CONTROLLED RELEASE DRUG DELIVERY SYSTEMS FOR OSTEOPOROSIS PHARMACEUTICALS BASED ON SILICA HYDROGELS

KONSTANTINOS E. PAPATHANASIOU

UNIVERSITY OF CRETE

CRYSTAL ENGINEERING GROWTH AND DESIGN LABORATORY

Department of Chemistry

University of Crete

This dissertation is submitted for the degree of Doctor of Philosophy

March 2017

ΣΥΣΤΗΜΑΤΑ ΕΛΕΓΧΟΜΕΝΗΣ ΑΠΟΔΕΣΜΕΥΣΗΣ ΦΑΡΜΑΚΩΝ ΚΑΤΑ ΤΗΣ ΟΣΤΕΟΠΟΡΩΣΗΣ ΜΕ ΒΑΣΗ ΥΔΡΟΓΕΛΕΣ ΤΟΥ ΔΙΟΞΕΙΔΙΟΥ ΤΟΥ ΠΥΡΙΤΙΟΥ

ΚΩΝΣΤΑΝΤΙΝΟΣ Ε. ΠΑΠΑΘΑΝΑΣΙΟΥ

ΠΑΝΕΠΙΣΤΗΜΙΟ ΚΡΗΤΗΣ

to my late Father,

Eleytherio A. Papathanasiou,

a Great Scientist and a Wonderful Person

…

DECLARATION

This dissertation is the result of my own work and includes nothing, which is the outcome of work done in collaboration except where specifically indicated in the text. It has not been previously submitted, in part or whole, to any University or Institution for any degree, diploma, or other qualification.

Signed:_____

Place and Date:_____

Name

University of Crete

SUMMARY / ABSTRACT

Gel systems have found extensive applications in the medicinal/pharmaceutical field because of their ease of preparation, ability for modifications, and responsiveness to external chemical or physicalstimuli. Gels usually act as hosts for active pharmaceutical agents for a variety of pathological conditions. They function as controllers of the release of pharmaceuticals that have proven to be "problematic" because they are either unsuitably insoluble to biological fluids, or they are metabolized unacceptably rapidly.

Among the known bone diseases (osteoporosis, osteoarthritis, multiple myeloma, Paget's disease and several others), the most challenging is osteoporosis, which burdens millions of people compromising patients' quality of life. The recommended pharmaceutical treatment is the use of bis-phosphonates (BPs, a.k.a. "-dronates"). Etidronic acid (**ETID**) is the first osteoporosis treatment to enter the market (1977), while zoledronic acid is one of the treatments that followed (2007). Studies with N-containing BPs have shown that they are taken up by mature osteoclasts and inhibit farnesyl pyrophosphatase synthase, an enzyme of the mevalonate pathway. Their success in mitigating osteoporosis notwithstanding, these "-dronate" drugs present a number of challenges including limited bioavailability, fast excretion, and numerous side-effects, such as osteonecrosis of the jaw, hypocalcemia, esophageal cancer, ocular inflammation, atrial fibrillation, etc.. It is, therefore, imperative to design and fabricate "smart" systems that allow controlled delivery of the active BP agent, which will depend on the patient's needs and idiosyncrasies.

In this study, we report a detailed study on an easy-to-prepare a silica hydrogel-type DDS that can host and incorporate a variety of BPs. Several factors have been found to influence the controlled release of the active BP, such as cations present in the gel, active groups on the BP backbone, gel density, and temperature. These systems are intended for potential biomedical applications.

ACKNOWLEDGEMENTS

TABLE OF CONTENTS

1 PHOSPHONATES IN MATRICES

1.1 Introduction.Phosphonic acids as versatile molecules.

Phosphonic acids constitute a special class of molecules within phosphorus-containing compounds.[1] The phosphonic acid group is a pentavalent, tetrahedral P atom connected via a double bond to O (P=O), while it forms two P-O single bonds with two OH groups, Figure 1-1 The P atom also has a single bond with carbon (P-C), the latter originating from an aliphatic or aromatic fragment.
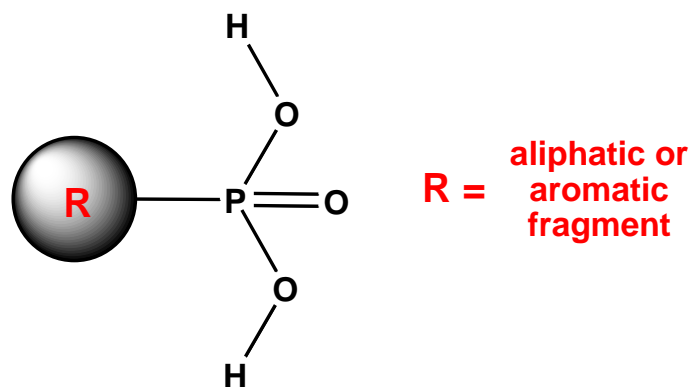
Figure 1-1. The chemical identity of the phosphonic acid group.

The H atoms exhibit variable acidity. A thorough review has been published on the acid behavior of several phosphonic acids.[2] In this review the authors make available experimental data on stability constants of proton and metal complexes for ten phosphonic acids. These are: methylphosphonic acid, 1-hydroxyethane-1,1-diylbisphosphonic acid, dichloromethylenebisphosphonic acid, aminomethanephosphonic acid, N-(phosphonomethyl)glycine, imino-N,N-bis(methylenephosphonic acid), N-methylamino-N,N-

bis(methylenephosphonic acid), nitrilotris(methylenephosphonic acid), 1,2-diaminoethane-N,N,N′,N′-tetrakis-(methylenephosphonic acid), and diethylenetriamine-N,N,N′,N″,N″-pentakis-(methylenephosphonic acid). The data were taken from papers published in the time frame 1950–1997. The acid-base behavior of phosphonic acids will be discussed further in a subsequent part of this chapter.

Phosphonic acids are widely used in a variety of applications. Their ability to prevent precipitation of alkaline-earth metal sparingly-soluble salts at substoichiometric concentrations (threshold inhibition effect) finds wide application in chemical water treatment for scale inhibition.[3] Others are used extensively in laundry detergent formulations.[4] Some are also used as corrosion inhibitors,[5] in industrial cleaning[6] and in peroxy bleach stabilization.[7] Uses of organophosphonates span applications in flame-resistant polymers,[8],[9],[10],[11],[12] photographic processing,[13] ore flotation (aminophosphonic surfactants),[14] actinide separation processes,[15],[16] and analytical chemistry.[17] Recently, organophosphonates have been identified as promising reagents for the creation of so-called "structurally tailored" materials[18] and microporous materials,[19] in catalysis[20]and in the electrochemical treatment of polluted soils.[21]

The high biological activity of carboxyalkylphosphonates, aminoalkylphosphonates, and alkylenediphosphonates makes them useful agents as components of microfertilizers and pesticides in agriculture,[22] as well as drugs and diagnostic reagents in biology and medicine.[23] Annual industrial output of organophosphonates is in the thousands of tons.[24]

1.2 Acid-Base chemistry of phosphonic acids

As mentioned before, the phosphonic acid group exhibits variable acidity. There are two, step-wise deprotonation processes, as shown in Figure 1-2.
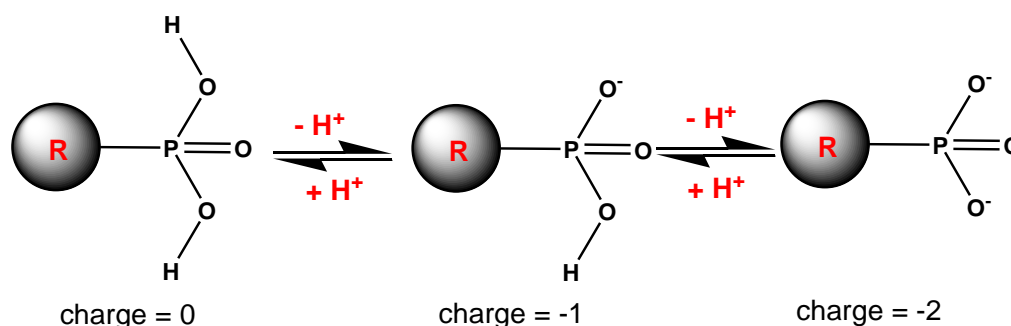
Figure 1-2. The two deprotonation processes in the phosphonic acid group.

The pKa values depend on the backbone of the phosphonic acid molecule, and the presence of other functional groups (eg. amino, sulfonate, carboxylate, etc).

We will refer to some notable examples of phosphonic acids and their acid-base behavior. Hence, the schematic structures of some (poly)phosphonic acids are shown in Figure 1-3.
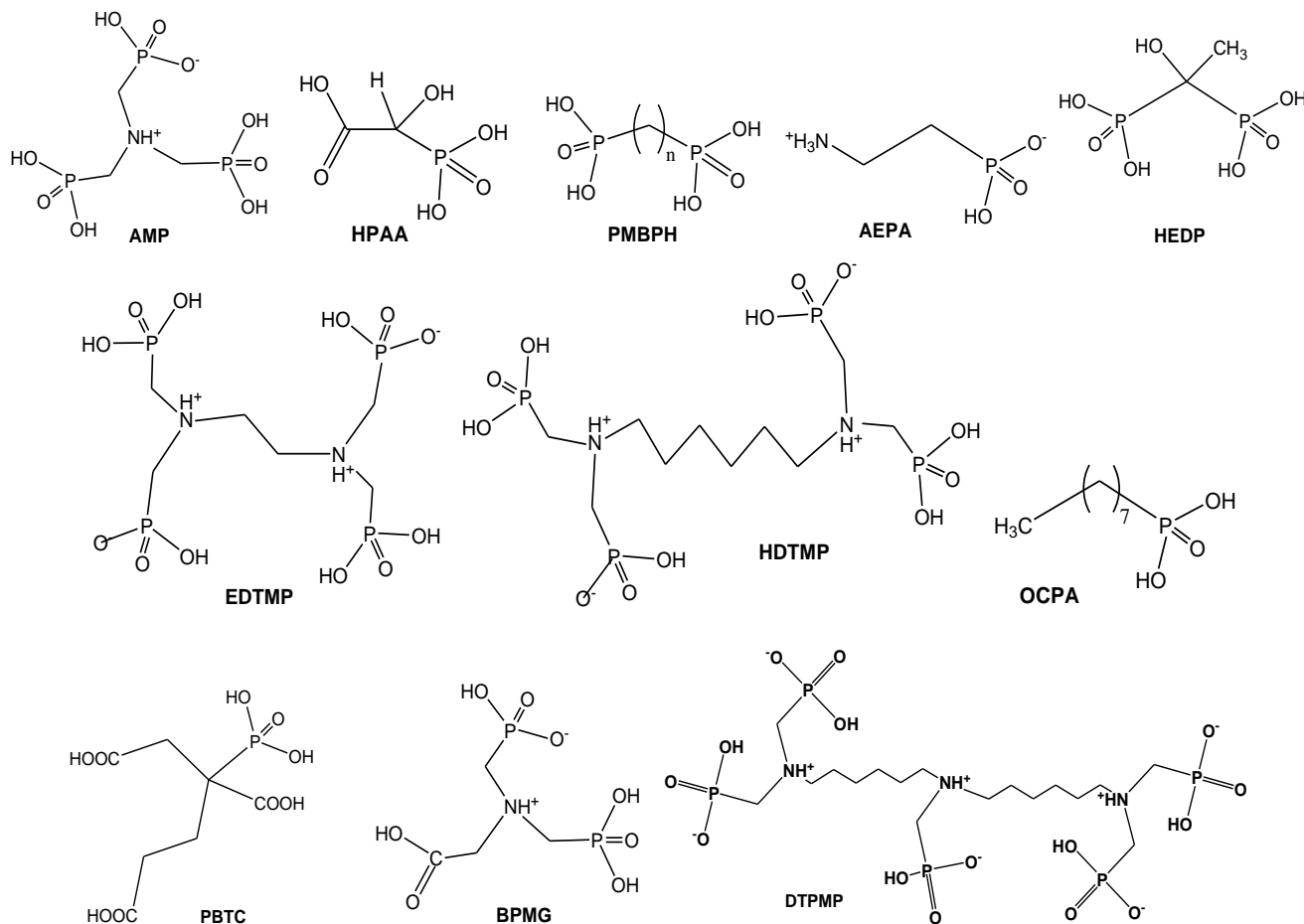
Figure 1-3. Schematic structures of different structure types of (poly)phosphonic acids.

The protonation constants of iminobis(methylenephosphonic acid) (IDPH, H$_4$idph, H$_4$L), N-methyliminobis(methylenephosphonic acid) (MIDPH, H$_4$midph, H$_4$L) and nitrilotris(methylenephosphonic acid) (NTPH, H$_6$ntph, H6L) were determined by ^{31}P NMR spectroscopy at 25 °C in 0.1 M KNO$_3$ at 11 < pH < 14. For equilibrium L + H $\leftrightarrow$ HL, log K = 11.5 (0.1), 12.2 (0.1) and 12.9 (0.1), respectively.[25]

Protonation constants for three common polyphosphonic acids (AMP, HEDP, and DTPMP) have been reported, see Table 1-1.[26]

Table 1-1.Protonation Constants of AMP, HEDP and DTPMP (for chemical structures see Figure 1-3).

	AMP[a]	HEDP[a]	DTPMP[b]
Log K_1	12.5 ± 0.2	11.0 ± 0.2	12.58
Log K_2	7.22 ± 0.03	6.9 ± 0.1	11.18
Log K_3	5.90 ± 0.02	2.7 ± 0.1	8.30
Log K_4	4.59 ± 0.03	1.6 ± 0.2	7.23
Log K_5	1.6 ± 0.3		6.23
Log K_6	0.5 ± 0.3		5.19
Log K_7			4.15
Log K_8			3.11
Log K_9			2.08
Log K_{10}			1.04

[a] *Data taken from Ref. [27]. Conditions: $I = 0.1$ mol·L^{-1} (KNO_3), $T = 25 \pm 0.5$ °C.*

[b] *Data taken from Ref. [28].*

An important observation is the very high acidity of the first acidic proton. Speciation graphs, like the one shown in Figure 1-4, are useful in gaining an overview of acid-base behavior of phosphonic acids, particularly when they interact with metal ions of variable charge to form hybrid materials or salts, as we will see in a following paragraph.
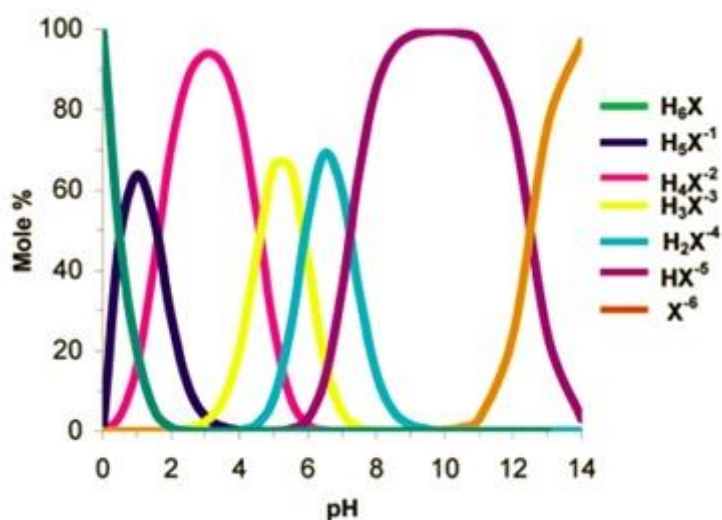
Figure 1-4. Distribution of AMP phosphonate ionic species as a function of pH. Reprinted with permission from Reference 21, Copyright (2006) American Chemical Society.

The group of Vepsäläinen has studied the protonation constants of a series of bis-phosphonic acids, of the "dronate" family, used as therapeutics for osteoporosis.[29] The following general trend can be found in the results of this study: the lengthening of the CH_2 chain between BP and amino

groups decreases the value of the first protonation constant (pKa5, amino group) and increases the values of the other protonation constants (phosphonate groups) in most cases (Table 2).

Table 1-2.The stepwise protonation of compounds 1,2,3,4 and 5, as reported by Vepsäläinen et.al.[29].
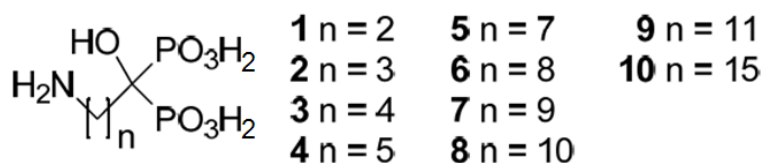
Protonation	log K					
Reaction	1	2	3	4	5	pKa
$L^{4-} + H^+ \leftrightarrow HL^{3-}$	12.86	12.13	12.05	11.94	11.65	pKa_5
$HL^{3-} + H^+ \leftrightarrow H_2L^{2-}$	10.04	10.69	10.78	10.86	10.67	pKa_4
$H_2L^{2-} + H^+ \leftrightarrow H_3L^-$	5.90	6.26	6.44	6.62	6.75	pKa_3
$H_3L^- + H^+ \leftrightarrow H_4L$	1.70	2.12	2.30	2.38	2.52	pKa_2
$H_4L + H^+ \leftrightarrow H_5L^-$	1.06	0.60	0.62	0.94	1.08	pKa_1

1.3 Interactions between metal ions and phosphonate ligands.

The simplest organophosphonate, methylphosphonic acid, reveals higher ML complex stability than acetic acid (by about one order of magnitude) for both alkaline earth and 3d-metal ions. This fact demonstrates the almost equal importance for coordination compound stability of an increase in ligand basicity and an increase in number of ionic and covalent bonds. Within the 3d-elements definite but small deviations from the Irving–Williams sequence can be seen: Cu > Mn > Co ~ Ni. Although the systematic error is higher than some of the differences in lgK_{ML}, the relative error is expected to be small enough to make this a valid conclusion.

Bisphosphonates have significantly higher stability constants than those of monodentate alkylphosphonic acids owing to both higher basicity and bidentate coordination. The lgK_{ML} values for HEDPA and CMDPA are also much higher than those for the dicarboxy analog malonic acid. For the pair HEDPA/CMDPA, there is a reasonable difference in stability that can be attributed to the electron withdrawing effect of the two Cl substituents.

Aminomethylenephosphonic acids (AMPH, IDPH, MIDPH, NTPH) also demonstrate generally higher affinity to cations than their carboxy analogs, see Table 1-3.[30],[31], [32],[33],[34],[35]

Table 1-3.Stability constants (lgK$_{ML}$) of aminomethylenephosphonates and their carboxy analogs (I = 0.1 M, T = 25 °C).

Cation	AMPH	Gly	MIDPH	MIDA	NTPH[25]		NTA	EDTPH[25-30]		EDTA
H$^+$	10.07	9.60	12.1	9.65	14.2	12.7	9.7	13.8	13.0	10.26
Mg^{2+}	1.99	-	5.1	3.44	9.0	7.5	5.43	9.1	8.4	8.69
	1.67	-	4.6	3.75	9.4	7.9	6.45	10.1	9.4	10.7
Ca^{2+}	1.34	-	4.0	2.85	8.0	6.5	5.0	8.3	7.6	8.6
	4.5	4.66	9.4	7.62	15.5	14.0	10.4	17.8	17.1	16.11
Sr^{2+}	5.3	5.8	9.5	8.73	13.2	11.7	11.5	17.1	16.4	18.6
Co^{2+}	8.10	8.2	14.2	11.09	18.7	17.2	13.0	23.9	23.2	18.8
	-	5.0	10.2	7.66	16.1	14.6	10.7	19.5	18.8	16.26

The complexation constants of AMP and HEDP with different metal cations were determined.[36] These two phosphonic acids are used in detergents as builders, because of their complexing properties, especially the complexation with calcium and heavy metal cations. The cations studied were those usually encountered in natural waters (Ca^{2+}, Zn^{2+}) and anthropogenic heavy metals (Cu^{2+}, Ni^{2+}, Cd^{2+}, Pb^{2+}).

The equilibrium constant values and the titration curves point out the following order:

AMP: Cu^{2+}>Zn^{2+}>Pb^{2+}>>Cd^{2+}>Ni^{2+}>>Ca^{2+}

HEDP: Cu^{2+}> Zn^{2+}>>Cd^{2+}>Ni^{2+}>Ca^{2+}

The affinity order for all the cations is the same for AMP and HEDP. The AMP complexiatiomn constants for each cation are higher than those of HEDP, particularly with Cu^{2+} and Zn^{2+}(difference of six log units).

Stone et al. have studied the formation of metal ion-chelating agent complexes in aqueous solution in an excellent review.[37] They also studied and compared the adsorption of various phosphonates onto (hydr)oxide mineral surfaces, Figure 1-5. Interconnections between the coordination chemistry and chemical reactivity of phosphonates were also made.
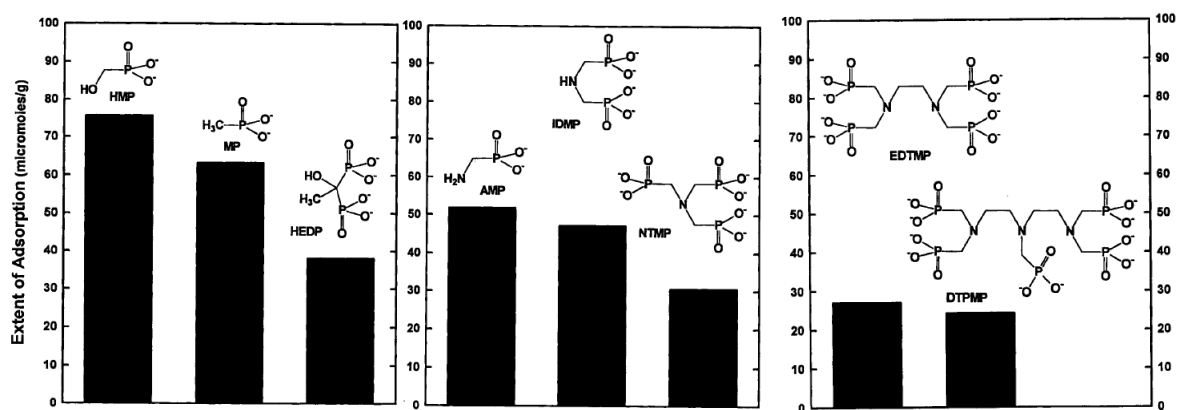
Figure 1-5. Adsorption of five phosphonate molecules onto goethite surfaces. Reprinted with permission from Reference[37], Copyright (2002) American Chemical Society.

Synthetic manipulation of organic platforms by introducing phosphonate groups often yields highly selective ligands. For example, Gałezowska et al. described the synthesis of two new ligands (L2 and L3) composed of ethylenediamine (EN), pyridyl (Py) moieties and phosphonic groups, designed to bind metal ions with the donor set based on four nitrogen atoms and two phosphonic units (Figure 1-6).[38] These ligands were used to evaluate their coordination abilities towards Cu^{2+}, Ni^{2+} and Zn^{2+}, and compare those to ligand L1.

L¹ 2,2'-(ethylenedi-imino)bis(benzylphosphonic-acid)
L² 2,2'-(ethylenedi-imino)bis(3-pirydylphosphonic-acid)
L³ 2,2'-(ethylenedi-imino)bis(2-pirydylphosphonic-acid)
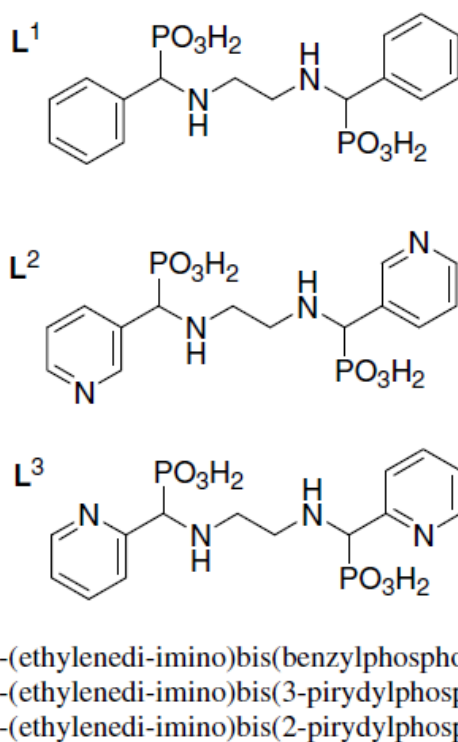
Figure 1-6. Chemical structures of studied ligands L1, L2, L3. Reprinted with permission from Reference [38], Copyright (2009) Elsevier.

Ligands L1 and L2 possessing the ethylenediamine core situated closely to the phosphonic acid units bind the Cu^{2+}, Ni^{2+} and Zn^{2+} ions using the same donor set, two N atoms from ethylenediamine and two O atoms from phosphonate. The presence of the pyridyl moieties in L3 leads to very effective ligand (pM 15.27) for Cu^{2+} ions, with tetradendate coordination mode and axial involvement of two phosphonate groups in Zn^{2+} and Ni^{2+} octahedral complexes. Ligand L3 is able to involve a four-nitrogen donor system and additionally two phosphates and is unusually an effective ligand for both planar and octahedral complexes

1.4 Phosphonates in "all-organic" polymeric salts

When phosphonic acids deprotonate they can interact in solution or in the solid state with organic cations. The salts that form could be envisioned as "all-organic", since they do not contain metal ions. In this section we will review some representative examples of materials that conform to the general type "organic cation-phosphonate".

An example of an "intramolecular" salt is the heterotopic phosphonic acid, 3-amino-5-(dihydroxyphosphoryl)benzoic acid, which was synthesized and structurally characterized,[39]Figure 1-7.
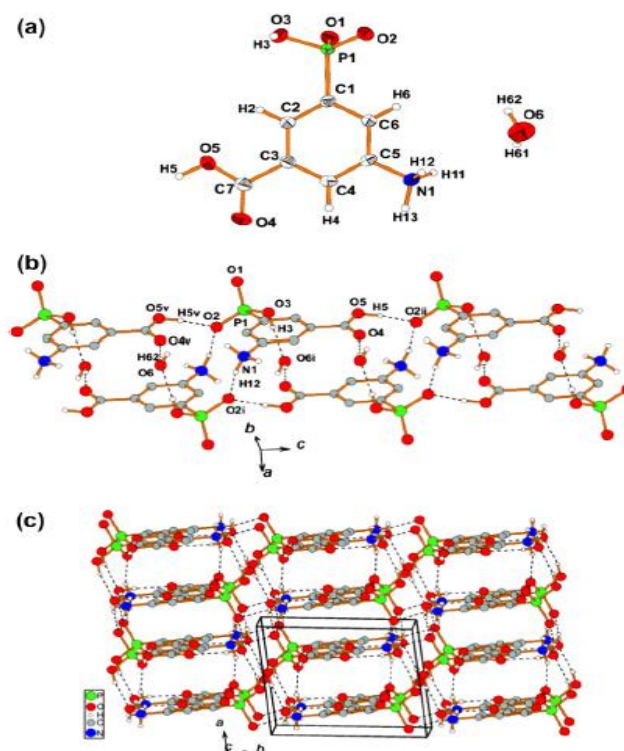
Figure 1-7. (a) View of the molecular structure of 3-amino-5-(dihydroxyphosphoryl)benzoic acid. (b) View of the O-H---O hydrogen bonded chains of zwitterionic 3-amino-5-

(dihydroxyphosphoryl)benzoic acid molecules. (c) Crystal packing of 3-amino-5-(dihydroxyphosphoryl)benzoic acid showing the layered structure. Dashed lines represent the O-H···O and N-H···O hydrogen bonds. Reprinted with permission from Reference [39], Copyright (2013) Elsevier.

Long-chain monophosphonates with ammonium and ethylenediammonium cations have been structurally characterized. Specifically, the crystal structure of ammonium 1-decylphosphonate, and ethylenediamonium 1-decylphosphonate 1.5 hydrate have been reported.[40] The layered structure of the crystal of ammonium 1-decylphosphonate is dominated by the complex system of hydrogen bonds between phosphonate group and ammonium ion (Figure 1-8). The 1-decylphosphonate ions are situated in the head-to-head and tail-to-tail relation. The very wide amphiphilic layers (26.345(5) Å) parallel to the ab crystallographic plane are built of the hydrophilic central part and the external, hydrophobic part. The interlayer contacts are of the very weak Van der Waals type, since the aliphatic chains do not interdigitate.
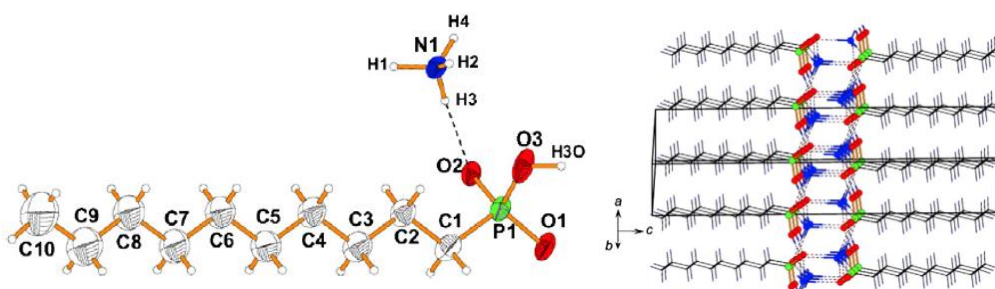
Figure 1-8. View of the molecular unit of ammonium 1-decylphosphonate (left) and the crystal packing (right). Reprinted with permission from Reference [40], Copyright (2012) Elsevier.

The organization of the crystal of ethylenediamonium 1-decylphosphonate is very similar to that of the crystal of ammonium 1-decylphosphonate, Figure 1-9. The crystal structure of the latter is more compact than that of the former because the aliphatic chains interdigitate. The phosphonate groups interact with ethylenediamonium cations through four strong hydrogen bonds.
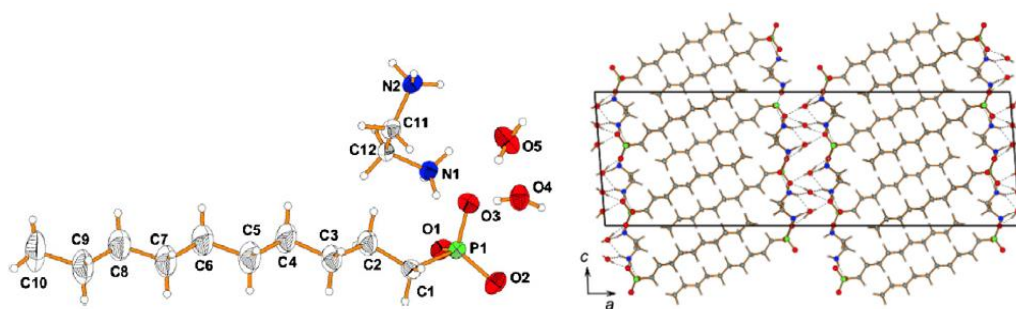
Figure 1-9. View of the molecular unit of ethylenediamonium 1-decylphosphonate 1.5 hydrate (left) and the crystal packing (right). Reprinted with permission from Reference [40], Copyright (2012) Elsevier.

Co-crystallization of melamine (ma) with m-sulfophenylphosphonic acid (sppH$_3$) from water in different molar ratios (2:1 and 4:1) offer [(maH)$_2$(sppH)]·3H$_2$O and [(maH)$_3$(spp)(ma)]·12H$_2$O, respectively.[41] Structure analysis reveals that two very intricate hydrogen-bonded networks are formed in them, with two or three protons of the m-sulfophenylphosphonic acid being transferred to melamine, Figure 1-10. The resultant (sppH)$^{2-}$ or (sppH)$^{3-}$ anion can form as many as 12 or 14 hydrogen bonds with melamine and water molecules, showing a very high hydrogen-bonding capability.
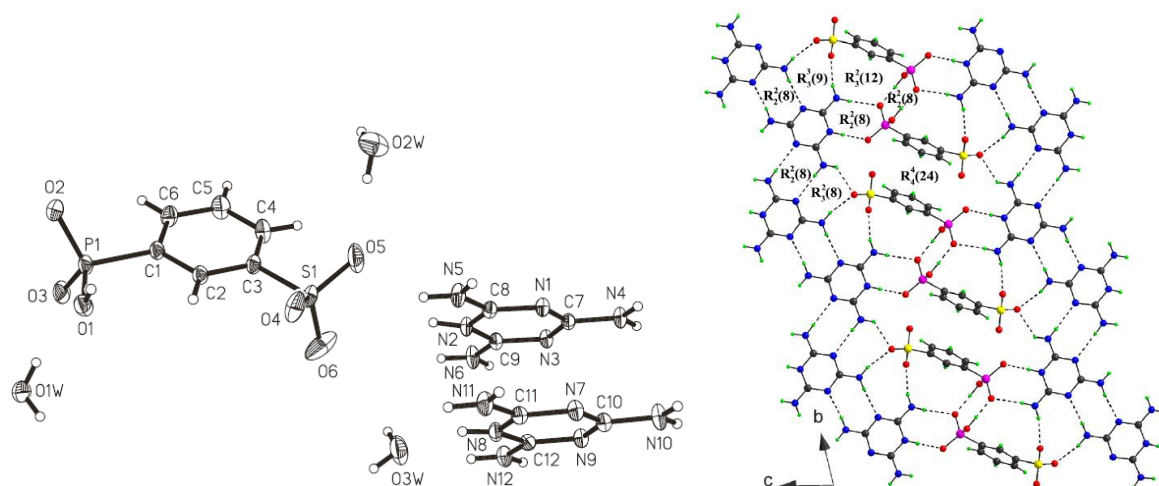
Figure 1-10. Asymmetric unit of [(maH)$_2$(sppH)]·3H$_2$O (left) and one-dimensional ladder-like chain formed by hydrogen bond interactions between the (sppH)$^{2-}$ and (maH)$^+$ ions in [(maH)$_2$(sppH)]·3H$_2$O (right). Reprinted with permission from Reference[41], Copyright (2013).

Hexamethylediamine-N,N,N′,N′-*tetrakis*(methylenephosphonic acid) (HDTMP) has been isolated as a crystalline solid with the ethylenediammonium (en) dication, as (en)(HDTMP)·2H$_2$O. The crystal structure of the solid has been determined.[42] The molar ratio between the dication and dianion has been found 1:1. The disposition of the ionic pair is shown in Figure 11. The presence of waters of crystallization, HDTMP^{2-} dianions and en^{2+} dications leads to a complicated network of hydrogen bonds, finally yielding a 2D layered structure (shown in Figure 12). They are described in detail below. The –NH$_3^+$ portion of the en molecule is hydrogen-bonded with one of the two water molecules of crystallization (at a distance of 2.974 Å), and with three O-P moieties (all from different phosphonate groups) (at distances 2.708 Å, 2.804 Å and 2.984 Å).
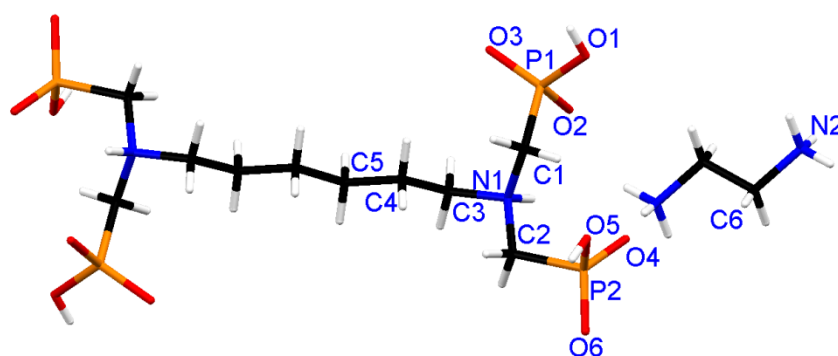
Figure 1-11. Structure of HDTMP^{2-} with the en^{2+} dications (the water molecules are omitted for clarity). Reprinted with permission from Reference [42], Copyright (2009) Elsevier.
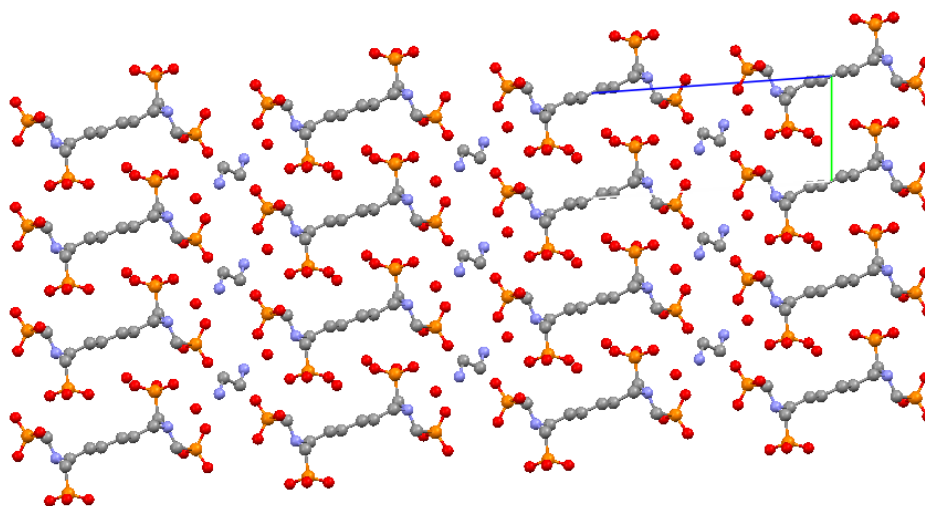
Figure 1-12. Layers of HDTMP^{2-} and en^{2+} dications (lower) down the b-axis. Hydrogen atoms are omitted for clarity.

The two waters of crystallization are located in the vicinity of the en^{2+} dication. One water molecule forms hydrogen bonds with one of the N-H$^+$ moieties of the phosphonate ligand (2.963 Å), with the $^+$H$_3$N group of the en^{2+} cation (2.974 Å), and with and the O atoms from a deprotonated

phosphonate ligand, ⁻O-P (2.999 Å). The second water molecule participates in three hydrogen bonds, one with a –P-OH group (2.553 Å), and two hydrogen bonds with two deprotonated P-O⁻ moieties (2.729 and 2.743 Å) from neighboring phosphonate ligands. There are several other hydrogen bonds in the structure that are described in detail in the original paper.

Ethylenediamine-N,N'-tetrakis(methylenephosphonic acid) (EDTMP) is structurally related to HDTMP, except that the N atoms are connected by two methylene groups. A crystalline solid was isolated which contains two ammonium cations per one EDTMP dianion.[42] In the structure of $(NH_4)_2(EDTMP)$ there are discrete $EDTMP^{2-}$ dianions and NH_4^+ cations, see Figure 1-13.
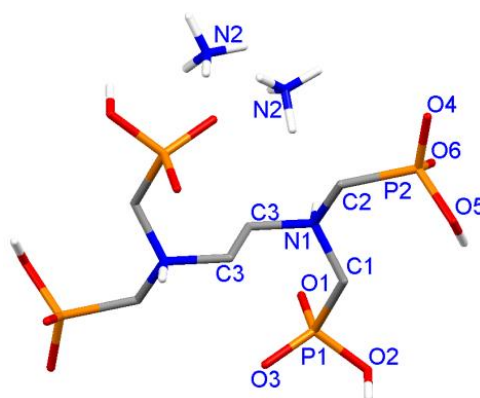
Figure 1-13. Structure of $EDTMP^{2-}$ with the two NH_4^+ cations.Reprinted with permission from Reference [42], Copyright (2009) Elsevier.

The presence of $EDTMP^{2-}$ dianions and NH_4^+ cations leads to a complicated network of hydrogen bonds, finally yielding a 2D layered structure, see Figure 1-14.
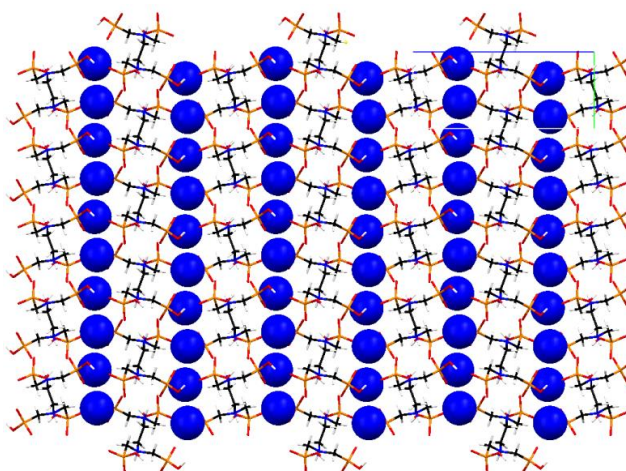
Figure 1-14. Layers of $EDTMP^{2-}$ and NH_4^+ cations, shown as spheres, shown down the a-axis.Reprinted with permission from Reference[42], Copyright (2009) Elsevier.

Each of the ammonium cations participates in five hydrogen bonds, all with non-protonated P-O groups from different phosphonate ligands, with O···N distances ranging from 2.799 to 2.949 Å. The $P(1)O_3H^-$ phosphonate group participates in five hydrogen bonds. Protonated P-O(2)H participates in a hydrogen bond with the ammonium N(2) group of the NH_4^+ cation (2.929 Å) and the non-protonated group O(4)-P(2) from a neighboring phosphonate (2.559 Å). The group P-O(1) forms only one H-bond with the protonated $N(1)H^+$ group belonging to another EDTMP molecule (2.648 Å). Finally, P-O(3) forms two H-bonds with two symmetry-related N(2) groups from two different en molecules (2.799 Å and 2.895 Å). The $P(2)O_3H^-$ phosphonate group also participates in five hydrogen bonds. Protonated P-O(5)H participates in a hydrogen bond with the non-protonated P(2)-O(6) group from a neighboring phosphonate. At the same time non-protonated P(2)-O(6) hydrogen bonds with the protonated P(2)-O(5)-H moiety with the same phosphonate group. This creates a hydrogen-bonded dimer, the structure of which is shown in Figure 15. A similar phosphonate hydrogen-bonded dimmer has been observed in the structure of 2-Phosphonobutane-1,2,4-Tricarboxylic Acid Monohydrate (PBTC·H_2O).[43]
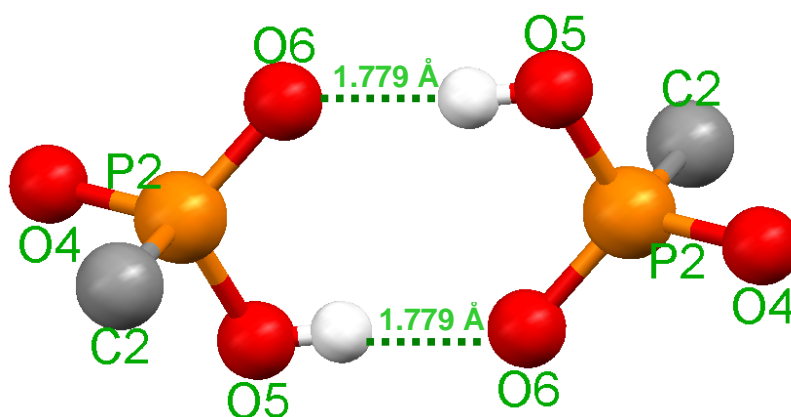
Figure 1-15. Structure of the hydrogen-bonded dimer in the structure of $(NH_4)_2(EDTMP)$.

Tetraphosphonates are biomimetic hosts for bisamidinium cations in drugs such as pentamidine and DAPI (4',6-diamidino-2-phenylindole). Similar to their insertion into DNA's minor groove, these drugs are often sandwiched by two tetraphosphonate hosts in a 2:1 ratio, as shown in Figure 1-16.[44]
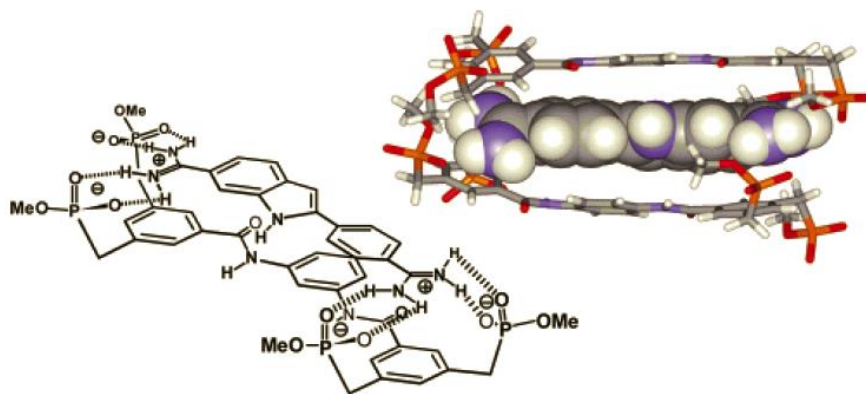
Figure 1-16. 1:1 complex between a tetraphosphonate and DAPI according to Monte Carlo simulations in water.Reprinted with permission from Reference [44], Copyright (2003) American Chemical Society.

1.5 Phosphonates in coordination polymers

The field of coordination polymers has exploded in the last decades. Since a substantial number of original research papers, reviews, book chapters and books have been published on the subject, we will attempt a concise look into this topic, with a focus on metal phosphonate-based coordination polymers. A concise source on the topic is the only book available on the topicby Clearfield and Demadis.[45]

There is a battery of structurally characterized metal phosphonate materials of essentially all metal ions of the periodic table. We briefly note those of alkali metal ions,[46],[47],[48],[49],[50],[51],[52]alkaline-earth ions,[53],[54],[55],[56],[57],[58],[59], [60],[61],[62],[63],[64],[65]transition elements of the first period, [66],[67],[68],[69],[70],[71], [72],[73],[74],[75] the second period,[76],[77],[78],[79],[80],[81],[82],[83],[84],[85] third period,[86],[87],[88],[89],[90],[91],[92],[93],[94],[95]lanthanides [96],[97],[98],[99], [100],[101], [102],[103],[104],[105]and actinides.[106],[107],[108],[109],[110]

Among the plethora of anionic ligands used for the construction of inorganic-organic hybrids polycarboxylates are predominant. Polyphosphonates have also attracted significant interest. because they exhibit a number of similarities, but also differences to the carboxylates: (a) Phosphonate building blocks possess three O atoms linked to the phosphorus atom in the coordinating moiety, compared to two O atoms in the case of carboxylates. This increases the possibilities for access to novel structures. (b) The phosphonic acid moiety can be doubly

deprotonated in two well-defined successive steps, depending on solution pH.[2] Carboxylic acid ligands can only be deprotonated once, see Figure 1-17.

Again, this allows access to a variety of potential novel phosphonate-containing structures, by simply varying the pH. (c) The phosphonate group can be (potentially) doubly esterified, in contrast to the carboxylate group that can only be monoesterified.[46],[69],[111],[112] Introduction of at least one phosphonate ester in the building block is expected to enhance solubility (in the case of very insoluble materials), or by virtue of its hydrolysis,[68] to yield structural diversity in the end material. (d) Synthesis of metal phosphonate materials can be carried out via a number of different routes that do not necessarily give products with the same structure. There is hence a greater potential of structural diversity in the products derived. Several of these methods lend themselves to a combinatorial approach allowing high-throughput screening of candidate materials to be achieved.[113] In this context, a recent review was published on "non-carboxylate" MOFs.[114]

Because the focus of this chapter is not metal phosphonate frameworks, we will refer the reader to the relevant book mentioned above and its chapters, for further details and extensive literature.[45]
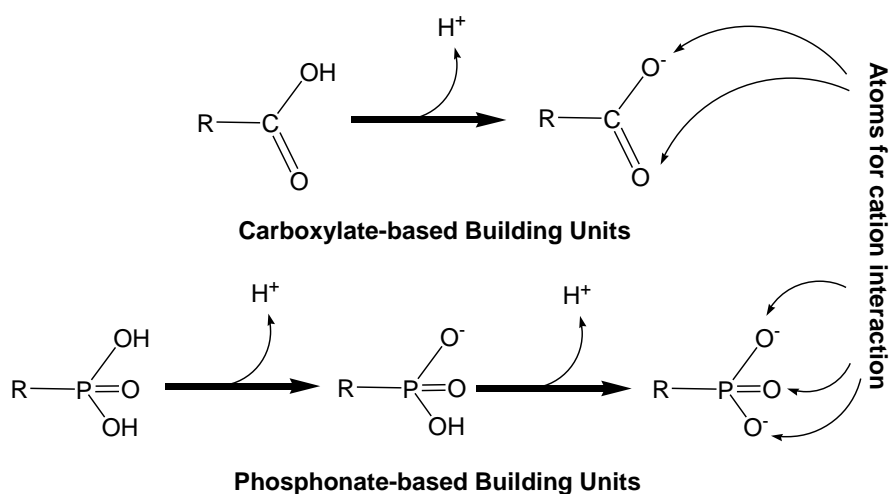
Figure 1-17. Structural and functional differences between carboxylic and phosphonic acids.

1.6 Phosphonate-grafted polymers

A phosphonate moiety can be grafted on a polymeric chain or matrix, by use of established organic synthetic methodology. We will briefly examine these grafting methods, and also review the types of polymers that result.

The Michaelis-Arbuzov reaction isa method for C-P bond formation, leading to a dialkoxyphosphonate. The reaction was discovered by Michaelis and investigated and developed by Arbuzov. It proceeds mainly between primary alkyl halides and trialkyl phosphite and is usually thermally initiated, see Figure 1-18.[115]
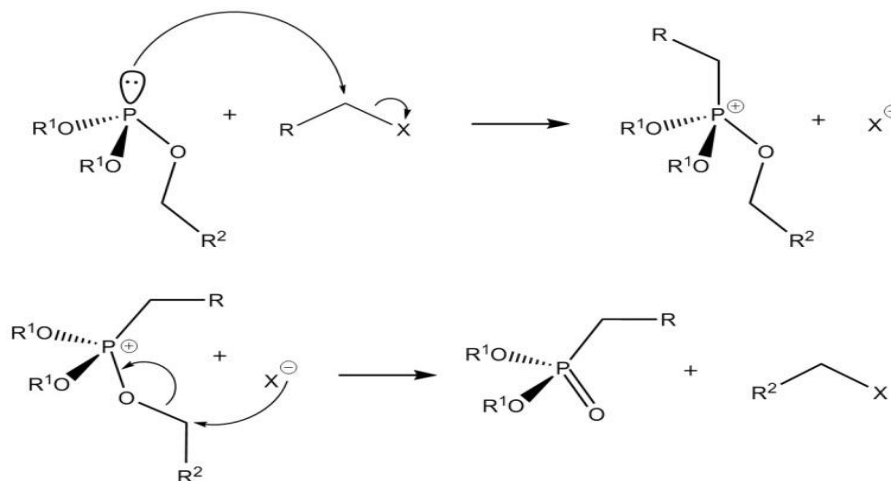
Figure 1-18. Mechanism of the Michaelis-Arbuzov reaction.Reprinted with permission from Reference [45], Copyright (2012) Royal Society of Chemistry.

The Mannich-type condensation (occasionally called the Moedritzer-Irani reaction)[116] is a convenient approach for synthesis of *N,N*-disubstituted aminomethylphosphonic acids or *N*-substituted iminobis(methylphosphonic acids). The reaction is conducted in highly acidic solutions. Zon *et al.* have proposed a mechanism for this reaction, Figure 1-19.[117]
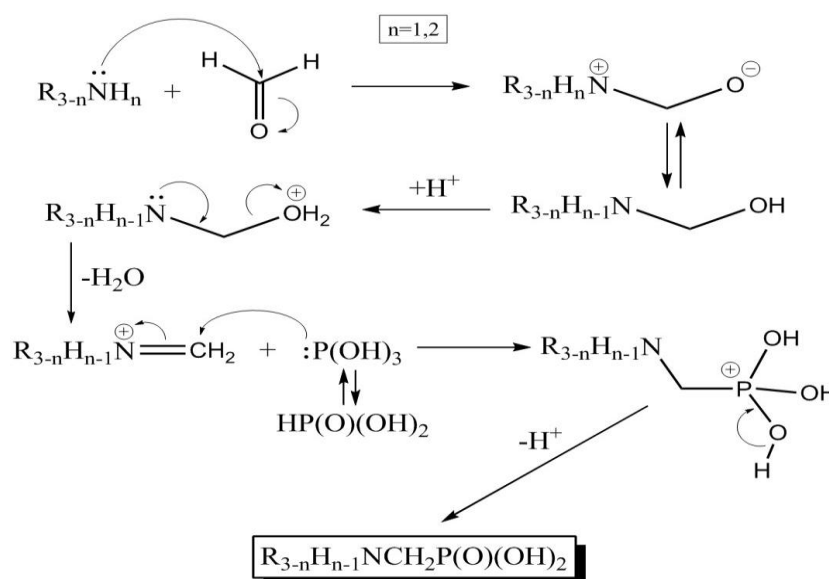
Figure 1-19. Mechanism of the Mannich-type (Moedritzer-Irani) reaction.Reprinted with permission from Reference [45], Copyright (2012) Royal Society of Chemistry.

Zon et al. explained that the first step of the reaction is a nucleophilic attack of *N,N*-dialkylamine nitrogen. Further rearrangement gives *N*-hydoxymethylamine which in strong acidic condition undergoes elimination of water molecule yielding an iminium salt. Phosphorous acid in acidic conditions behaves as a nucleophile and therefore attacks the electrophilic iminium salt. The charged adduct is stabilized by loss of a proton to give *N,N*-disubstituted aminomethylphosphonic acid. *N*-substituted iminobis(methylphosphonic acid) is formed when one starts from primary alkylamine. Below, we present an example of the formation of an aromatic tetraphosphonic acid ligand, Figure 1-20, which has been used before for the construction of metal phosphonate frameworks.
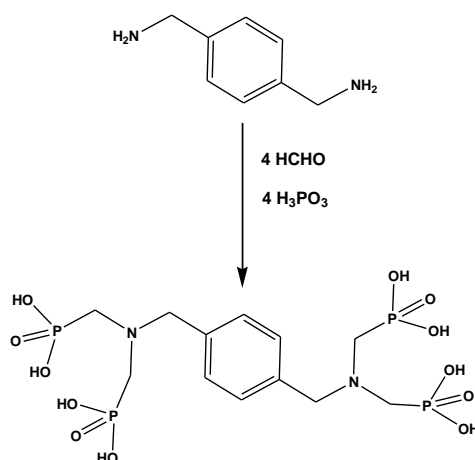
Figure 1-20. Synthesis of the xylene-diamine-tetrakis(methylenephosphonic acid) ligand.

Below, we will present several examples of phosphonate incorporation into polymeric matrices. Biomaterials such as inulin, chitin, chitosan and their derivatives have a significant and rapid development in recent years. They have become the focus of intense research because of an unusual combination of biological activities together with mechanical and physical properties. However, the applications of chitin and chitosan are limited due to insolubility issues in most solvents. The chemical modification of chitin and chitosan are of keen interest because these modifications would not change the fundamental skeleton of chitin and chitosan but would keep the original physicochemical and biochemical properties. They would also improve certain properties. The chemical modification of chitin and chitosan by phosphorylation is expected to be biocompatible and is able to promote tissue regeneration. Thus, we will start with these polymers.

A novel conjugate of a polysaccharide and a Gd(III) chelate with potential as contrast agent for magnetic resonance imaging (MRI) was synthesized.[118] The structure of the chelate was derived from H_5DTPA by replacing the central pendant arm by a phosphinic acid functional group,

which was covalently bound to the polysaccharide inulin. On the average, each monosaccharide unit of the inulin was attached to approximately one chelate moiety. The ligand binds the Gd^{3+} ion in an octadentate fashion via three nitrogen atoms, four carboxylate oxygen atoms, and one P-O oxygen atom, and its first coordination sphere is completed by a water molecule. This compound shows promising properties for application as a contrast agent for MRI thanks to a favorable residence lifetime of this water molecule (170 ns at 298 K), a relatively long rotational correlation time (866 ps at 298 K), and the presence of two water molecules in the second coordination sphere of the Gd^{3+} ion. The synthesis of this interesting polymer is shown in Figure 1-21.
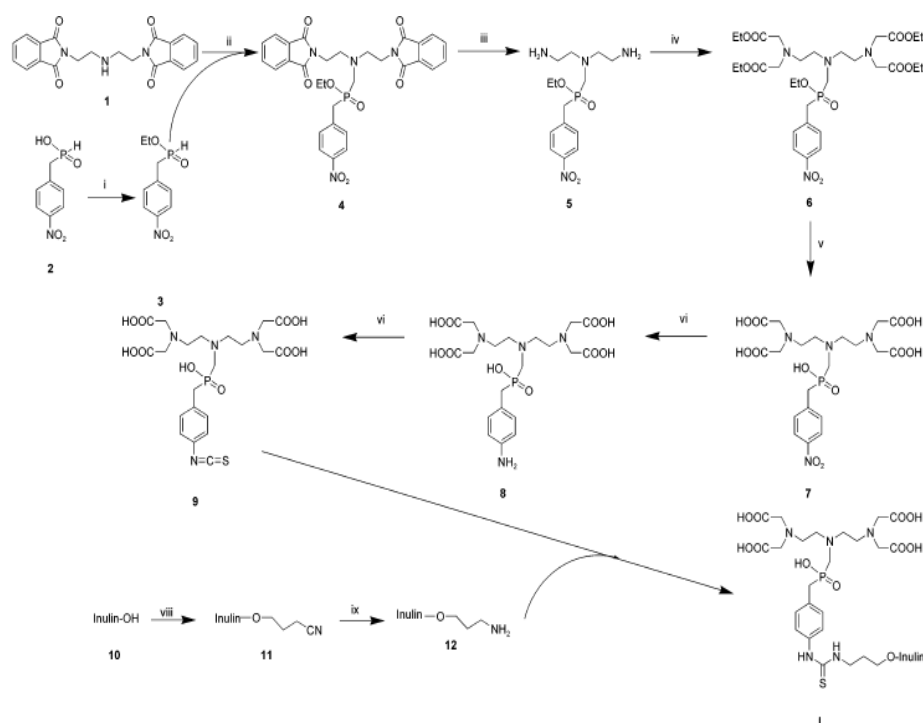
Figure 1-21. Synthesis of an inulin-bound chelate.Reprinted with permission from Reference [118], Copyright (2004) American Chemical Society.

A water-soluble chitosan derivative carrying phosphonic groups was synthesized using a one-step reaction.[119],[120]Detailed NMR studies permitted the identification of the structure by the substituent distribution of the product, which is partly N-monophosphonomethylated (0.24) and N,N-diphosphonomethylated (0.14) and N-acetylated (0.16) without modification of the initial degree of acetylation, Figure 1-22.

$$R_1 = H, R_2 = CH_2PO_3H_2$$
$$R_1 = R_2 = CH_2\text{-}PO_3H_2$$
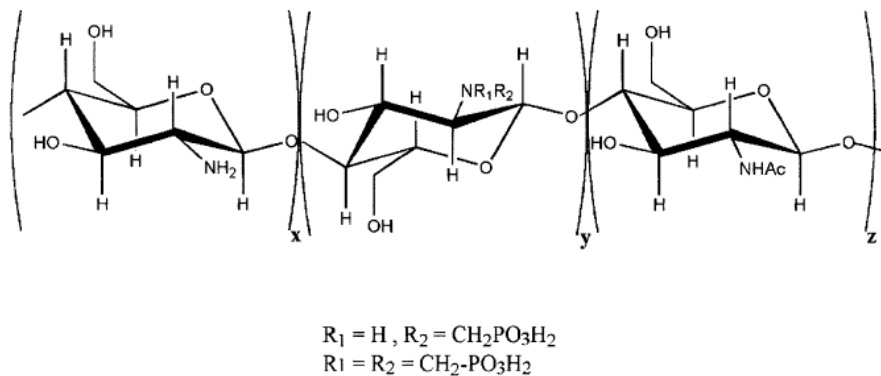
Figure 1-22. Synthesis of phosphono-substituted (N-methylene phosphonic) chitosan. Reprinted with permission from Reference [119], Copyright (2001) Elsevier.

The introduction of an alkyl chain onto a water soluble, modified chitosan (N-methylene phosphonic chitosan) allows the presence of hydrophobic and hydrophilic branches for control of solubility properties.[121] A simple methodology for the preparation of a new chitosan derivative surfactant, N-lauryl-N-methylene phosphonic chitosan, was developed. The degree of lauryl substitution was estimated to be 0.33.

A simple methodology for the preparation of a new chitosan derivative called N-propyl-N-methylene phosphonic cahitosan (PNMPC) was proposed. As before, the introduction of a propyl chain onto a modified chitosan (N-methylene phosphonic chitosan) offers the presence of hydrophobic and hydrophilic branches for controlling solubility properties of the new derivative. The degree of propyl substitution was 0.64. An SEM image of the solid polymer is shown in Figure 1-23.[122]
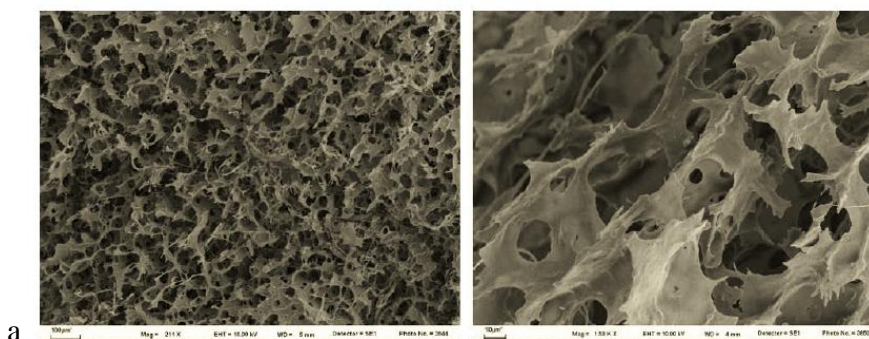
Figure 1-23. SEM images of the N-propyl-N-methylene phosphonic chitosan (PNMPC). Reprinted with permission from Reference [122], Copyright (2010) Elsevier.

Phosphorylation of chitosan but at the hydroxy and amino groups under the conditions of the Kabachnik-Fields reaction was reported (Figure 1-24)[123]. Conditions were found under which the reaction yields chitosan derivatives containing N-phosphonomethylated and chitosan phosphite fragments.
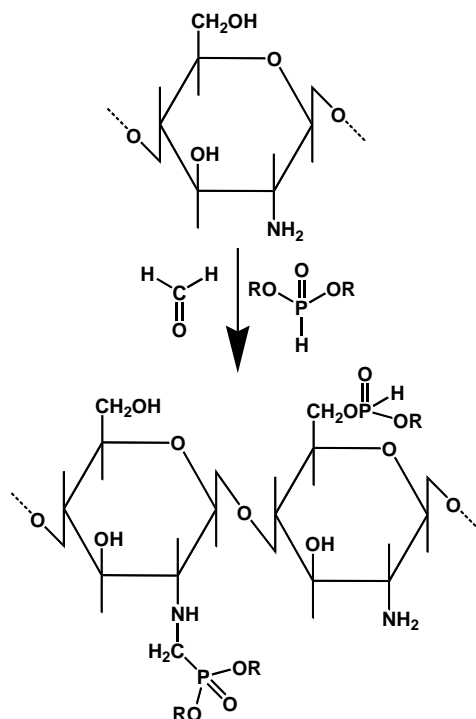
Figure 1-24. Kabachnik-Fields synthesis of chitosan derivatives containing N-phosphono methylated and chitosan phosphite fragments.

Recently, several derivatives of 2-(-arylamino phosphonate)-chitosan (2-AAPCS) were prepared by reactions of various Schiff bases of chitosan with di-alkyl phosphite in benzene solution (Figure 1-25).[124]
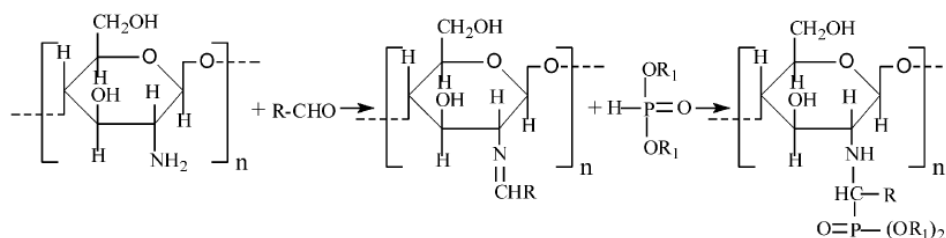
Figure 1-25. Synthetic pathway of 2-(-arylamino phosphonate)-chitosan. Reprinted with permission from Reference [124], Copyright (2009) Elsevier.

The structures of the derivatives (2-AAPCS) were characterized by FT-IR spectroscopy and elemental analysis. In addition, the antifungal activities of these derivatives against four kinds of fungi were evaluated. The results indicated that all 2-AAPCS congeners had a significant inhibition effect on the tested fungi at a concentration ranged from 50 to 500 g/L. Furthermore, the antifungal activities of the derivatives increased upon the molecular weight and concentration.

Jayakumara et al. have presented the recent developments in the preparation of phosphorylated chitin and chitosan with different methods.[125] These are presented in Figure 1-26.
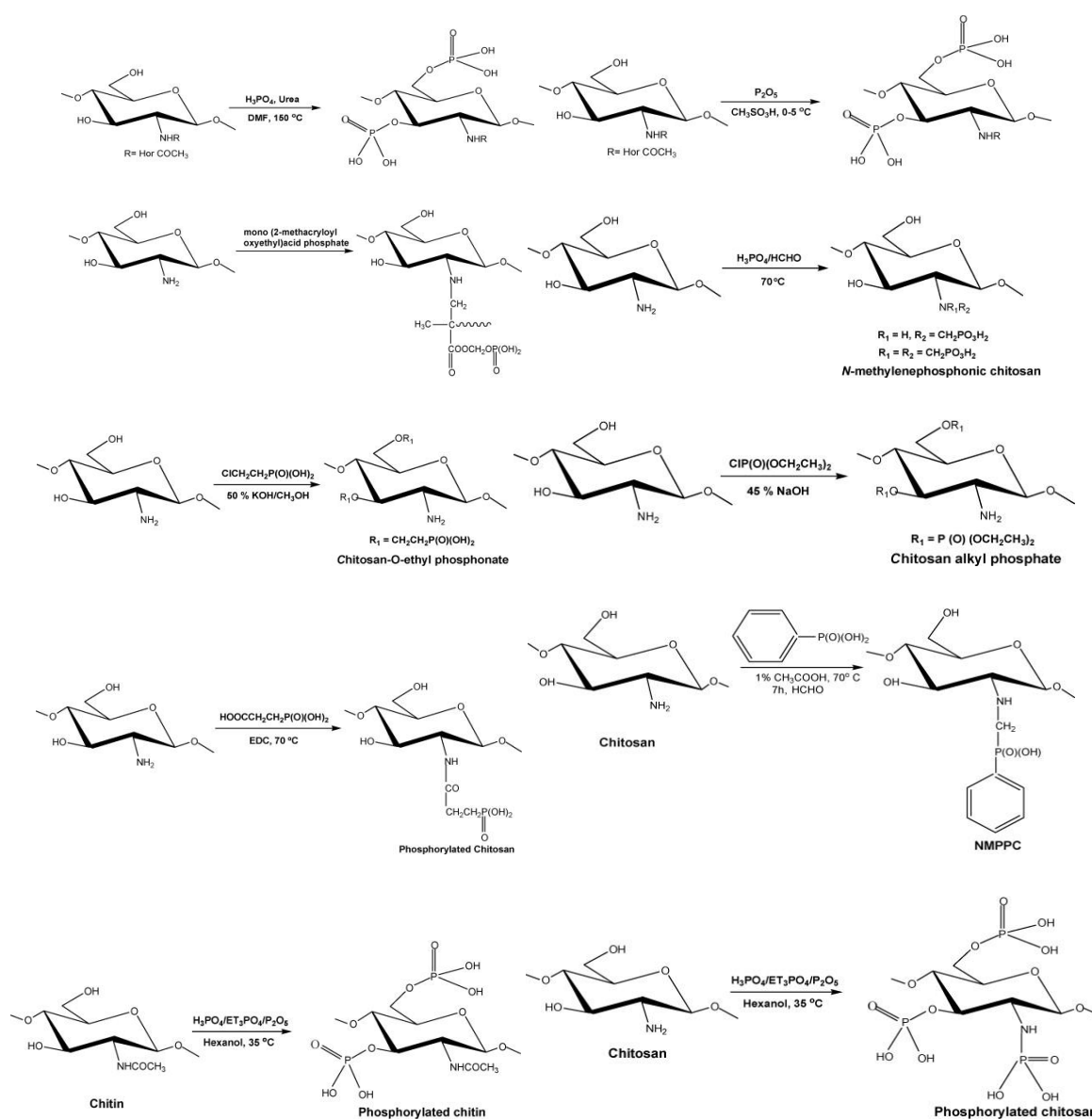
Figure 1-26. Preparation of phosphorylated chitin and chitosan with different methods. Reprinted with permission from Reference [125], Copyright (2008) Elsevier.

Chitosan was also phosphorylated by P_2O_5 in methanesulfonic acid and the product, water-soluble phosphorylated chitosan, was characterized by P elemental analysis, IR and ^{31}P NMR spectroscopy (Figure 1-27).[126] The phosphorylated chitosans were used to improve the mechanical properties of calcium phosphate cement (CPC) systems of two types: (a) monocalcium phosphate monohydrate (MCPM) and calcium oxide (CaO) and (2) dicalcium phosphate dihydrate (DCPD) and calcium hydroxide [Ca(OH)$_2$]. The results were successful (based on the compressive strength (CS) and Young's modulus of both CPC formulations). The results indicated that P-chitosan-reinforced calcium phosphate cements have some good characteristics for clinical applications.

Derivatives of chitin and chitosan
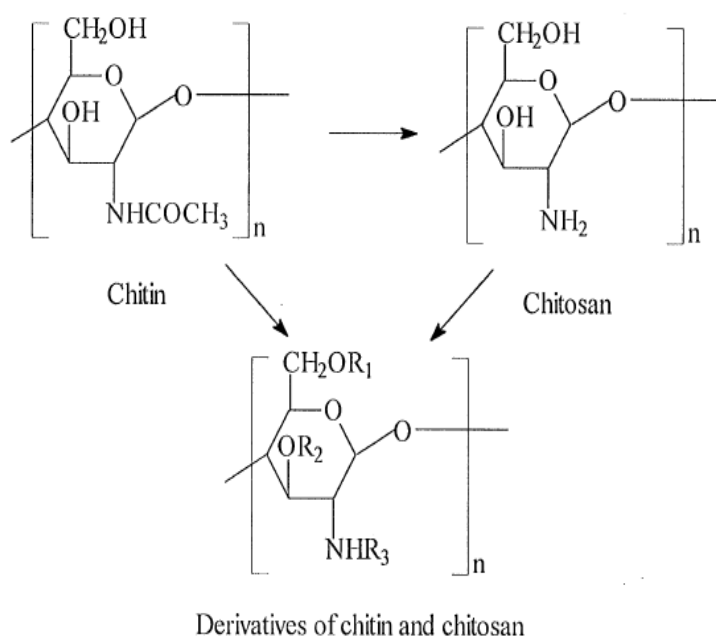
Figure 1-27. Schematic structures of chitin, chitosan and derivatives (R_1, R_2, R_3 = -COCH$_3$, -CH3, -CH$_2$COOH, -SO$_3$H, -P(O)(OH)$_2$. Reprinted with permission from Reference [126], Copyright (2001) Elsevier.

A series of phosphonate-functionalized pH-responsive chitosans were directly synthesized via Michael addition of chitosan with mono-(2-acryloyloxyethyl) phosphonate (Figure 1-28).[127] The results indicated that the inter- or intra-chain electrostatic interactions of the phosphonate-functionalized chitosans could be controlled via adjusting the solution pH, leading to the reversible conformational and phase transitions of these chitosans.
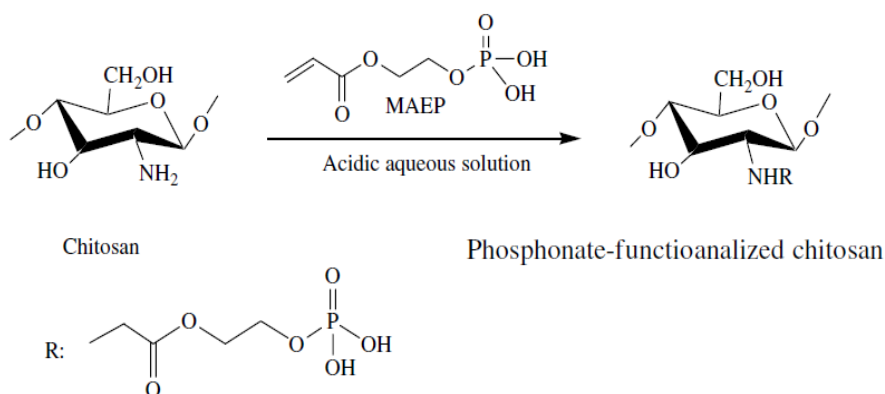
Figure 1-28. Synthesis of phosphonate-functionalized chitosan.Reprinted with permission from Reference [127], Copyright (2006) Elsevier.

New phosphorus-containing chitosan derivatives were prepared in good yield under mild conditions from 6-O-triphenylmethyl-chitosan and native chitosan. The three reactions used are thioacylation by a phosphonodithioester, alkylation by a halogeno-phosphonate, and Michael addition using a tetraethyl vinylidenebisphosphonate (Figure 1-29).[128] The modified chitosan derivatives were fully characterized and their solubilities and thermal properties were evaluated.
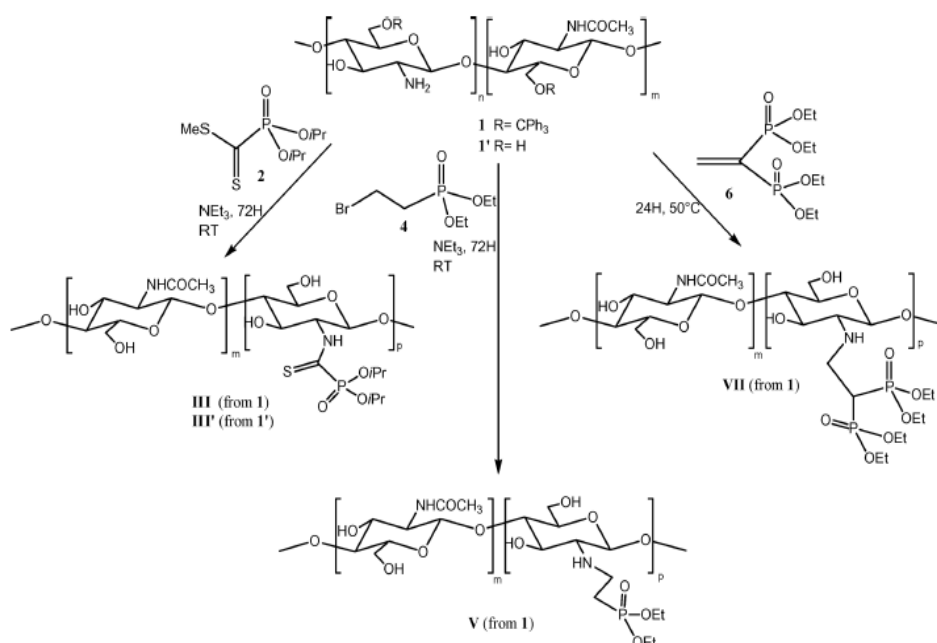
Figure 1-29. Synthesis of phosphorus-containing chitosans. Reprinted with permission from Reference [128], Copyright (2009) Taylor & Francis.

Poly[(1-vinyl-1,2,4-triazole)-co-(vinylphosphonic acid)] (poly(VTAz/VPA)) hydrogels were prepared by ^{60}Co γ-irradiation of binary mixtures of 1-vinyl 1,2,4-triazole and vinylphosphonic acid in the presence of $NaHCO_3$. The polymers form hydrogels under certain conditions (Figure 1-30).[129]
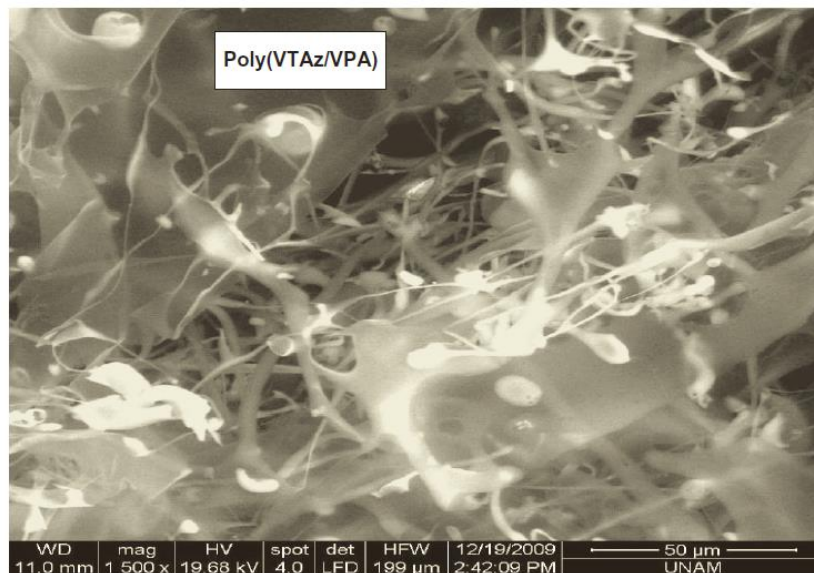
Figure 1-30. SEM image of poly(VTAz/VPA) hydrogels. Reprinted with permission from Reference [129], Copyright (2013) Taylor & Francis.

Preparation and characterization of some chelating resins, phosphonate grafted on polystyrene-divinylbenzene supports, were reported.[130] The resins were prepared by an Arbuzov-type reaction between chloromethyl polystyrene-divinylbenzene copolymers and triethylphosphite, yielding the phosphonate ester copolymer (resin A), Figure 1-31. This can be hydrolyzed by HCl to yield the phosphonate/phosphonic acid copolymer (resin B), Figure 1-31. The phosphonate resins A and B were characterized by determination of the phosphorus content, infrared spectrometry and thermal analysis. The total sorption capacity of the phosphonate ester-functionalized resin (A) and phosphonate/ phosphonic acid-functionalized resin (B) for divalent metal ions such as Ca^{2+}, Cu^{2+} and Ni^{2+} was studied in aqueous solutions. Resin A retains ~ 3.25 mg Ca^{2+}/g copolymer , 2.75 mg Cu^{2+}/g copolymer, but retains no Ni^{2+} at pH = 1. On the other hand, Resin B retains 8.46 mg Ca^{2+}/g copolymer , 7.17 mg Cu^{2+}/g copolymer, and no Ni^{2+} at pH = 1. Efficient Ni^{2+} retention was observed at pH = 7 only for the phosphonate/phosphonic acid-functionalized resin (B) at the level of 19 mg Ni^{2+}/g polymer B. Polymer A was incapable of retaining Ni^{2+} at pH = 7.
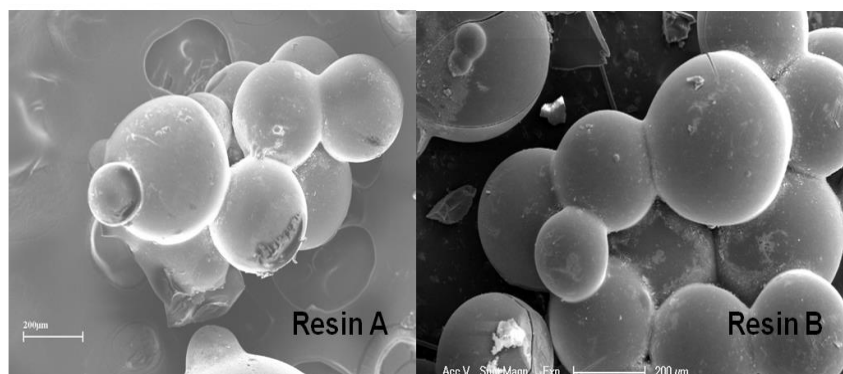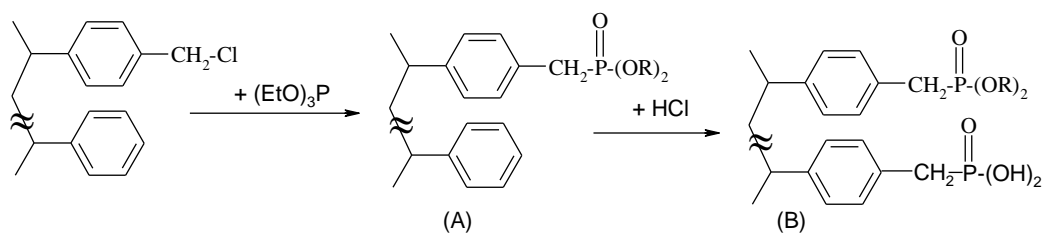
Figure 1-31. Phosphonate grafting on polystyrene-divinylbenzene supports (upper). SEM images of the produced resins (lower). The bars for both images are 200 μm. Reprinted with permission from Reference [130], Copyright (2008) American Chemical Society.

The Mannich-type reaction was used to graft methylenephosphonic acid groups to polyethyleneimine (PEI) to produce an ion exchange polymer, polyethylenimine methylenephosphonic acid (PEIMPA).[131] Removal of various heavy metal ions such as Cu^{2+}, Co^{2+}, Zn^{2+}, Ni^{2+}, and Pb^{2+} from aqueous solutions by induced flocculation of phosphonomethylated-polyethyleneimine (PPEI)–heavy metal complex with Ca^{2+} ions was studied (Figure 1-32).[132]
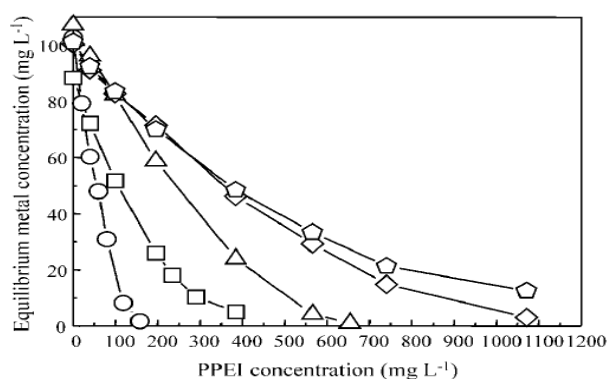
Figure 1-32. Removal of heavy metals by the PPEI–Ca2+ flocculant system. Squares = Cu, circles = Pb, triangles = zinc, rhombs = nickel, pentagons = cobalt. Reprinted with permission from Reference [132], Copyright (2002) Taylor & Francis.

Considerable floc formation accompanying metal sequestration was demonstrated, even at low initial concentration of the target metals. The PPEI–Ca^{2+} flocculant system was also effective for heavy metal scavenging purposes.

1.7 Polymers as hosts for phosphonates and metal phosphonates

Phosphonates have been studied as enzyme inhibitors. Since this action requires incorporation of the phosphonate into an enzyme matrix, we will mention a few representative examples here.

Phosphonates were found to competitively inhibit phosphotriesterase from Pseudomonas by chelating both zinc atoms of a binuclear metal center in the enzyme's active site.[133] The inhibitory properties of a series of substituted phosphonates were also measured for the bacterial phosphotriesterase. The incorporation of fluorine, hydroxyl, thiol, carbonyl, and carboxyl groups adjacent to the phosphoryl group was designed to assist in the direct coordination with one or both of the metal ions contained within the structure of the binuclear metal center. Of the compounds tested the diethyl thiomethylphosphonate was by far the most potent inhibitor identified.

Foscarnet (phosphonoformate trisodium salt), an antiviral used for the treatment of HIV and herpes virus infections, also acts as an activator or inhibitor of the metalloenzyme carbonic anhydrase (CA, EC 4.2.1.1). Interaction of the drug with 11 CA isozymes has been investigated kinetically, and the X-ray structure of its adduct with isoform I (hCA I-foscarnet complex) has been resolved (Figure 1-33).[134] The first CA inhibitor possessing a phosphonate zinc-binding group was thus evidenced, together with the factors governing recognition of such small molecules by a metalloenzyme active site (Figure 1-34). Foscarnet is also a clear-cut example of modulator of an enzyme activity which can act either as an activator or inhibitor of a CA isozyme.
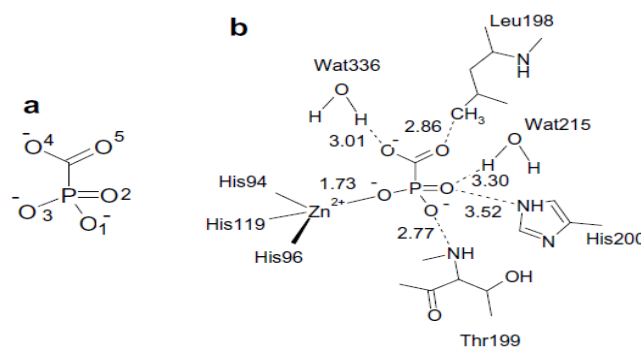
Figure 1-33. Scheme of the interactions between inhibitor (foscarnet, A) and the active site amino acid residues, B. Reprinted with permission from Reference [134], Copyright (2007) Elsevier.
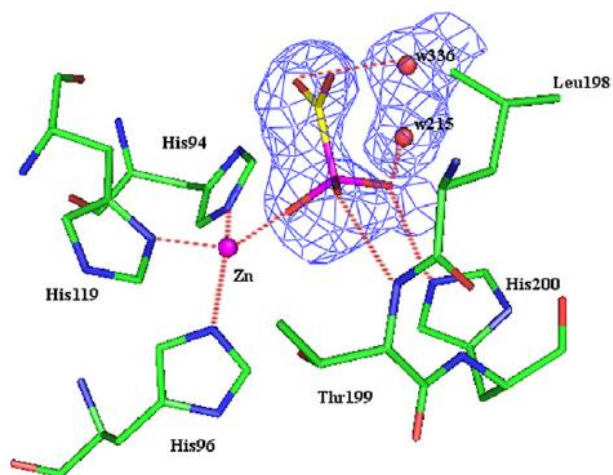
Figure 1-34. Electron density map showing the zinc ion coordinated by three histidine ligands and a phosphonate oxygen. Reprinted with permission from Reference [134], Copyright (2007) Elsevier.

Oldfield et al. investigated the docking of a variety of inhibitors and substrates to the isoprene biosynthesis pathway enzymes farnesyl diphosphate synthase (FPPS), isopentenyl diphosphate/dimethylallyl diphosphate isomerase (IPPI) and deoxyxylulose-5-phosphate reductoisomerase (DXR) using the Lamarckian genetic alogorithm program, AutoDock.[135] The structures of three isoprenoid diphosphates docked to the FPPS enzyme reveal strong electrostatic interactions with Mg^{2+}, lysine and arginine active site residues (Figure 1-35).
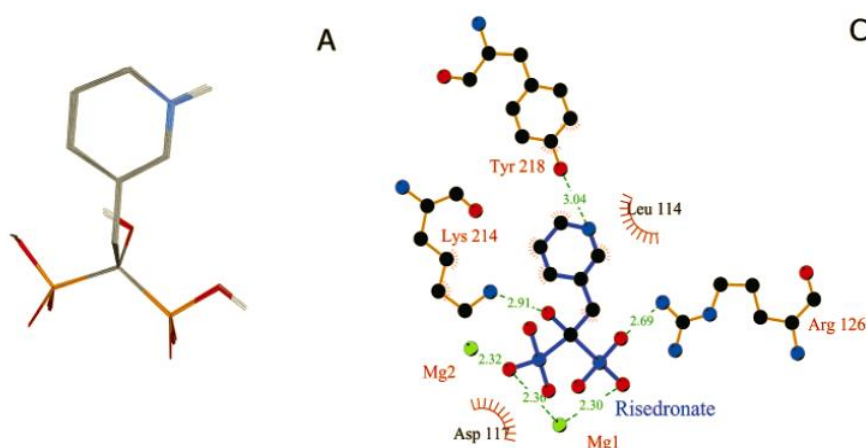
Figure 1-35. Docked structures and Ligplot interactions between bisphosphonate inhibitors and an avian FPPS.A, Risedronate, 10 lowest energy conformations.Ligplot diagram showing the main interactions between risedronate and FPPS.Reprinted with permission from Reference [135], Copyright (2004) American Chemical Society.

Similar results are obtained with the docking of four IPPI inhibitors to the IPPI enzyme. Bisphosphonate inhibitors are found to bind to the allylic binding sites in both eukaryotic and prokaryotic FPPSs, in good accord with recent crystallographic results (Figure 1-36). Overall, these results show for the first time that the geometries of a broad variety of phosphorus-containing inhibitors and substrates of isoprene biosynthesis pathway enzymes can be well predicted by using computational methods, which can be expected to facilitate the design of novel inhibitors of these enzymes.
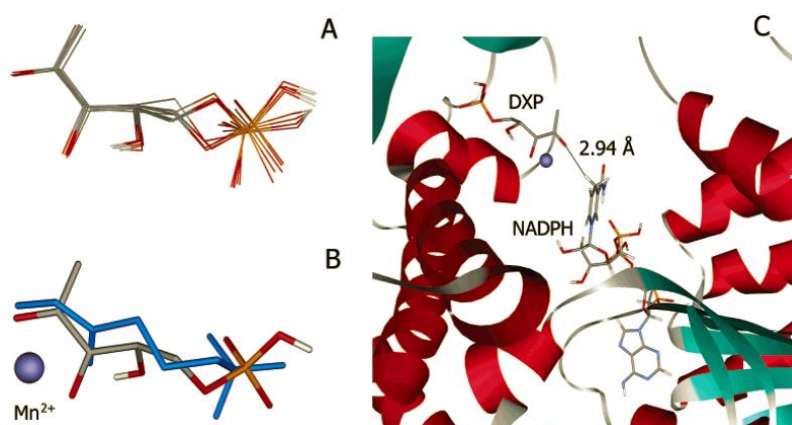
Figure 1-36. Docked structures of deoxyxylulose-5-phosphate (left) bound to NADPH-DXR (right). Reprinted with permission from Reference [135], Copyright (2004) American Chemical Society.

Another detailed inhibition study of five carbonic anhydrase (CA, EC 4.2.1.1) isozymes with inorganic phosphates, carbamoyl phosphate, the antiviral phosphonate foscarnet as well as formate was reported.[136] The membrane-associated isozyme hCA IV was the most sensitive to inhibition byphosphates/phosphonates. Foscarnet was the best inhibitor of this isozyme highly abundant in the kidneys, which may explain some of the renal side effects of the drug.

Thus far, phosphonate incorporation of "free" phosphonates (no metals) into organic matrices was presented. In the remaining part of this section we will present incorporation of metal phosphonates into selected organic and inorganic matrices.

Eddaoudi et al. reported the successful growth of highly-crystalline homogeneous MOF thin films of HKUST-1 and ZIF-8 on mesoporous silica foam, by employing a layer-by-layer (LBL) method.[137] The newly-constructed MOF hybrid materials on mesoporous silica foam, were characterized and evaluated using various techniques (PXRD, SEM and TEM) (Figure 1-37).
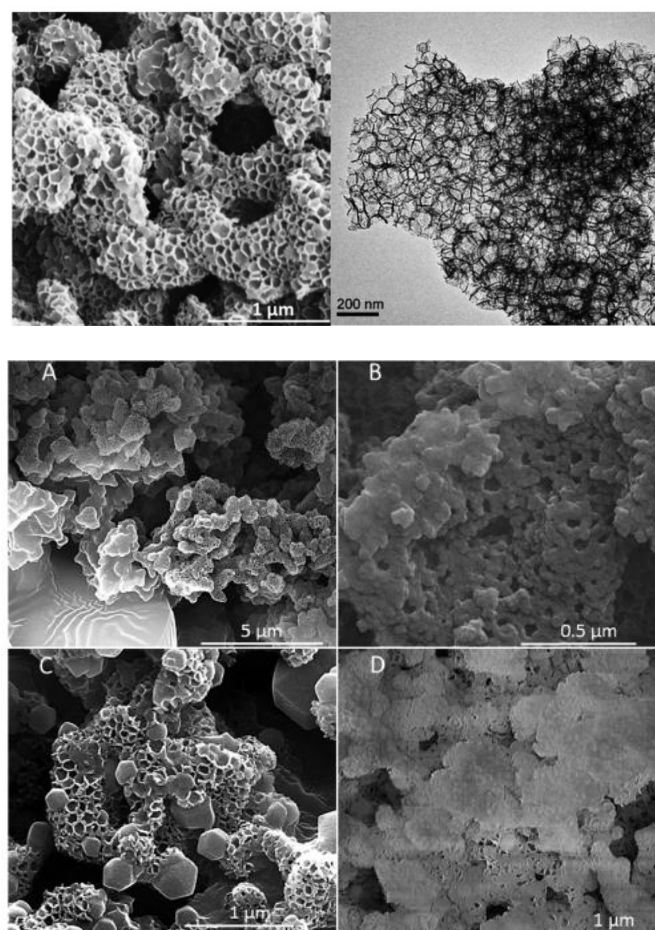
Figure 1-37. SEM images of the mesoporous silica foam, SEM (upper left) and TEM (upper right). SEM images of HKUST-1 grown on silica foam (middle left and right). SEM images of ZIF-8 grown on silica foam (lower left and right). Reprinted with permission from Reference [137], Copyright (2012) Royal Society of Chemistry.

This study confirms the unique potential of the LBL method for the controlled growth of desired MOF thin films on various substrates, which permits rational construction of hierarchical hybrid porous systems for given applications. The ability to control and direct the growth of MOF thin films on confined surfaces, using the stepwise LBL method, creates new opportunities for new prospective applications, such as hybrid systems construction of pure MOF-based membranes, as well as coating a variety of polymers for gas separation applications.

Hydrolysis and condensation reactions of diethylphosphato-ethyltriethoxysilane (SiP) and a mixture of SiP and tetraethoxysilane (TEOS) have been studied in ethanol and N-methylacetamide (NMA) as solvent. The reactions were investigated by high resolution ^{29}Si NMR. The hydrolyzed and condensed species, from SiP and TEOS were identified and quantified as a function of reaction

time. The influence of the amide medium as well as the catalytic effect of the phosphonate function of SiP on TEOS hydrolysis were established.[138]

A zinc silico-phenylphosphonate was synthesized.[139] The substitution of phosphorus by silicon induced a deficit of the positive charges that were balanced by cations located in the interlayer space. The XRD powder diffraction pattern corresponds to a lamellar structure and exhibits a series of sharp peaks assigned to the series (*00l*) reflections with a d_{001} of 2 nm. SEM micrographs of this material show a morphology similar to the one observed for clay minerals and especially smectites ''gypsum-like morphology'' (Figure 1-38). TEM images exhibit a rods' arrangement for the layered materials (Figure 1-38). Q4 sites were identified by ^{29}Si solid state NMR indicating a full polymerization of silica.
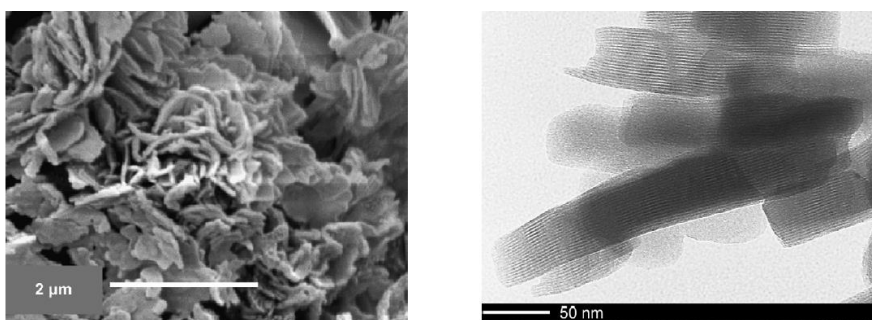
Figure 1-38. SEM (left) and TEM images (right) of the zinc silico-phenylphosphonate. Reprinted with permission from Reference [139], Copyright (2007) Elsevier.

Thermally stable proton-conducting composite sheets of 50–100 μm thick have been prepared from phosphosilicate gel (P/Si = 1 molar ratio) powders and polyimide precursor.[140],[141] Polyimide was selected as an organic polymer matrix because of its excellent thermal stability and good sheet-forming property. Proton conductivity, mechanical properties and chemical durability of the resultant composite sheets in the low and medium-temperature range have been examined. In addition, a single test fuel cell has been fabricated using the composite sheet as an electrolyte.

1.8 Applications

The importance of phosphonic acids and derivatives in the field of supramolecular chemistry, crystal growth and materials chemistry has been well recognized.[142],[143][144],[145],

[146],[147],[148],[149] Besides basic chemistry, phosphonates play a significant role in several other technologically/industrially important areas, such as water treatment,[150]oilfield drilling,[151],[152],[153],[154],[155],[156],[157],[158]minerals processing, [159],[160] corrosion control,[161],[162],[163],[164],[165],[166] metal complexation and sequestration,[167],[168] dental materials,[169],[170],[171],[172] bone targeting,[173],[174],[175], [176] cancer treatment,[177],[178],[179] etc.

1.8.1 Proton Conductivity.

Solid-state ion conductors are an important class of materials because of their use as electrolytes in batteries and fuel cells, gas sensors, etc. The mechanism of ion conduction in solids depends on structural considerations. Specific important factors are concentration, mobility, and charge of conductive ions. Control of the spatial distribution and dynamic behavior of target ions in solids are also significant. Ion conductivity is also dependent on temperature because ions need to overcome the activation energy between the hopping sites in various structures. Commonly, organic polymers exhibit ion conductivity below 200 °C and inorganic materials (such as metal oxides, and metal halides) above 400 °C.

In this section, we will deal with proton conductivity exhibited by phosphonate-containing materials (either organic or hybrid). A number of reviews have appeared on the subject.[180],[181],[182],[183]

A novel proton conducting polymer blend was prepared by mixing poly(vinylphosphonic acid) (PVPA) with poly(1-vinylimidazole) (PVI) at various stoichiometric ratios via changing molar ratio of monomer repeating unit to achieve the highest protonation. The network was used for immobilization of invertase, and then the enzyme activity was studied. The results reveal that the most stable and highly proton conducting polymer network may play a pioneer role in the biosensors applications as given by FT-IR, elemental analysis, impedance spectroscopy and storage stability experiments.[184]

Sulfophenylphosphonic acid was used for the synthesis of two zirconium salts, $Zr(HO_3SC_6H_4PO_3)_2 \cdot 2H_2O$ and $Zr(HPO_4)_{0.7}(HO_3SC_6H_4PO_3)_{1.3} \cdot 2H_2O$.[185] Powder patterns indicate that these layered compounds are structurally derived from alpha modification of zirconium phosphate monohydrate, in which the zirconium atoms are octahedrally coordinated by six oxygen atoms of the phosphate groups. In the case of phosphonates, the fourth oxygen atom of the

phosphate group is replaced by an organic residue which points into the interlayer space. In $Zr(HPO_4)_{0.7}(HO_3SC_6H_4PO_3)_{1.3} \cdot 2H_2O$ the incorporation of the phosphate group causes structural disorder in the whole system, increases the amount of "labile" protons and changes their behavior. This is in agreement with the increased conductivity of this compound. The conductivity of both compounds increases from 0.028 to 0.063 $S \cdot cm^{-1}$ in the relative humidity (RH) range 50–90 %.

Recently, two similar series of lanthanide carboxyphosphonates were synthesized and structurally characterized. [186] The ligand used was hydroxyphosphonoacetic acid (HPAA). The presence of 1D channels, filled with water molecules, in the crystal structures of both series (see Figure 1-39), suggests the possibility of proton conductivity behaviour.
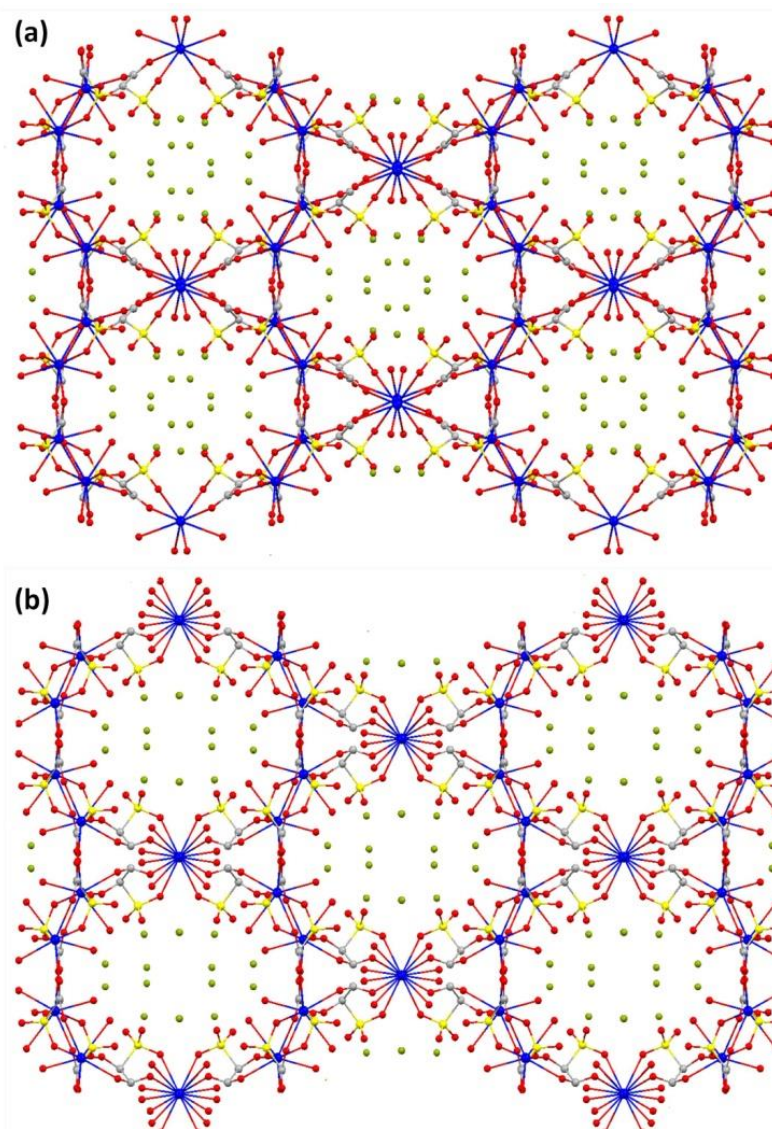
Figure 1-39. Lanthanide hybrids showing the 1D channels along the c-axis filled with lattice waters for: (a) La-HPAA-II and (b) La-HPAA-I. The lattice water molecules occupying the channels are as single dots. Reprinted with permission from Reference[186], Copyright (2012) American Chemical Society.

Furthermore, there are certain structural features that make these good candidates as proton-conductors at room temperature. These include the –POH groups pointing towards the interior of the channels, the network of hydrogen bonds within the channels and the proximity between the lattice water molecules. Therefore, conductivity studies have been carried out for one representative member of each series.

When GdHPA-II is exposed to the highest % RH value of 98 %, a spike is observed which has an associated capacitance of ~1 μF. Since the spike is inclined to the Z´ axis by ~ 70°, it indicates a partial-blocking electrode response that allows limited diffusion; therefore, the conducting species must be ionic, *i.e.* H$^+$ ions. The total pellet resistance, R$_T$, was obtained from the intercept of the spike and/or the arc (low frequency end) on the Z´ axis. At 98 % RH and T = 21 °C, σ$_T$ was 3.2 × 10^{-4} S·cm^{-1}.

Shimizu et al. have reported a Zn material with the ligand 1,3,5- benzenetriphosphonic acid.[187] At 90% relative humidity and 85 °C, the proton conductivity reaches 2.1 × 10^{-2} S·cm^{-1}. This is the highest proton conductivity reported for a phosphonate-based MOF.

A new flexible ultramicroporous solid, La(H$_5$DTMP)·7H$_2$O, has been crystallized at room temperature using the tetraphosphonic acid H$_8$DTMP, hexamethylenediamine-*N,N,N',N'*-*tetrakis*(methylenephosphonic acid).[188] Its crystal structure, solved by synchrotron powder X-ray diffraction, is characterised by a 3D pillared open-framework containing 1D channels filled with water (Figure 1-40).
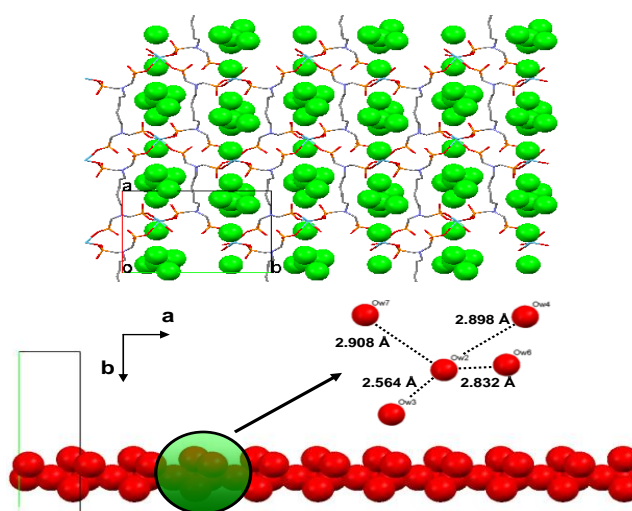
Figure 1-40. Upper: 3D framework for La(H$_5$DTMP)·7H$_2$O showing the 1D channels running along the c-axis and defined by 30-membered rings. The water molecules within the channels are depicted as exaggerated spheres. Lower: One-dimensional chain of hydrogen-bonded lattice water molecules within the channel along the *c* axis. H-bonding distances in the 5-water cluster are shown in the inset.

Upon dehydration, a new related crystalline phase, La(H$_5$DTMP) is formed. Partial rehydration of La(H$_5$DTMP) led to La(H$_5$DTMP)·2H$_2$O. These new phases contain highly corrugated layers showing different degrees of conformational flexibility of the long organic chain. Impedance data indicates that proton-conductivity takes place in La(H$_5$DTMP)·7H$_2$O with a value of 8·10^{-3} S·cm^{-1} at 286 K and 99 % of relative humidity RH.

A new multifunctional light hybrid, Mg(H$_6$ODTMP)·2H$_2$O(DMF)$_{0.5}$, was synthesized using the tetraphosphonic acid H$_8$ODTMP, octamethylenediamine-*N,N,N',N'-tetrakis* (methylenephosphonic acid), by high-throughput methodology. Its crystal structure, solved by synchrotron powder X-ray diffraction, is characterized by a 3D pillared open-framework containing cross-linked 1D channels filled with water and DMF (Figure 1-41).[189] Upon H$_2$O and DMF removal and subsequent rehydration, Mg(H$_6$ODTMP)·6H$_2$O is formed. These processes take place through crystalline-quasi amorphous-crystalline transformations, during which the integrity of the framework is maintained. Impedance data indicates that Mg(H$_6$ODTMP)·6H$_2$O has high proton conductivity, σ = 1.6 10^{-3} Scm^{-1} at T = 292 K at ~100% relative humidity, with an activation energy of 0.31 eV.
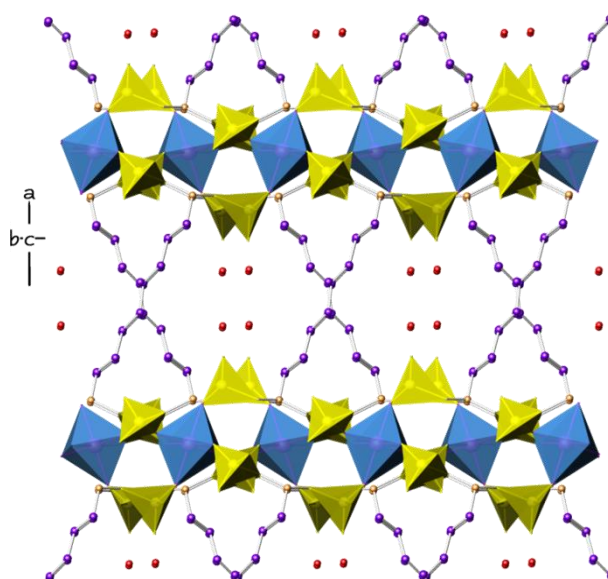
Figure 1-41. Crystal structure of Mg(H$_6$ODTMP)·2H$_2$O(DMF)$_{0.5}$. The framework constructed as MgO$_6$ and PO$_4$ polyhedra and ball-and-stick for the organic ligand, with lattice water molecules shown as red spheres, creating 1D channels vertical to the page. molecules are not shown. Reprinted with permission from Reference 152, Copyright (2012) American Chemical Society.

A new 3D metal−organic framework, $[La(H_5L)(H_2O)_4]$, L = 1,2,4,5-tetrakisphosphono methylbenzene), was reported which conducts protons above 10^{-3} Scm^{-1} at 60 °C and 98 % relative humidity.[190] The MOF contains free phosphonic acid groups, shows high humidity stability, and resists swelling in the presence of hydration. Channels filled with crystallographically located water and acidic groups are also observed.

Shimizu has published a comprehensive review on proton conductivity in metal phosphonate frameworks, which provides useful further reading.[191]

1.8.2 Metal Ion Absorption.

A great deal of research has been performed with a variety of materials that absorb metal ions from aqueous solutions, with obvious environmental implications.[192] In this section we will present selected phosphonate-based systems that are capable for metal ion absorption.

A flexible open-framework sodium-lanthanum(III) tetrakis-phosphonate, $NaLa[(HO_3P)_2$-CH-C_6H_4-$CH(PO_3H)_2]\cdot 4H_2O$ was published by Bein *et al*.[193]They studied the exceptional ion-exchange selectivity between the Na^+ ions of the material and alkaline earth, alkaline and selected transition metal ions. Exchange between the hosted Na^+ ions and other monovalent ions with ionic radii ranging from 0.76 A (Li^+) to 1.52 A (Rb^+) was accomplished. The divalent ions with approximately the same size did not appear to be exchanged.

Also, the $[Pb_7(HEDTP)(H_2O)]\cdot 7H_2O$ and $[Zn(H_4EDTP)]\cdot 2H_2O$ $[H_8EDTP = N,N,N',N'$-ethylenediamine-*tetrakis*(methylenephosphonic acid)] showed very high adsorption (> 96 %) of Fe^{3+} ions in aqueous medium. Excellent ion adsorption performance was also found for other divalent ions such as Ca^{2+}, Cr^{2+}, Mn^{2+}, Cu^{2+}, Zn^{2+} and Cd^{2+}.[194]

Polyethyleneimine Methylenephosphonic Acid (PEIMPA) was investigated in liquid – solid extraction of a mixture of Cd^{2+}, Co^{2+}, Cu^{2+}, Fe^{3+}, Ni^{2+}, Pb^{2+}, and Zn^{2+} cations from a mineral residue of zinc ore dissolved in nitric acid. The selectivity of this polymer was studied as a function of pH. PEIMPA can adsorb much higher amounts of Fe^{3+} ion than Cd^{2+}, Co^{2+}, Cu^{2+}, Ni^{2+}, Pb^{2+}, and Zn^{2+} ions. The recovery of Fe^{3+} is almost quantitative.[195]

A polyelectrolyte complex of PEIMPA (polyanion) and PEI (polycation) was found useful for the removal of various heavy metal ions such as Cu^{2+}, Co^{2+}, Zn^{2+}, Ni^{2+} and Pb^{2+} from aqueous solutions by the co-precipitation method. Heavy metal binding with PEIMPA was initially allowed to occur and then upon equilibration, PEI was added to initiate precipitation of the polyelectrolyte complex together with the heavy metal ion. The PEIMPA–PEI system was found effective for

heavy metal scavenging purposes even in the presence of high concentrations of non-transition metal ions like Na^+. Heavy metal concentration may be reduced beyond emission standards for industrial wastewaters. The PPEI–PEI polyelectrolyte complex was found to be more effective than traditional precipitation methods for the treatment of a representative electroless Ni plating waste solution.[196]

PEIMPA was used as an effective sorbent for solid-phase extraction of Pb^{2+} ions from an aqueous solution.[197] Conditions for effective sorption are optimized with respect to different experimental parameters in a batch process. The results showed that the amount of extraction decreases with solution pH in the range between 3.5 and 5.8. The sorption capacity is 609 mg·g^{-1}. Also, PEIMPA was tested in the recovery of Pb^{2+} from a synthesized binary solution of Pb^{2+}–Zn^{2+} and from real Zn^{2+}-electrolyzed wastewaters. The presence of Cd^{2+}, Co^{2+}, Cu^{2+}, Fe^{3+}, Ni^{2+}, and Zn^{2+} in large concentrations has a significantly negative effect on extraction properties (Figure 1-42).
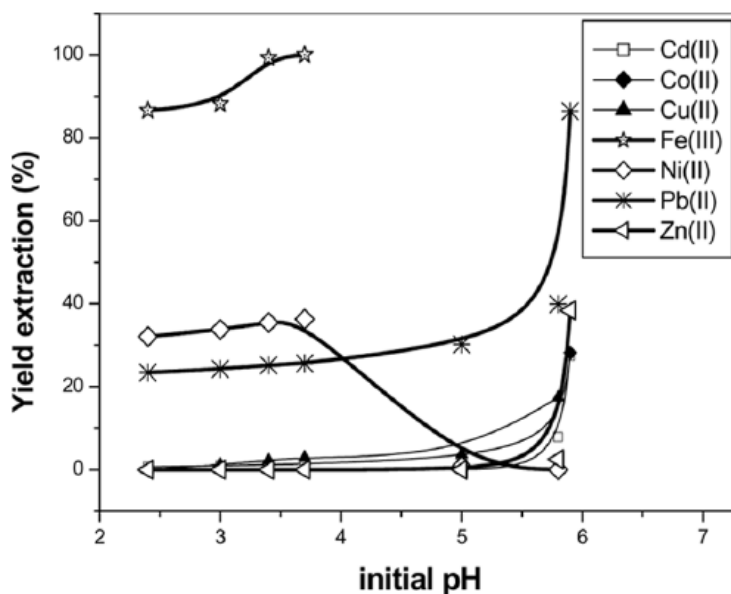
Figure 1-42. Recovery of indicated metal ions by PEIMPA, as a function of pH. Reprinted with permission from Reference [197], Copyright (2009) Taylor & Francis.

A very promising application specially for treatment of some technological solution and waste comes from some new Sn^{4+}nitrilo-*tris*(methylenephosphonates). These materials have been synthesized by a gel method in granular form (spherical beads).[198] The ion exchange behavior between the ligands and alkali, alkaline earth and some transition metal ions was studied. It is worth

mentioning that even at very acidic conditions the ion exchangers operate efficiently because of the highly acidic adsorption sites.

Some phosphonic acids have the ability to graft onto polymeric matrices. Popa *et al.* synthesized a group of resin-type materials for the removal of metal ions from aqueous solutions.[130] An Arbusov-type reaction between chloromethyl polystyrene-divinylbenzene copolymers and triethylphosphite took place and led to phosphonate ester copolymer (resin A). In the presence of HCl resin A hydrolyzes to yield the phosphonic acid copolymer (resin B). Then, the total sorption capacity in aqueous solutions of the two resins was studied for divalent metal ions such as Ca^{2+}, Cu^{2+} and Ni^{2+}. Resin A retains ~3.25 mg Ca^{2+}/g copolymer, 2.75 mg Cu^{2+}/g copolymer, but retains no Ni^{2+} at pH=1. Resin B retains 8.46 mg Ca^{2+}/g copolymer, 7.17 mg Cu^{2+}/g copolymer and no Ni^{2+} at pH = 1. Efficient Ni^{2+} retention is observed at pH = 7 only for the resin B and at the level of 19 mg Ni^{2+}/g polymer. The first polymer was incapable of retaining Ni^{2+} at pH = 7. A number of proposed metal binding modes were proposed for these phosphonate polymers, Figure 1-43.
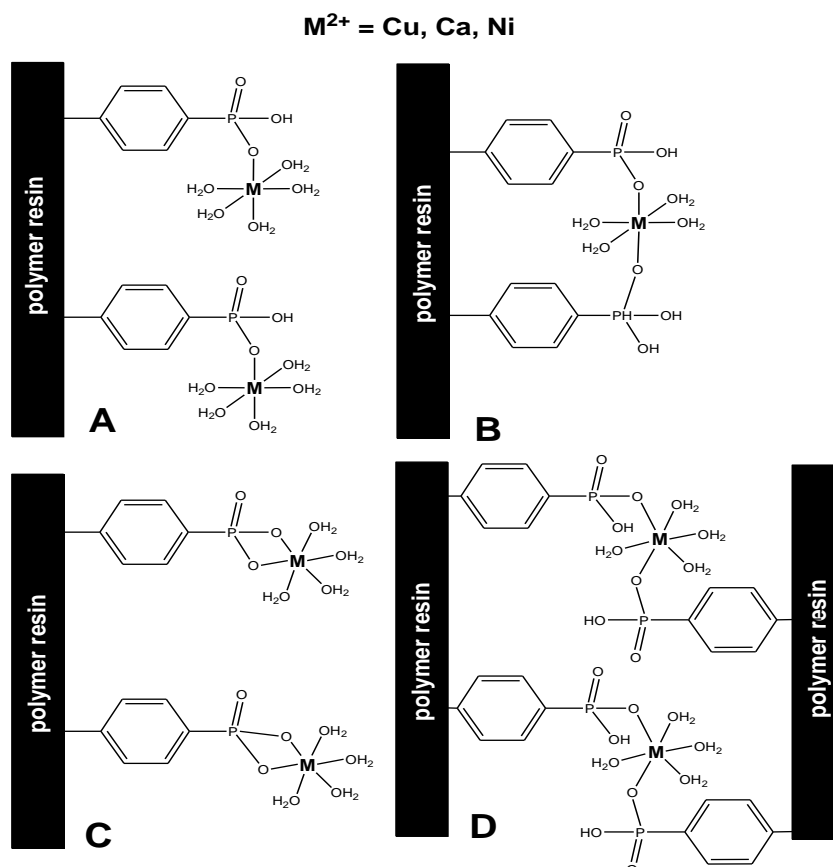
Figure 1-43. Various metal binding modes of the phosphonate resins. A: monodentate terminal binding, B: monodentate chelating binding, C: bidentate chelating binding, D: monodentate bridging binding. Reprinted with permission from Reference [130], Copyright (2008) (2008) American Chemical Society.

A three-dimensionally ordered macroporous titanium phosphonate material was synthesized by an inverse opal method using 1-hydroxy ethylidene-1,1-diphosphonic acid (HEDP). This material was tested for the adsorption of Cu^{2+}, Cd^{2+}, and Pb^{2+}, showing 10-20 % removal efficiency, depending on metal ion.[199]

The same researchers reported an improvement by synthesizing organic–inorganic hybrid materials of porous titania–phosphonate using tetra- or penta-phosphonates, ethylenediamine-tetrakis(methylenephosphonic acid) (EDTMP) and diethylenetriamine-pentakis(methylenephosphonic acid) (DTPMP).[200] These were anchored to the titania network homogeneously. The synthesized titania–phosphonate hybrids possess irregular mesoporosity formed by the assembly of nanoparticles in a crystalline anatase phase. The Titania-DTPMP sample achieved the highest adsorption capacity for each metal ion (Cu^{2+}, Cd^{2+}, and Pb^{2+}), probably due to the phosphonate binding sites than in Titania-EDTMP: for Cd(II) up to 88.75 and 89.17%, respectively.

1.8.3 Controlled release of phosphonate pharmaceuticals.

Prodrugs of phosphonoformic acid (PFA), an anti-viral agent used clinically as the trisodium salt (foscarnet), are of interest due to the low bioavailability of the parent drug, which severely limits its utility. Neutral PFA triesters are known to be susceptible to P–C bond cleavage under hydrolytic de-esterification conditions, and it was previously found that P,C-dimethyl PFA P–N conjugates with amino acid ethyl esters did not release PFA at pH 7, and could not be fully deprotected under either acid or basic conditions, which led, respectively, to premature cleavage of the P–N linkage (with incomplete deprotection of the PFA ester moiety), or to P–C cleavage.[201] Fully deprotected PFA-amino acid P–N conjugates (compounds 4a-c in Figure 44) can be prepared via coupling of C-methyl PFA dianion 2 (in Figure 44) with C-ethyl-protected amino acids using aqueous EDC, which gives a stable monoanionic intermediate 3 (in Figure 1-44) that resists P–C cleavage during subsequent alkaline deprotection of the two carboxylate ester groups. At 37 °C, the resulting new PFA-amino acid (Val, Leu, Phe) conjugates (4a–c) undergo P–N cleavage near neutral pH, cleanly releasing PFA. A kinetic investigation of 4a hydrolysis at pH values 6.7, 7.2, and 8.5 showed that PFA release was first-order in [4a] with respective $t_{1/2}$ values of 1.4, 3.8, and 10.6 h.
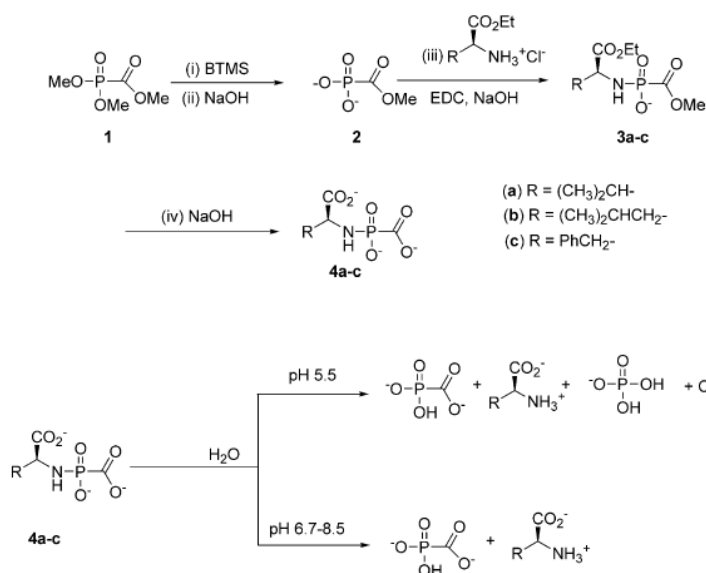
Figure 1-44. Hydrolytic processes of the conjugates at various pH values. Reprinted with permission from Reference [201], Copyright (2004) Elsevier.

Foscarnet inhibits two RNA polymerases but with different patterns of inhibition. Influenza virus RNA polymerase is inhibited in a non-competitive manner with respect to nucleoside triphosphates, apart from GTP which gives a mixed pattern of inhibition. It was also found that initiation of influenza virus mRNA synthesis by the polymerase, when primed by exogenous mRNA, could occur in the presence of foscarnet but that the elongation was inhibited.[202] This block of mRNA formation by foscarnet occurred during or after the synthesis of the 12 nucleotide-long conserved sequence, ending at a GMP, found at the 5'-end of the viral message (Figure 1-45).
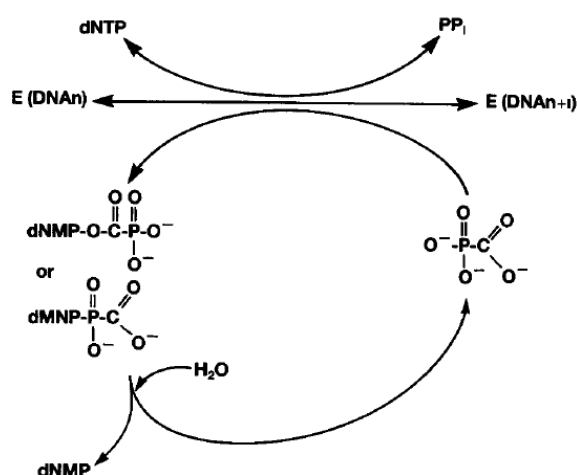
Figure 1-45. Hypothetical model for inhibition of DNA polymerase (E) by foscarnet. Two different reaction products can be envisioned for the degradative reaction (none was isolated). Reprinted with permission from Reference [202], Copyright (1989) Elsevier.

Pamidronate, one of the therapeutic bisphosphonates for osteopenic diseases, directly inhibits bone healing in the traumatic defect model of the rabbit calvaria. The inhibition effect of pamidronate on bone healing was supported by radiographic and histological analyses. Radiographic analysis showed that pamidronate combined with PLGA (poly L-lactide-*co*-glycolide) had less bone formation than that of the defect only or PLGA only group. Histological analysis further confirmed that pamidronate inhibited bone healing.[203]

The intercalation of 1-hydroxyethylidene-1,1-diphosphonic acid (HEDP), which is also a drug for osteoporosis (known as etidronic acid), in layered double hydroxide (LDH) was examined with the goal of developing a novel drug delivery system of HEDP (Figure 46). To prevent side reactions, the intercalation reaction was carried out at pH 4–6. The uptake of HEDP was determined as 3.5 mmol·g^{-1} of LDH, and the interlayer distance increased from 7.8 to 13.0 Å. The HEDP-release profiles into K_2CO_3 aqueous solution and into various buffer solutions were also examined.[204]
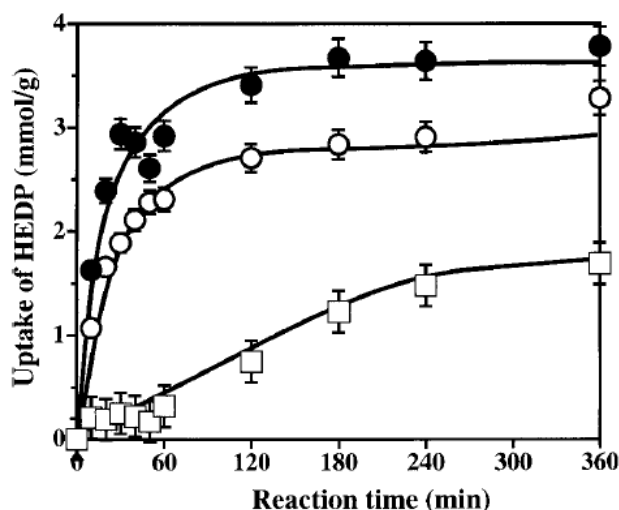
Figure 1-46. Uptake of HEDP by three different LDH materials (full circles LDH(Cl), empty circles LDH(CO3), squares LDH calcined at 500 °C). Reprinted with permission from Reference [204], Copyright (2003) Wiley.

Calcification is the principal cause of the clinical failure of bioprosthetic heart valves (BHV), fabricated from glutaraldehyde-treated porcine valves of bovine pericardium. A study examined the dose-response of local controlled-release disodium HEDP therapy for BHV calcification and its mechanism of action.[205] Controlled release of HEDP from ethylene-vinyl acetate matrices was regulated by co-incorporation of the insert filler inulin, and subdermal calcification of BHV cusps was studied with the co-implantation of these matrices in rats (Figure 1-

47). Subdermal BHV tissue calcification was inhibited in vivo for 7, 60, and 84 days, without any adverse effects. At 84 days matrices (0.2, 2 and 20% w/w HEDP) co-implanted with BHV resulted in explant calcification levels of 210.4, 39.1, and 11.7 pg/mg in comparison to control values of 213.2 pg/mg (a level equivalent to that of clinically failed BHV). The diffusion coefficient of HEDP through BHV was 0.8×10^{-10} cm^2/s reflecting low tissue permeability and high affinity. It was concluded that both in vitro and in vivo release of HEDP from the 20 % w/w HEDP matrices was suitable to inhibit BHV calcification and that this effect is most likely due to interaction of HEDP with the BHV tissue surface.
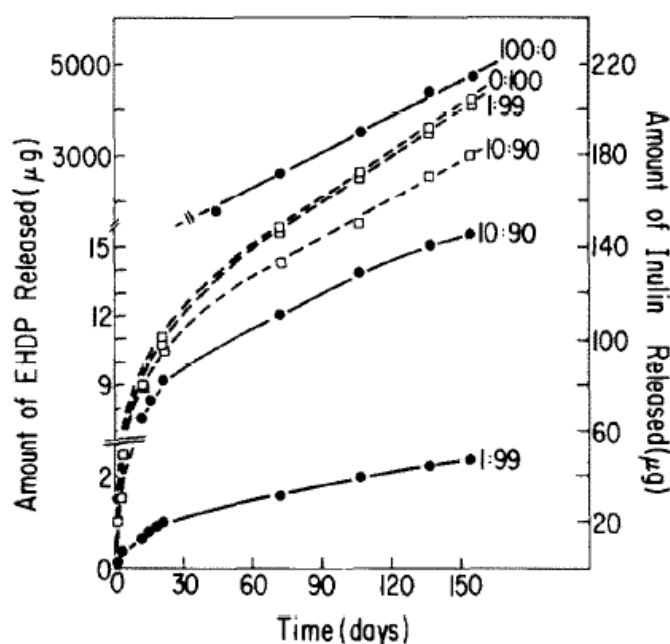
Figure 1-47. HEDP and inulin release profiles. HEDP:inulin ratio 0:100, 1:99, 10:90, 100:0. Reprinted with permission from Reference [205], Copyright (1986) Elsevier.

The controlled release of etidronic acid (HEDP), immobilized onto cationic polymeric matrices, such as polyethyleneimine (PEI) or cationic inulin (CATIN) was studied.[206] Several CATIN- and PEI-etidronate composites were synthesized at various pH regions and characterized. Tablets with starch as the excipient containing the active ingredient (polymer-etidronate composite) were prepared (Figure 1-48 left) and the controlled release of etidronate was studied at aqueous solutions of pH 3 (to mimic the pH of the stomach) for 8 hours. All studied composites showed a delayed etidronate release in the first 4 hours (Figure 1-48 right), compared to the "control" (a tablet containing only starch and etidronic acid, without the polymer).
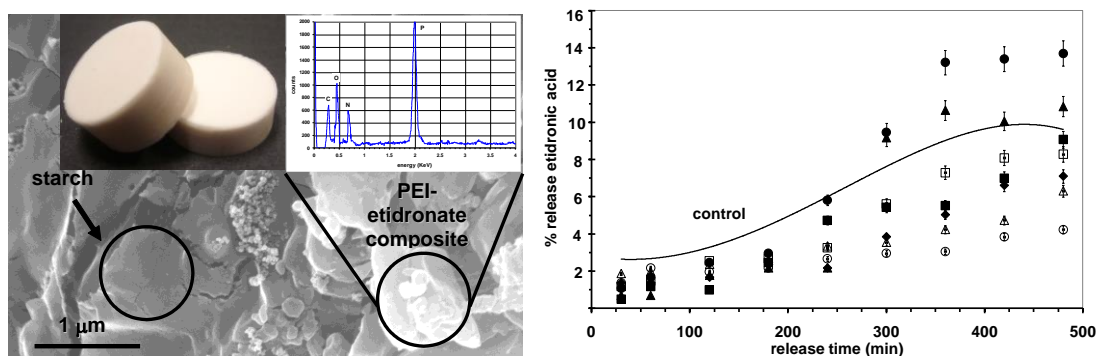
Figure 1-48. Left: Typical tablet containing polymer-etidronate active ingredient (upper left). SEM image of the tablet surface (lower). Surface particles of the PEI-etidronate composite are highlighted. EDS spectrum of the tablet showing the presence of P (from etidronic acid) and C, O, N from the polymer.Right:Controlled release curves for the PEI-etidronate and CATIN-etidronate composites. For clarity purposes the average release of free etidronic acid from a starch-only tablet (control) is presented as a continuous line. Filled symbols represent the release of etidronic acid from CATIN matrices and hollow symbols show the release from PEI matrices. Specifically: □ PEI (from pH 3), ○ PEI (from pH 4), △ PEI (from pH 5), ■ CATIN-3 (from pH 9), ♦ CATIN-2 (from pH 7), • CATIN-3 (from pH 7), ▲ CATIN-1 (from pH 9). Reprinted with permission from Reference [206], Copyright (2011) Americal Chemical Society.

1.8.4 Corrosion protection by metal phosphonate coatings.

Many phosphonic acids are used as corrosion inhibitors in the interdisciplinary field of corrosion science. The phosphonate based corrosion inhibitors are effective in decreasing metallic corrosion,[207] especially near neutral conditions by the formation of poorly soluble metal phosphonate compounds with the existing metal ions of these aqueous solutions. The necessity to develop inhibitors that are free from carcinogenic, chromates,[208]nitrates, nitrites, etc, fueled the interest in the area of phosphonic acids. Commonly the procedure is as follows. The phosphonate is introduced into the system in the acid form or as an alkali metal soluble salt. It then rapidly forms stable complexes with metal cations, such as Ca, Mg, Sr, or Ba that pre-exist in the process stream. Certain times, cations such as Zn^{2+} are purposely added to the system. A few representative examples follow.

For the protection of carbon steel a combination of Zn^{2+} and HDTMP in a 1:1 molar ratio offers excellent corrosion protection.[67] The corrosion rate for the control (absence of any additives) is 7.28 mm/year, whereas the corrosion rate for the Zn-HDTMP protected sample is 2.11 mm/year. That is a ~170% reduction in corrosion rate. The FT-IR, XRF and EDS studies show that the "anticorrosion" film is a material composed of Zn^{2+} (externally added) and P (from HDTMP) in an approximate 1:4 ratio, as expected.

Other metal phosphonate systems have also been reported. They include Sr/Ba-HPAA,[58],[59] Ca-HPAA,[64] Sr/Ba-HDTMP,[60] Ca-EDTMP,[62] Ca-PBTC.[56] Demadis et al. have published a series of reviews on the subject, which offer additional information and further literature.[209],[210],[211],[212],[213]

1.8.5 Gas storage.

The last decades have witnessed the explosion in the area of Metal Organic Frameworks (MOFs). Many microporous 3D framework structures, thermally stable up to 700 K, have been discovered. Among the most readily recognizable are certain carboxylate-based frameworks such as MOF-5,[214] MIL-100[215] and HKUST-1.[216] These materials show remarkable adsorption properties, very high surface areas, flexibility in their framework and unstaturated metal adsorption sites. There are also porous MOFs based on amines, such as zeolitic imidazoles,[217] amino acids,[218]and amino-carboxylates.[219]

Among the first organic-inorganic adsorbents investigated were also metal-phosphonate materials which offer an alternative set of chemical and structural possibilities, but until recently none of them was found to possess pores larger than 6 Å (in comparison to carboxylate-based materials that have pores up to ~ 20 Å). The competitive property of phosphonates is that the O_3P-C bond is stable at elevated temperatures. Examples include the syntheses of divalent metal piperazine-bis(methylenephosphonate)s of Co(II), Mn(II), Fe(II) and Ni(II), that showed remarkable pore volumes.[220] Other reactions with this ligand and Fe(II), Co(II), Ni(II) acetates at pH values below 6.5 led to porous solids. The structure can be described as inorganic columns of helical chains of edge-sharing NiO_5N octahedra which cause an hexagonal array of channels with a free diameter taking into account van der Waals radii of hydrogen atoms, of ~ 10 Å.

The nickel version of the above-mentioned materials is the first fully crystalline phosphonate MOF with pores approaching 1 nm and pore volume values observed for large pore zeolites.[221] This structure contains channels filled with physisorbed and chemisorbed water

molecules. The framework has a honeycomb arrangement that comes from helical chains of edge sharing NiO_5N octahedra and the ligand. Through the phosphonate oxygen atoms and the N atoms of piperazine the ligand coordinated with the nickel atoms, a feature that imparts thermal stability up to 650 K. Because of the reversible dehydration and rehydration and the changes in the local structure that temperature results, experiments showed that H_2 and CO are excellent probes of adsorption site at low temperatures, while CO_2, CH_3OH, CD_3CN and CH_4 are useful probes at room temperatures in terms of the fully dehydrates sample. In order to evaluate the adsorption properties of the materials for potential storage and separation all the measurements were carried out at 303 K.

Another use of phosphonic acids in the field of gas adsorption is featured in the materials UAM-150, UAM-151 and UAM-152.[222]Reaction of the rigid 4,4'-biphenyldiphosphonic acid (BPDP), phosphorus acid and aluminum salts, leads to amorphous products. The H_2 intake displayed by material UAM-152 is close to the highest reported for organoinorganic materials at 77 K and atmospheric pressure. From the study we extract the conclusion that H_2 adsorption increases as the amount of phosphorous acid incorporated increases.

1.8.6 Intercalation.

The field of intercalation chemistry is thriving, as more inorganic layered materials are discovered as potential "hosts" to "guest" molecules. The most important characteristics for the developing host materials are high thermal stability, resistance to chemical oxidation, selectivity to ions and molecules and the ability to expand their interlamellar space in the presence of guest molecules.[222],[223]

The role of metal phosphonates in the field of intercalation is being thoroughly studied.[224],[225]The majority of lamelar metal mono-phosphonates have the general formula $M(O_3PR)_x \cdot nH_2O$, where M is the metal ion, R is the aliphatic or aromatic group. Molecules such as n-alkylmonoamines,[226],[227],[228],[229]n-alkyldiamines,[230]aromatic amines (pyridines)[231] dendritic polyamines[232]have been intercalated into lamellar metal phosphonates. The interaction of Zirconium phenylphosphonate, $Zr(O_3PC_6H_5)_2$, with n-alkylmonoamines $R-(CH_2)_n-NH_2$ (n = 0-6) was studied by Ruiz and Airoldi.[233] Studies on the ability of pyridine (py) and a-, b- and c-picolines to intercalate into crystalline hydrated barium phenylphosphonate, $Ba[(HO)O_2PC_6H_5]_2 \cdot 2H_2O$ were reported by Lazarin and Airoldi.[234]

When $Zn(O_3PC_6H_5)\cdot H_2O$ is in contact with liquid amine, a replacement of the water molecule by amine molecule takes place. The product, $Zn(O_3PC_6H_5)\cdot(RNH_2)$ is thermally stable with the amine occupying the same coordination site as the water molecule in the monohydrate hybrid material.[235]

In the case of dehydration of $Cu(O_3PC_6H_5)\cdot H_2O$ and $Zn(O_3PCH_3)\cdot H_2O$ adsorption of amine can take place. The Cu center in the product is in an unusual 5-coordinated environment, with a water molecule occupying the equatorial position of a distorted square pyramid.[236]

Studies of Lima and Airoldi focused on intercalation of crystalline calcium phenylphosphonate[237] and calcium methylphosphonate[238] with n-alkylmonoamines. The hydrated compound $Ca(HO_3PC_6H_5)_2\cdot 2H_2O$ has two coordinated water molecules to the inorganic backbone, which in the presence of basic polar molecules are gradually replaced.[239]An increase in interlamellar distance takes place to accommodate the guest molecules in the interlayer space.[240]

Poojary and Clearfield used powder x-ray data to study the intercalated products formed by propyl-, butyl-, and pentylamine and zinc phenylphosphonates (hydrous and anhydrous structures).[241] In all three intercalates the zinc center is found in a slightly distorted tetrahedron. The three coordination sites are occupied by three different oxygen atoms from three different phosphonate groups. The fourth site is occupied by the nitrogen atom of the amine molecule.

2 SILICA-BASED POLYMERIC GELS AS PLATFORMS FOR DELIVERY OF PHOSPHONATE PHARMACEUTICS

2.1 Matrices in controlled delivery gel systems: the case of silica

Polymeric matrices are a prominent option for the construction of drug delivery carriers, due to their easy chemical or physical modification and wide variety of potential applications.[242] There are many different drug carrier matrix types depending on specific factors and the desired outcome, such as the drug type and the route of delivery. These are considered "open systems", therefore polymer gel carriers play a dominant role in the pharmaceutical field because they are able to transport molecules that could act as drugs, through cross linked networks. Hence, spontaneous, controlled release can be accomplished.

Gel formation can possess various degrees of difficulty depending on the choice of polymer, but research in the field is quite extensive. Some examples of gel types are hydrogels, stimuli-responsive, (bio)degradable,[243]just to mention a few. For example, hydrogels are typically formed from a network of polymer chains, constructing a colloidal gel that can contain, up to 99 % water.[244]

Silica gels have drawn substantial interest of the scientific community over the past few years due to their low toxicity, stability, low manufacturing cost and multiple usages. They appear in a variety of applications, such as promising polar adsorbents of e.g. amino acids,[245] and as drug carriers. Pure silica gels can be used as the stationary phase in chromatography (thin layer chromatography, reverse phase chromatography etc.) and functionalized silicon dioxide gels are often used in organic synthesis and purification of various reagents and products.[246]

Silicic acid [$Si(OH)_4$] polymerization has been the subject of intense research.[247] It can result in gel formation under adjustable pH values and appropriate supersaturated solutions. It is worth-while to take a closer look at some significant details of silicon chemistry. In diluted aqueous solutions, soluble silica is found as ortho / mono silicic acid $Si(OH)_4$. This is a monomer that exists in two forms in an about-neutral pH environment, the protonated species (major, $Si(OH)_4$) and the singly deprotonated species (minor, $Si(OH)_3O^-$). As pH increases, the concentration of the deprotonated form ($Si(OH)_3O^-$) increases. Increasing the silicate concentration and adjusting the pH value to ~ 7 leads to condensation of two monomers, with simultaneous loss of one water molecule. The procedure follows a S_{N2} – type mechanism, in which a deprotonated silicic acid molecule attacks a fully protonated one (see Figure 2-1).[248]
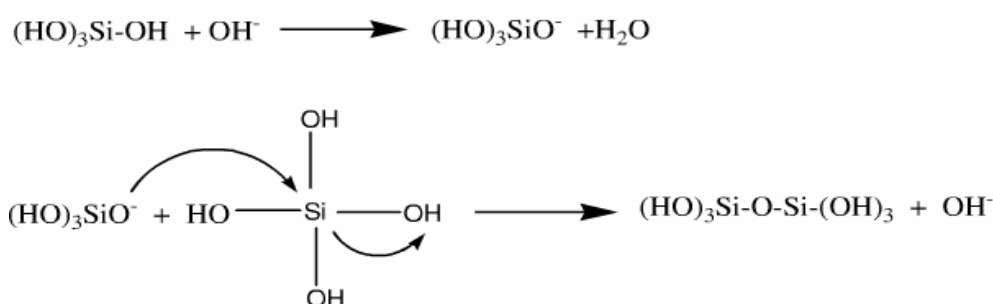
Figure 2-1. S_{N2} – like mechanism of silicic acid polycondensation.

The aforementioned step is the most crucial one as far as the kinetics of the polycondensation is concerned and is the rate-determining step in the complex silica polycondensation process.[249] The next steps involve the formation of trimers, tetramers and then higher oligomeric species until 1–2 nm amorphous silica nanoparticles are formed.[250]

It is worth-mentioning that the pKa of the polysilicic acids at these stages of the polymerization is about 6.5 and thus, above pH 7–8, negatively charged silicates become predominant.[251] In such conditions, silicic acid on the surface of colloidal species exists in equilibrium with dissolved silicic acid molecules and, hence, due to the Ostwald ripening process,

further particle growth occurs, leading to stable sols. In contrast, at pH regions below 7, particles can be only slightly charged, so no electrostatic repulsion prevents them from aggregation, leading to gel formation.[252]

A variety of methods have been published from different research groups regarding the fabrication of silica gels, which slightly differ from one another.[253],[254]The easiest and most widely-used method for gel preparation is a process that involves preparation of an aqueous solution of hydrated sodium silicate ($Na_2SiO_3 \cdot xH_2O$), which is then acidified to form a gelatinous precipitate. After mild washing, the product can be dehydrated and the percentage of dehydration depends on the exact end-use that it is intended for.

After gel formation, the remaining hydroxyl groups on the gel surface can either be immediately used as binding sites for other candidate molecules, or become guests of an array of chemical or physical modifications, due to their modifiable oxygen atoms. Thus, silica gels are ideal candidates for a huge array of applications.

Extensive research has been reported on controlled release systems involving silica-based drug carriers. The importance of the controlled release principle in a drug delivery system, liesin the need to deliver the desired drug in the right i) time, ii) area/location and iii) concentration.More specifically, a drug delivery system of controlled release properties should be able to maintain the optimum drug concentration in the blood, with minimum fluctuation, to achieve predictable and reproducible release rates for an extended time period and, last but not least, to eliminate side effects. Thus, the synthesis of the gels for a specific drug should be tailored considering the desired release kinetics, the loading level and, as expected, the physical properties of drugs.[255]

2.2 Controlled release systems

In the past of few decades several studies have been carried out on controlled delivery systems.[256],[257],[258],[259] Controlled release systems are designed to support and enhance the treatment under study. The goal of these systems is to control the drug release through the passage of time, assist the drug to overtake natural potential barriers, hinder and prevent possible elimination/excretion of the drug from the body, guide the drug to the desired site of action and minimize the potential exposure of the drug to undesirable degradation effects.[260]

The desired system should be able to maintain the optimum concentration of the drug in the blood, release the drug in a controlled and planned fashion, and have the ability to enhance the duration of action of the drug, particularly when it is short-lived. Also, a delivery system must be

designed so as not to cause side effects to the patient, to avoid frequent doses, which lead to drug wastage. The target of a delivery system should be to provide an optimized treatment.

There are two common methods of controlled release, the temporal control and the distribution control. In temporal control, the drug is protected by a device which has the ability for long-range transport at specific times during the treatment. This method is applicable to drugs which tend to be metabolized rapidly and eliminate from the body (see Figure 2-2).
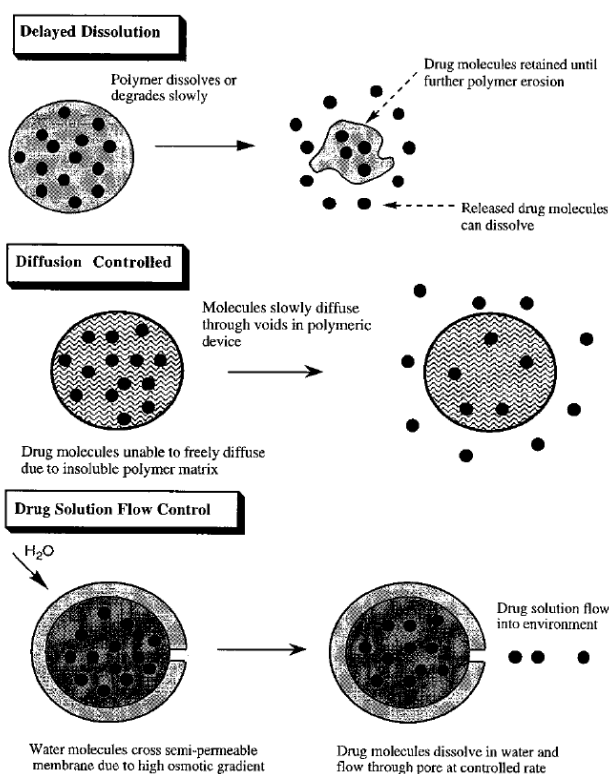
Figure 2-2. Examples of mechanisms of temporal controlled release. Reproduced with permission from Reference[261].

Temporal control may be accomplished by three mechanisms: delayed dissolution, diffusion controlled and drug solution flow control. In delayed dissolution polymeric devices protect drug release by delaying the dissolution of the drug molecules, thus inhibiting diffusion or controlling the flow. In diffusion controlled release an insoluble polymeric matrix delays and controls the diffusion of the drug molecules. The drug should in this case travel through a tortuous path to come out of the matrix. Drug solution flow control is used in osmotic potential across the semipermeable barrier of the transfer devices in order to create pressure chambers which contain aqueous solutions of the drug. This pressure is equalized by the transfer of the solvent of the drug out of the matrix.[262] In the case of distribution control, the delivery system is implanted directly to the area where the drug

needs to act.[263] The implants which are suitable for this controlled released system are those which have no harmful side effects for the patient and the drug is unable to leave from the implant.[262] Implantable drug delivery systems (IDDS) are classified into three major categories: biodegradable or non-biodegradable implants, implantable pump systems, and, the newest, atypical class of implants.[255]

In biodegradable or non-biodegradable implants, the drug release depends on the solubility and diffusion of the drug in the delivery device. In implantable pump systems controlled drug release is achieved by the micro-technology of electronic systems and the flow is controlled through the constant pressure difference. The atypical class of controlled released systems achieves targeted delivery of drug, minimization of wasting drug and side effects. In this case the efficacy of the drug and the treatment.[255]

2.3 Bisphosphonates (BPs) in controlled release systems

In the last ten years the scientific literature has seen about 10,000 scientific works on the topic of BPs. These compounds were first shown to inhibit calcification and hydroxyapatite dissolution *in vitro* and bone resorption *in vivo*.[264] The pharmacological effect of BPs is related to their ability to bind to the bone mineral (hydroxyapatite). Equally important is their biochemical effect on the cells, predominantly osteoclasts (for a comprehensive review on bisphosphonate pharmacology see Reference [265]). Representative members of the BP family are shown in Figure 2-3.
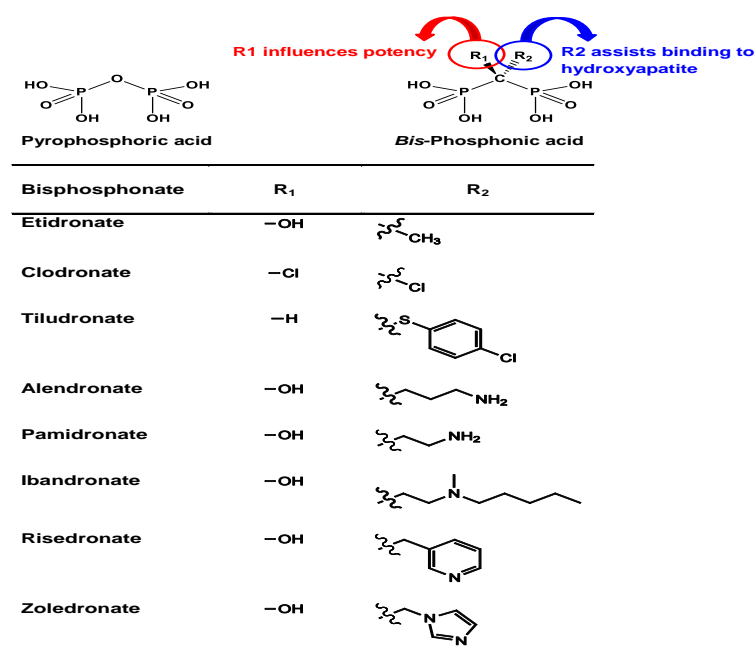
Figure 2-3. Schematic structures of bisphosphonates.

Etidronate and chlodronate (first generation of "-dronates") do not contain nitrogen atoms in their structure. These compounds act as analogs of pyrophosphates and metabolized to a cytotoxic analog of ATP, adenosine-5′-(β,γ-dichloromethylene)-triphosphate. That analog inhibits the mitochondrial adenine nucleotide translocase (ANT) and eventually triggers apoptosis.[266],[267]

When a BP contains a nitrogen atom in its alkyl side chain, for example Aledronic Acid or Pamidronic Acid (see Figure 2-3), it becomes 10–100 times more potent than the non-nitrogen analogs (first-generation BPs). Studies with amino-bisphosphonates have shown that they are taken up by mature osteoclasts and inhibit an enzyme of the mevalonate pathway called farnesyl pyrophosphatase synthase.[268],[269],[270],[271],[272]Inhibition of inactive osteoclasts is a result of the domino impact from the involvement of BPs in biochemical pathways.[273]

Still nowadays, the final and fatal stage of cancer, metastasis, is an uncharted and incurable activity. Scientists reported that in some types of human cancers, such as breast cancer, thyroid cancer, renal carcinoma, prostate cancer and multiple myelomas, more than 50 % will get metastasized probably at a bone site in the advanced stages.[274]As emphasized before, BPs are compounds/drugs that are able to reduce bone erosion and restore bone density in osteoporosis and other bone related diseases. There are many clinical trials which proved that bone homeostasis is restored by the use of BPs.[275] The use of BPs induces the apoptosis of osteoclasts and, as a result, the actions of osteoclasts that are responsible for the bone erosion are inhibited.[276] There is fast distribution and high accumulation in the bone (100 times) in comparison to C_{max} even after 6 months post use.[277] This is due to the BPs strong affinity towards bone mineral (hydroxyapatite). An additional reason for the widespread use of BPs as bone imaging agents (besides high selectivity and affinity) is their synergy with radiopharmaceuticals. Some studied synergy examples are: estradiol,[278] prostaglandin E2,[279] Src (protein tyrosine kinase pp60c-Src) homology 2 inhibitors,[280] diclofenac,[281] fluroquinolone, cis-platin, melphalan, methotrexate,[282] radiopharmaceuticals like technetium (^{99m}Tc) hydroxyethylidene disphosphonate,^{99m}Tc methylene disphosphonate,^{99m}Tc hydroxymethylene disphosphonate,[283] and samarium (^{153}Sm) lexidronam (QuadrametR).[284]

The phosphonate moiety (-PO$_3$H$_2$) exhibits excellent binding properties to hydroxyapatite and metallic surfaces. BPs have been evaluated as formulating agents, especially for the steric stabilization of nanoparticles.[285] Gittens et al. proposed peptides and proteins for conjugation with BPs to induce bone selectivity.[286]Hengst et al.[261]have suggested the use of CHOL-TOE-BP as a targeting moiety for liposomal drug delivery to the bone. Also, BP conjugates were used as delivery anchors for treatment of osteoporosis.[279] The use of alendronate-β-cyclodextrin as a bone anabolic agent was demonstrated by Liu et al.[287]

Studies on the applications of BPs in cardiac valve problems are discussed below in more detail. Tissue-derived valvular prostheses which consist of either human allograft or xenograft are commonly utilized in valve replacement surgery. Xenograft valve prostheses are most commonly built-up from bovine pericardium or porcine aortic valves that crosslink glutaraldehyde. These replacement valves present problems due to calcification, with cuspal mineral deposition, leading to valvular regurgitation or stenosis. This is the most important reason for the clinical failure of these devices. Furthermore, aortic wall calcification has been observed, leading to gradual rigidity in long-term implants. Fresh aortic explants appeared less calcified than the glutaraldehyde-cross-linked aortic wall grafts. In order to prevent the above model systems from mineral deposition, calcification inhibitors were used as pre-treatments or local controlled release polymer co-implants.[288],[289],[290]

A great deal of studies on controlled release of BPs has been performed. The principal reason is that the administration of BP compounds can limit the formation and growth of hydroxyapatite crystals. When these drugs are administered in efficient systemic dosages, severe adverse effects on skeletal mineral and overall calcium metabolism result, so the dosage level is a significant factor. Local therapy was achieved with controlled-release matrices that enclose the anticalcification factor, 1-hydroxyethylene diphosphonate (HEDP, or etidronate, **ETID**) dissipated in a copolymer of ethylene-vinyl acetate (EVA). These matrices were hemispherical (diameter 1 cm) and this geometric structure presented practically stable release rates in a plethora of test formulations. In cusps removed from animals with hemisphere implants containing ethylene-vinyl acetate-HEDP, exhibited minimal calcification.

Local controlled release of **ETID** from ethylene-vinyl acetate copolymer matrices directly into bioprosthetic cuspal implants inhibited calcification of the subcutaneous implants for up to 84 days without detectable problematic effects associated with the BP therapy. This long-term (84 days) controlled-release system delivered etidronate at a nearly total body dosage of 6 μg/kg and this very low dosage requirement for local therapy was undoubtedly the reason for effective anticalcification therapy, which importantly was not associated with any adverse effects. In contrast, the control implants showed progressive extensive calcification.[288][289][290]

In some studies silicone matrices including Na_2**ETID** or Ca_2**ETID** (which is ~ 1000 times less soluble) have demonstrated their efficacy as inhibitors for mineralization of bioprosthetic cusps. The drug load solubility affects the drug delivery rate. Thus, after 150 days approximately 80% of **ETID** was released from matrices containing exclusively Na_2**ETID** in comparison with lower levels of release from matrices loaded with (the less soluble) Ca_2**ETID**.[291]

It must be noted that the required duration of drug delivery can be accommodated to range from several months to 10 or more years by varying the matrix geometry, polymer composition, and solubility of the **ETID** salt used.

The BPs are capable of bone-specific delivery as it has been already reported. However, some of the BP derivatives exhibit some disadvantages from a toxicological point of view: after the BPs or their derivatives are taken up by the bone tissue, they can remain attached onto the bone mineral for a long time, thus causing side-effects.

A prodrug-based delivery system was designed in order to overcome such problems, known as novel osteotropic delivery system (ODDS). This system operated not only as a bone-specific, but also as a controlled delivery system. The affinity for hydroxyapatite is the most definitive feature in order to attain the osteotropic drug delivery. The three main groups of the chemical compounds which can attach to the surface of hydroxyapatite are usually oxygen-based, such as carboxylate, phosphonate and hydroxyl moieties. A drug is bound to a bisphosphonic promoiety via bioreversible bonds. The BP prodrug is principally taken up by the bone due to the chemical adsorption of bisphosphonic promoiety to hydroxyapatite. After systemic administration, a bisphosphonic prodrug is rapidly delivered to the bone and subjected to enzymatic and/or chemical hydrolysis to afford the parent drug, depending on its cleavage rate.

Because many previous studies showed that diphosphonic prodrug of carboxyfluorescein (CF-BP) is strongly adsorbed onto hydroxyapatite in vitro and strongly taken up into osseous tissues after intravenous injection, the CF-BP was synthesized as a standard compound. Moreover, CF was used because this compound and its prodrug (CF-BP) could be detected not only by a fluorescence detector but also by fluorescence microscopy. As soon as CF-BP was incorporated into the bone, it dissolved very slowly generating CF in the systemic compartment. It must be noted that the by-products, which are not taken up by the bone, are rapidly excreted from the body via the urinary system.

The P-C-P group in bisphosphonates is resistant to chemical and enzymatic degradation.[292] Hence, the elimination of CF-BP from the osseous tissue is the result of the hydrolysis of the ester bond, which was proposed on the basis of the presence of regenerated CF. Once the CF-BP is injected, the bone concentration of regenerated CF gradually increased during the following 7 days. In contrast, CF presents a really small skeletal distribution (0.9 % of dose) when it is injected intravenously. As a consequence, CF itself has no affinity for the bone. This phenomenon could be explained by the mechanism of the diffusion-limited release of regenerated CF through the bone mineral matrix. So, a skeletal diffusion-controlled system like the one

described, has the capacity to retain the plasma drug concentration for a long term and it could be helpful for effective therapies.[293],[294],[295]

There are a variety of research efforts on biological and biologically-inspired silica formation. These research studies put forth useful observations and conclusions. Based on such studies, it is now certain that an abundance of biomolecules (typically rich in amines), play a crucial role in biosilica deposition. It is now possible to develop new bioinspired green routes to nanostructured and porous silica by utilizing a wide variety of "additives" (analogues of biomolecules).[296] The use of "Green Nanosilica" has a variety of advantages. Some of these are related to the safety of the process, routinely performed on the bench-top at room temperature, in water and takes about 5 minutes. The composition of "Green Nanosilica" can be controlled in order to modify the system properties, such as the pore and particle size.[297] This can be achieved by making the "right" choice of an additive and synthesis conditions, as is shown by some SEM images (see Figure 4-4) from a study of Steven *et al.*[298]. It is clear that the utilization of this approach offers a one-step, "green" synthesis in contrast tothe time-, energy- and material-intensive methods for traditional materials.[296],[299],[297]
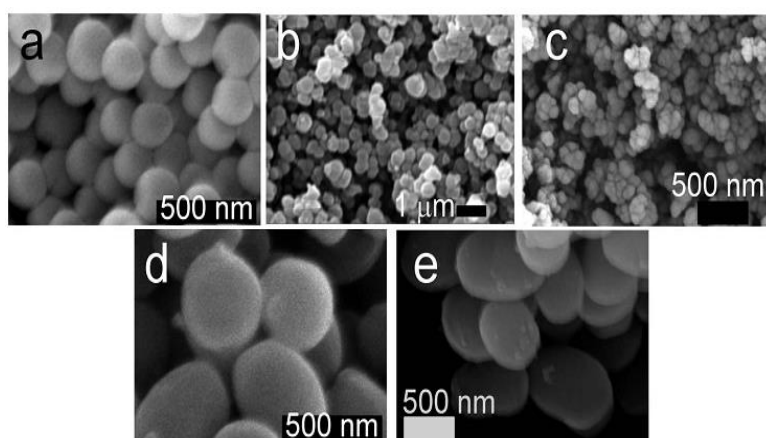
Figure 2-4. Scanning electron micrographs of silica particles used: (a) Stöber silica, (b) PEHA–GN, (c) PAH–GN, (d) APMSN and (e) SAMSN. Reproduced with permission from Reference[253].

A very intuitive application of siliceous ordered mesoporous materials combined with bisphosphonates was studied by Balas *et al.*[300] Aledronate in two different types of hexagonal ordered mesoporous materials, MCM-41 ($D_P = 3.8$ nm) and SBA-15 ($D_P = 9.0$ nm). Thomas et al. reviewed the adsorption from these systems/matrices (Figure 2-5).[301] In both cases, the surface of

the pore internal walls had undergone modification with amine groups (Chong and Zhao 2003).[302]
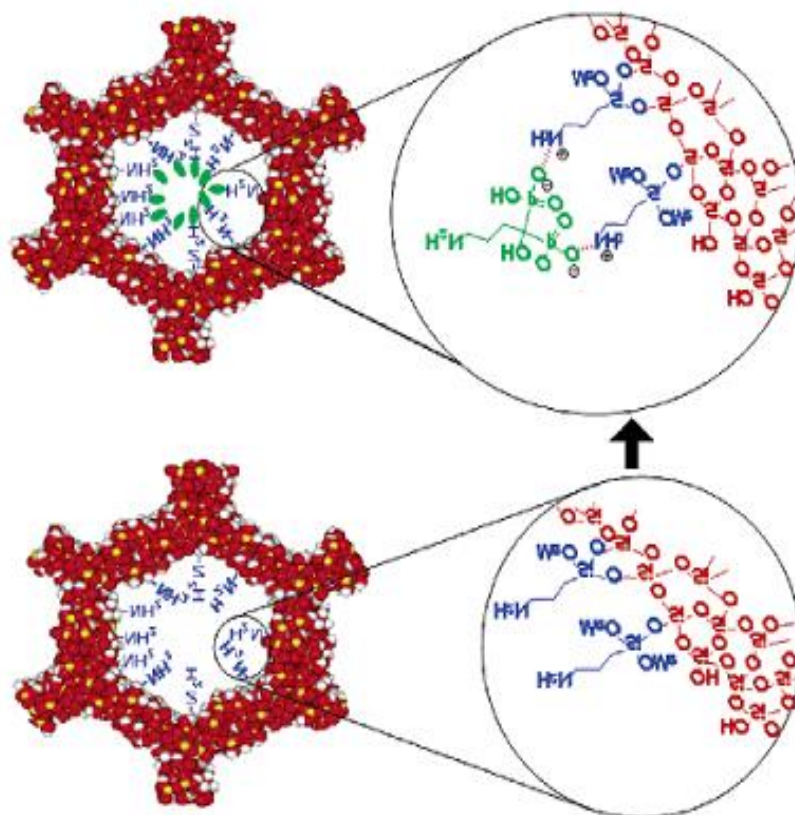
Figure 2-5. Alendronate adsorption on hexagonally ordered mesoporous silica, functionalized with propylamine groups. Reproduced with permission from Reference [301].

The amine functionalization was confirmed with the use of FT-IR, N_2 adsorption, and elemental analysis techniques. X-Ray diffraction patterns ensured that the ordered mesoporous framework of the materials was unaffected by the modification conditions. The grafting of propylamine to the pore walls in the modification process results to a decrease in the total pore volume and diameter, ca. 60 % for MCM-41 and ca. 40 % for SBA-15. After 24 h of immersion in an aqueous alendronate solution, the amine-modified materials showed a drug loading almost 3 times larger than that of the unmodified materials (Figure 2-6). This difference a consequence of the interaction between the phosphonate groups in alendronate and the silanol groups in the case of unmodified materials and from the amine groups covering the surface of the mesopore walls of the modified materials.[303]
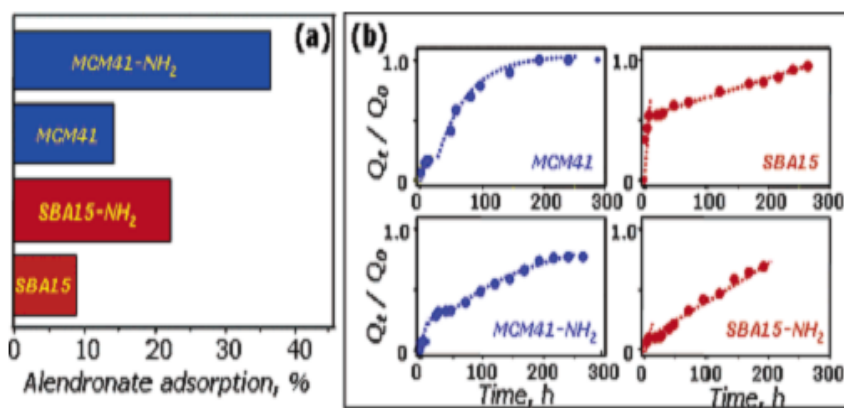
Figure 2-6.(a) Maximum load of alendronate in ordered mesoporous materials. (b) Release profiles of alendronate from the pure siliceous and amino-modified ordered mesoporous materials. Reproduced with permission from Reference [303].

The interaction between silanol and phosphonate of the adsorbed drug is weaker than that of the amine to phosphonate under pH 4.8 loading conditions. This ends to an adsorption of alendronate molecules when the materials are amine-modified, 22 % in SBA-15-NH$_2$ and 37 % in MCM-41-NH$_2$. The diffusion of bisphosphonate molecules to the liquid media, in materials with high surface areas and small mesopores as a surface-dependent phenomenon, can be predicted by a first-order kinetics model (see Figure 2-6b).[304],[305]

The contents of the present Chapter have been published in:

"Polymeric Matrices for the Controlled Release of Phosphonate Active Agents for Medicinal Applications".Papathanasiou, K.E.; Demadis, K.D. in Handbook of Polymers for Pharmaceutical Technologies, Bioactive and Compatible Synthetic/Hybrid Polymers, Volume 4, Thakur, V.K.; Thakur, M.K. Editors, Wiley-Scrivener Publishing LLC, **2015**, Chapter 4, pp. 87–122, ISBN: 9781119041467.

and

"Silica-Based Polymeric Gels as Platforms for Delivery of Phosphonate Pharmaceutics".Papathanasiou, K.E.; Moschona, A.; Spinthaki, A.; Vassaki, M.; Demadis, K.D. in *Polymer Gels: Synthesis and Characterization*, Thakur, V.K. Editor, Springer, **2017**, *in press*.

3 EXPERIMENTAL SECTION

3.1 General description

In our effort to study the diffusion of various bisphosphonic acids from a silica-based hydrogel, we fabricated a hydrogel host system based on amorphous silica. This kind of hydrogels is well-known since the beginning of the lastcentury.[306]The experimental setup used for this study of release is shown below (see Figure 3-1). Identical shape and diameter borosilicate glass beakers were used to synthesize four (4) identical hydrogels with at total volume of 10 ml. Twelve hours after the formation of the gel a total volume of 50ml of DI water at pH value of 3 was carefully deposited on top of the gel mass. The detailed experimental procedure and sequence of measurements are presented below. In four (4)identical beakers 10 ml of DI water were added. Subsequently, 0.66 gr of sodium metasilicate penathydrate (3.14 mmol) were dissolved together with~1.5 mmol of each bisphosphonic acid studied. The pH value of final solution was about 12.5. With the use 0.75 ml of concentrated HCl (37%) the pH was adjusted to 7, a value at whichthe polymerization of silicic acid has the highest rate. [307],[308],[309],[310],[311],[312],[313], [314],[315],[316],[317],[318]
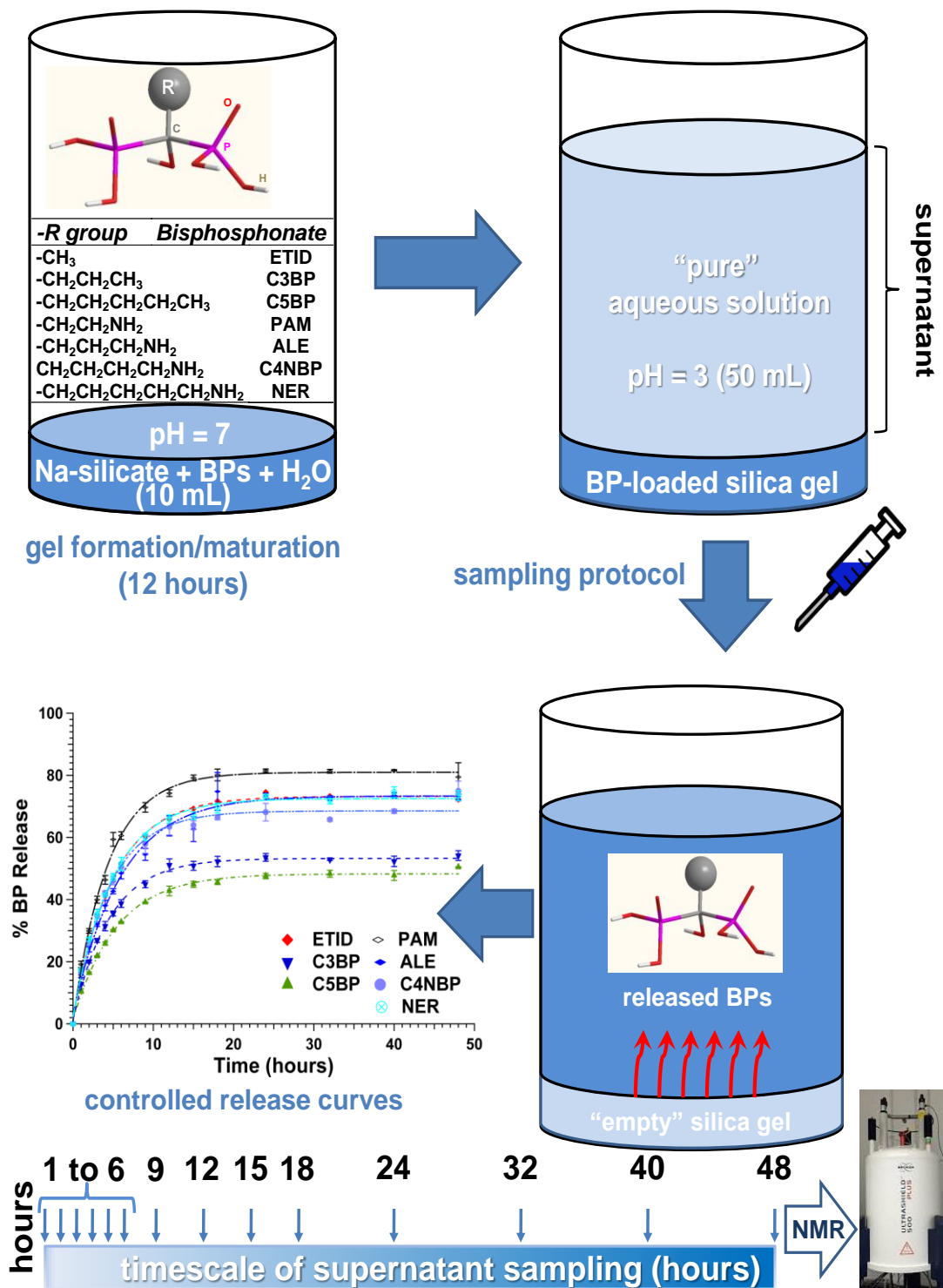
Figure 3-1. Experimental set-up, sampling and experimental procedure.

Twelve (12) hours later in each of the beakers a shapely and translucent gel was formed, upon which fifty (50) ml of DI water were carefully deposited, pre-adjusted at pH of 3. We chose

this particular value of pH as a simulation of the acidic conditions found in the human stomach. That point in time was the onset of the 48 hours-experiments of consecutive and parallel measurements on the four identical hydrogels devices. For the period of first six (6) hours sample of0.350ml were withdrawn from the supernatant every hour. During the following twelve (12) hours sampling was done every three (3) hours and the last sampling was done at the 24th hour. Afterwards, the sampling timing comprised of three equal time segments every 8 hours (see Figure 3-1). All samples of the supernatant were measured using NMR spectroscopy. The quantification was made possible by the presence of deuterium oxide, D_2O,99.9 atom % D (contains 0.05 wt. % 3-(trimethylsilyl)propionic-*2,2,3,3-d4* acid, sodium salt) as the internal standard.

3.2 Materials

Sodium silicate pentahydrate, $Na_2SiO_3 \cdot 5H_2O$, silicic acid (< 20 micron, refined, 99.9%) and potassium hydroxide was purchased from Sigma Aldrich. Rubidium hydroxide hydrate was purchased from Alfa-Aesar. **ETID** (either as solid tetrasodium salt or as acid in aqueous solution) was used as received from Solutia Inc. Deuterium oxide (99.9 atom % D) that contained 0.05 wt. % 3-(trimethylsilyl)propionic-2,2,3,3-d4 acid, sodium salt purchased also from Sigma Aldrich. Deionized water from an ion-exchange resin was used for all experiments and stock solution preparations.

3.3 Instrumentation

Solid state NMR experiments (by our collaborators Mr. Stephan Brueckner and Professor Eike Brunner, TUD, Dresden, Germany) were performed on a Bruker Avance 300 NMR spectrometer with a 7 mm MAS wide bore probe. The operating resonance frequency (rf) of 300.1 MHz for ^{1}H, 59.6 MHz for ^{29}Si and of 121.5 MHz for ^{31}P measurements. 7 mm Zirconia rotors with KEL-F inserts were used. For direct excitation measurements $\pi/2$ pulses at rf fields of 34.7 kHz on ^{29}Si and 65.8 kHz on 31P were applied. The interscan delay was set to 180 s for ^{31}P and 120 s for ^{29}Si. During acquisition TPPM decoupling with rf field at 50.0 kHz was used. Measurements were performed at a sample spinning speed of 7 kHz. For the ^{1}H-^{31}P CP MAS experiments a ramped CP by using an rf field of 53.2 kHz for the spinlock on ^{31}P, an 80%-100% ramp on the proton channel, and a contact time of 1.5 ms were applied. The corresponding decoupling was performed using the TPPM decoupling scheme at an rf field of 50.0 kHz during

acquisition. The interscan delay was set to 5 s. An AVANCE 300 (Bruker, Karlsruhe, Germany) spectrometer was used (University of Crete, Department of Chemistry, Greece) for the BP release experiments. SEM data and images collected with a JOEL JSM-6390LV electron microscope (University of Crete, Crete, Greece).

3.4 General comments on the synthesis of bisphosphonates

(Data and information were kindly provided by our collaborators from the University of Eastern Finland, School of Pharmacy, Kuopio, Finland)

Alendronate and neridronate were synthesized and characterized as reported elsewhere.[319]The C3BP (disodium salt) and C5BP (disodium salt) were synthesized according to the procedure described Egorov *et al.* and can be found in detail with NMR and HRMS characterization data in supporting information.[320]

3.4.1 General.

^{1}H and ^{31}PNMR spectra were recorded on a 600 MHz spectrometer operating at 600.2 and 243.0 MHz, respectively; ^{13}C NMR spectra were recorded on a 500 MHz spectrometer operating at 125.8 MHz. The solvent residual peak was used as a standard for ^{1}H measurements in D_2O (4.79 ppm) and in ^{13}C measurements CD_3OD were added to be as a reference (49.00 ppm) [Gottlieb, H.E.; Kotlyar, V.; Nudelman, A. NMR Chemical Shifts of Common Laboratory Solvents as Trace Impurities. *J. Org. Chem.* **1997**, *62*, 7512-7515]. 85% H_3PO_4 was used as an external standard in the ^{31}P measurements. The $^nJ_{HH}$ couplings were calculated from proton spectra and all *J* values are given in Hz. The $^nJ_{CP}$ couplings were calculated from carbon spectra with the coupling constants given in parenthesis as Hz. Mass spectra were recorded with a Finnigan LCQ quadrupole ion trap mass spectrometer (Finnigan MAT, San Jose, CA, USA) equipped with an electrospray ionization source. The purity of the products was determined from ^{1}H and ^{31}P NMR spectra and was $\geq$ 95 % unless stated otherwise.

3.4.2 Synthesis of 1-hydroxybutane-1,1-bisphosphonic acid disodium salt (C3BP).

1 M catecholborane solution in THF (36.5 mL, 36.5 mmol) was added to a flask containing butyric acid (3.2 g, 36.3 mmol) under an nitrogen atmosphere at room temperature. The mixture was stirred for about 1 hour until no more gas evolution was observed. Tris(trimethylsilyl)

phosphite (22.3 g, 25.0 mL, 74.8 mmol, 2.05 equiv.) was added and stirring was continued for 20 h. Methanol (120 mL) was added and, after stirring for 4-5 h., the solvents were evaporated *in vacuo*. The residue was dissolved in water (15 mL) and about 75 mL of MeOH was added. pH was adjusted to 8-9 by adding 40% NaOH with stirring. White precipitate formed and after 0.5 h it was filtered, washed with H_2O/MeOH (1:5) and dried *in vacuo* for several days with warming (MeOH was extremely "tightly" in crystal product). 1-hydroxybutane-1,1-bisphosphonic acid disodium salt (6.01 g, 60%) was obtained as a white powder. ^{1}H NMR (D$_2$O): δ 1.88-1.79 (m, 2H, CH_2), 1.56-1.47 (m, 2H, CH_2), 0.89 (t, 3H, ^3J = 7.4). ^{13}C NMR (D$_2$O, CD$_3$OD as ref.) δ 75.4 (t, $^1J_{CP}$ = 130.8, P-*C*-P), 37.2, 18.2 (t, $^2J_{CP}$ = 6.3), 15.2. ^{31}P NMR (D$_2$O) δ 18.79. MS (ESI$^-$) calc d. for $C_4H_{11}O_7P_2^-$ [M-H]$^-$ 232.9986, found: 232.9985.

Table 3-1. Molecular structure, ^{1}H, ^{31}P, ^{12}C spectrum respectively for C3BP.
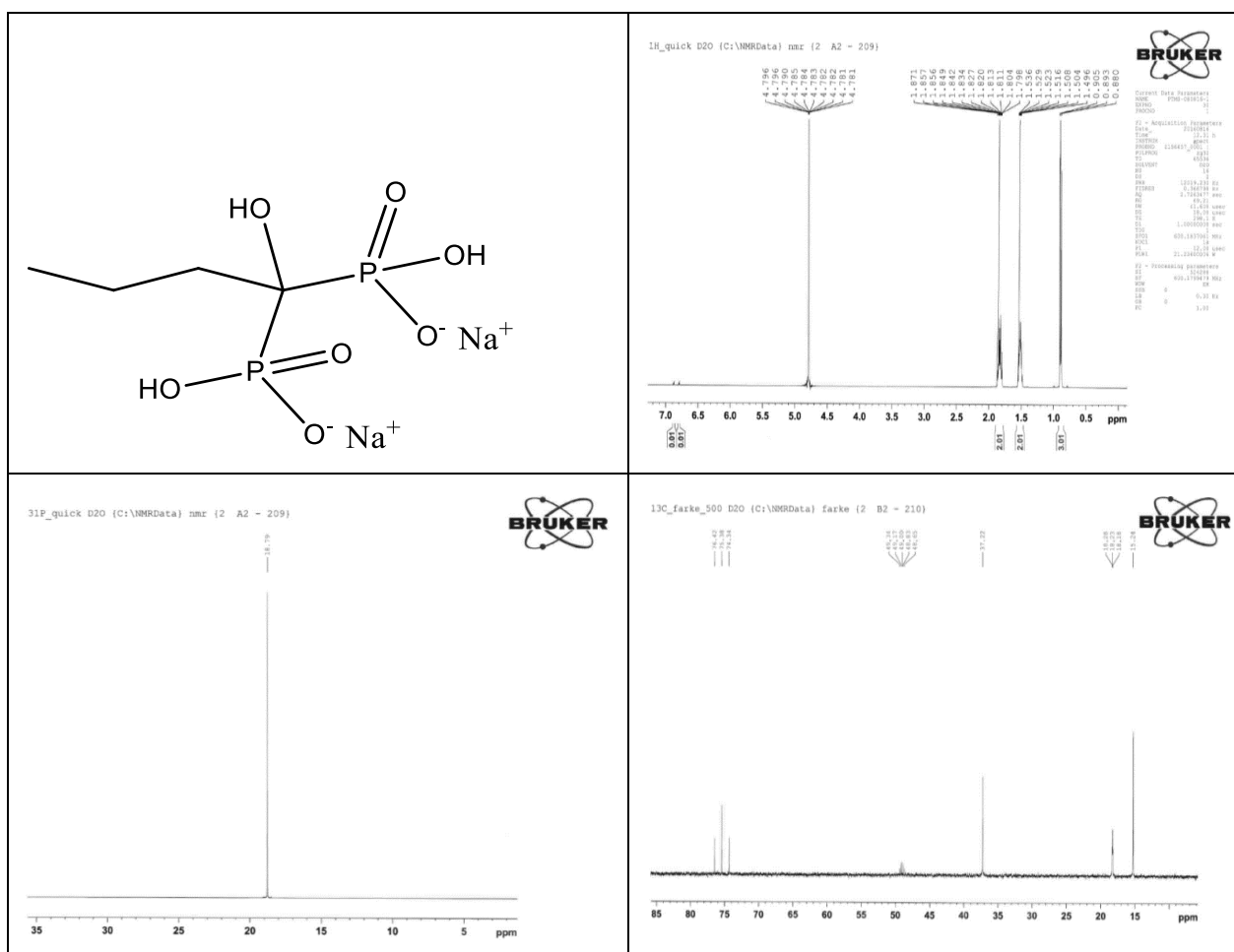
3.4.3 Synthesis of 1-hydroxyhexane-1,1-bisphosphonic acid disodium salt (C5BP).

Prepared similarly to compound **C3BP** from hexanoic acid (4.23 g, 36.4 mmol), 1 M cathecolborane solution in THF (36.4 mL, 36.4 mmol) and tris(trimethylsilyl) phosphite (22.3 g, 25.0 mL, 74.8 mmol, 2.05 equiv.). 1-hydroxyhexane-1,1-bisphosphonic acid disodium salt (7.34 g, 66%) was obtained as a white powder. ^{1}H NMR (D$_2$O): δ 1.92-1.83 (m, 2H,CH_2), 1.57-1.50 (m, 2H,CH_2), 1.36-1.24 (m, 4H, 2 x CH_2), 0.87 (t, 3H, ^3J = 7.2). ^{13}C NMR (D$_2$O, CD$_3$OD as ref.) δ 75.3 (t, $^1J_{CP}$ = 132.0, P-C-P), 34.9, 33.1, 24.4 (t, $^2J_{CP}$ = 5.7), 22.9,14.4. ^{31}P NMR (D$_2$O) δ 18.72. MS (ESI$^-$) calcd.for C$_6$H$_{15}$O$_7$P$_2^-$ [M-H]$^-$ 261.0299, found: 261.0297.

Table 3-2.Molecular structure, ^{1}H, ^{31}P, ^{12}C spectrum respectively for C5BP.
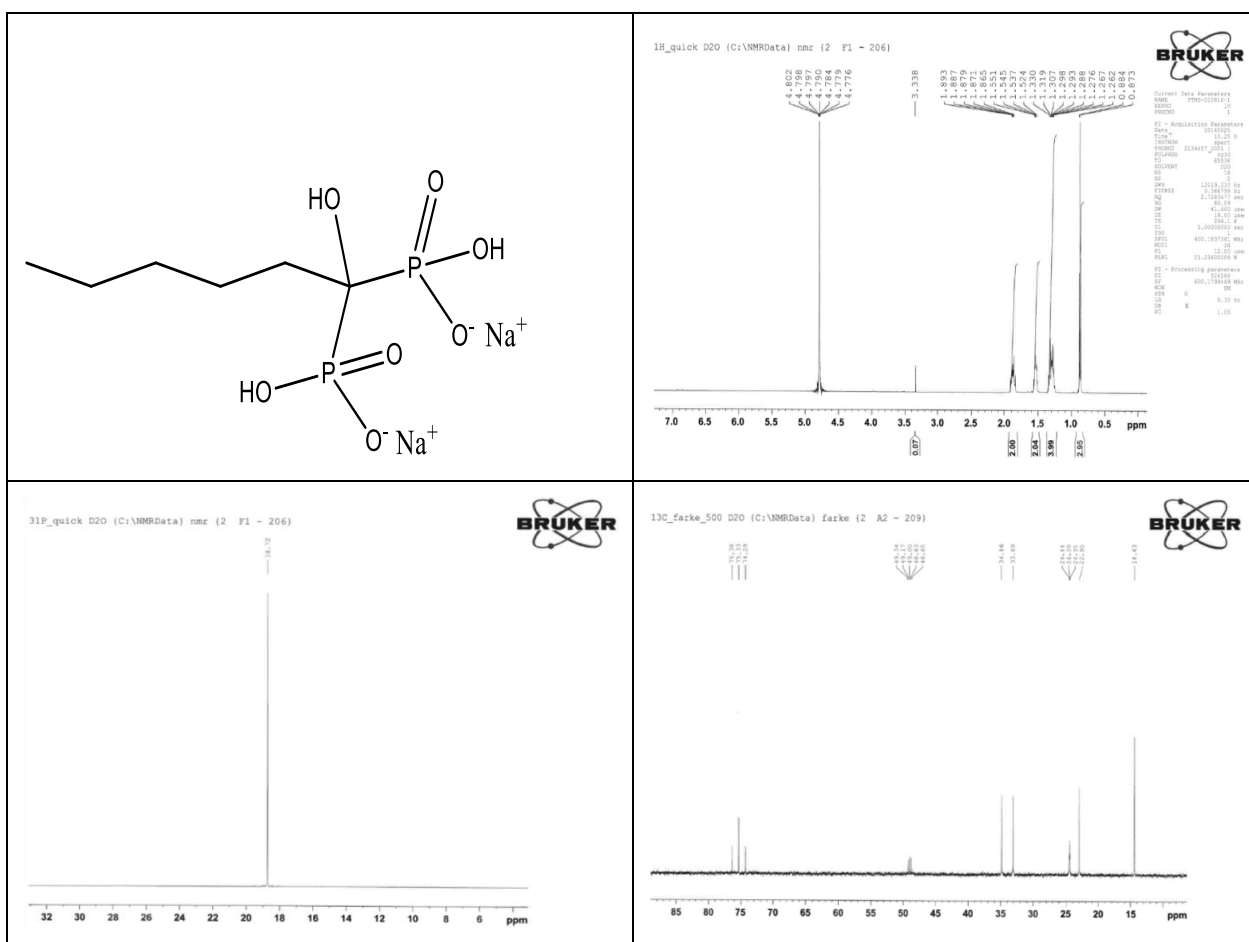
3.5 Preparation of gels

Herein, the synthesis of an **ETID**-loaded gel is described, as an example. All other BP-loaded gels were prepared in the same manner. The synthesis of each BP-loaded gel was repeated four (4) times using identical shape and diameter borosilicate glass beakers. In a beaker 10 mLof DI water was added. In this a quantity (0.66g, 3.14 mmol) of sodium metasilicate pentathydrate was dissolved, together with 0.50 g, 1.70 mmol) of tetrasodium **ETID**, while keeping the solution under stirring. The pH value of this solution was ~ 12.5. The pH was adjusted to 7.00 with the use 0.75 mL of concentrated HCl (37 %). This particular pH value was selected because the polymerization of silicic acid has the highest rate there. Gel formation commences within 10 minutes, however the freshly formed and "loose" gel was allowed to mature for 12 hours, after which a shapely and translucent gel formed. Gel preparation can be reproducibly repeated and can be modified by altering the amount of Na^+ ions, replacing the alkali ion, or changing the entrapped BP.BP-containing gels for all remaining BPs were prepared in the same manner, using quantities shown in the Table 3-3.

Table 3-3.BP-containing gels for all remaining BPs were prepared in the same manner, using quantities shown.

BP	Mass (g)	mmoles
ETID	0.50 g	1.70 mmol
C3BP	0.38 g	1.36 mmol
C5BP	0.48 g	1.56 mmol
PAM	0.29 g	1.22 mmol
ALE	0.37 g	1.25 mmol
C4NBP	0.35 g	1.31 mmol
NER	0.35 g	1.25 mmol

3.6 Controlled release of BPs from gels

On top of the solidified gel, a volume of deionized (DI) water (50 mL), pre-acidified to pH ~ 3 was carefully poured. This marked the initiation of the controlled release process (t = 0), which continued for 48 hours. For the initial 6-hour period an aliquot of 0.350 mL was withdrawn from the supernatant every hour. After the 6th hour and for the next 12 hours, sampling was performed every 3 hours. Finally, after the 18th hour and until the end of the release experiment (at the 48[th]hour) sampling was performed every 8 hours. The withdrawn samples were mixed with 0.150 mL of deuterium oxide (99.9 atom % D) that contained 0.05 wt. % (4.3375 µmol) 3-(trimethylsilyl)propionic-2,2,3,3-d_4 acid, sodium salt, TSP) as standard. ^{1}H NMR spectra were recorded on a Bruker AVANCE 300 MHz NMR (Bruker, Karlsruhe, Germany) spectrometer at 293.2 K operating at a proton NMR frequency of 300.13 MHz. Standard solvent (D_2O) was used as internal lock. Each ^{1}H spectrum consisted of 32 scans requiring 3 min. and 39 min. acquisition time with the following parameters: Spectral width = 20.5671 µs, pulse width (P1) = 15.000 µs, , and relaxation delay (D1) = 4.000 seconds. Polynomial 4th-order baseline correction was performed before manual integration of all NMR spectra. Proton and carbon chemical shifts in D_2O are reported relative to TSP. The characteristic peaks for each compound were integrated using the integration tool available from the Bruker software (TopSpin 3.2). For each compound we selected the integration value of the sharpest peak. However, all results derived from the integration values of the sharpest peaks were cross-checked and confirmed by using other peaks in the ^{1}H NMR spectra of each compound (Table 3-4).

Table 3-4.^{1}H NMR spectra for ETID, C3BP, C5BP, PAM, ALE, C4NB, NER respectively.
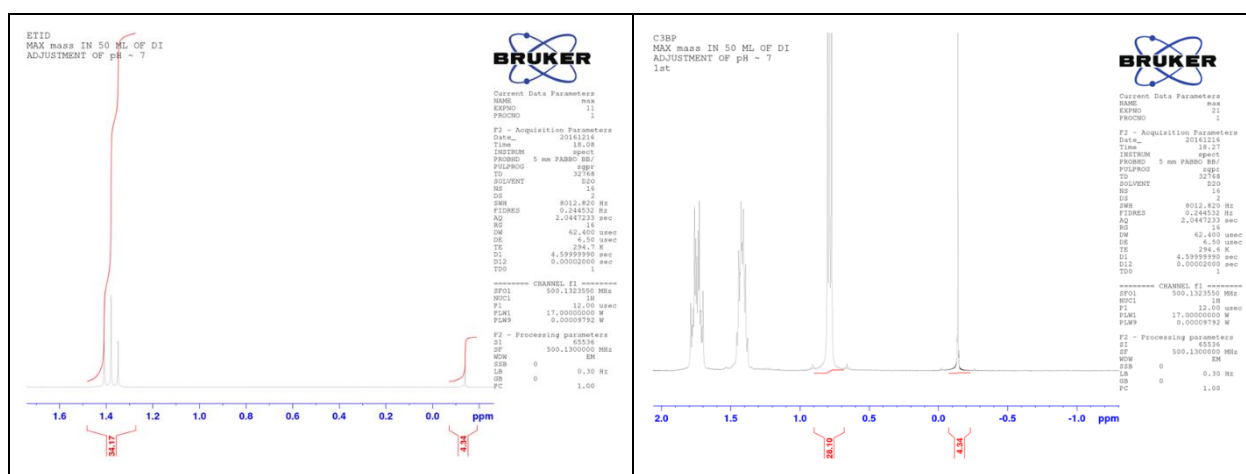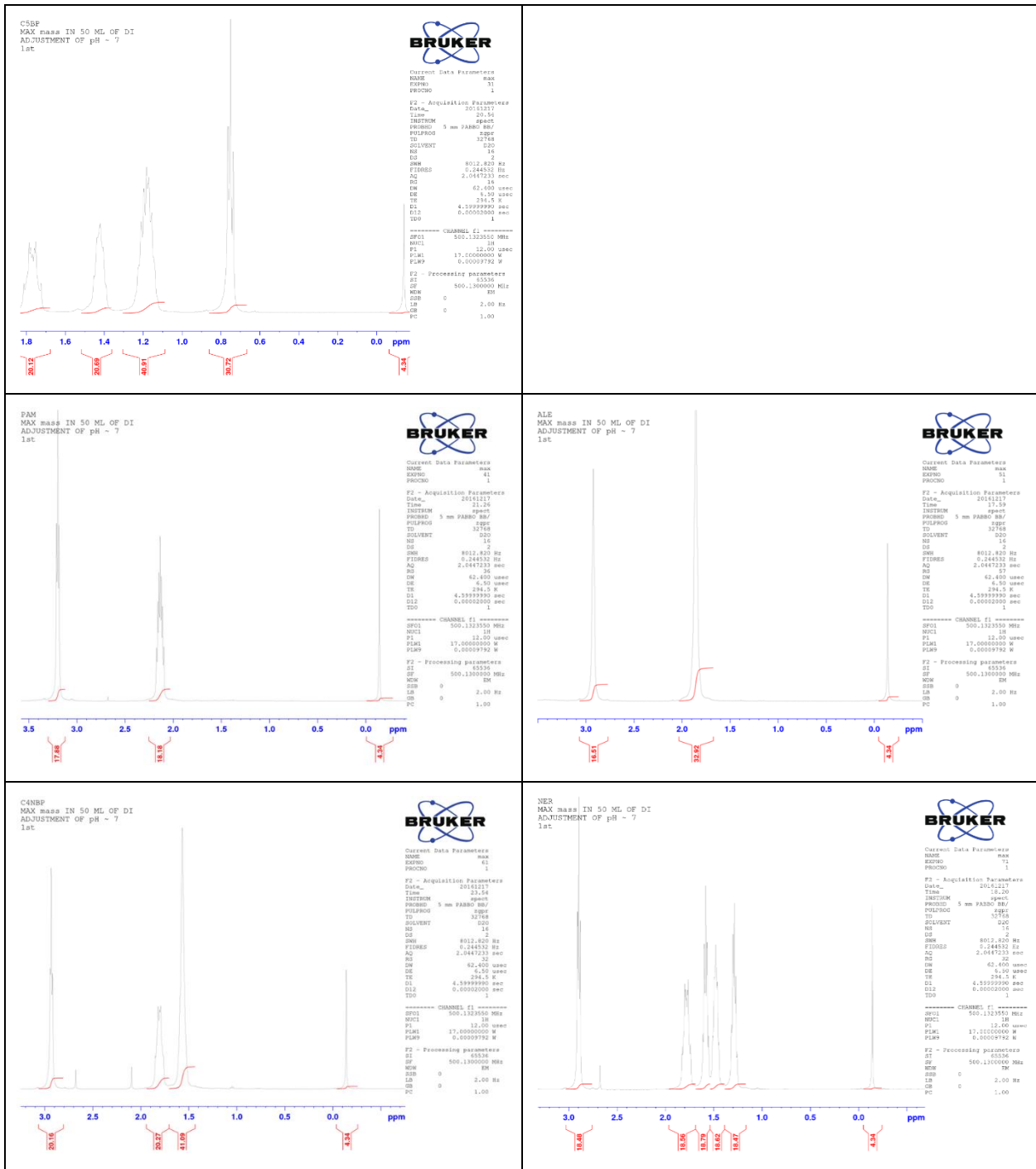
3.7 SEM studies

3.7.1 SEM characterization and imaging of "empty", "drug-loaded","used" gels.

Samples of all studied hydrogels ("empty", ETID-loaded, "emptied" and "used" gels) were treated several times and in series with Ethanol/H$_2$O solutions, 30/70, 50/50, 70/30, 90/10, and

finally 100/0, in order to achieve complete dehydration. Then a typical protocol of CPD was followed before the SEM studies.

Table 3-5.SEM images (surface and cross-sections) of silica gels prepared in the absence of BP(ETID) drug.
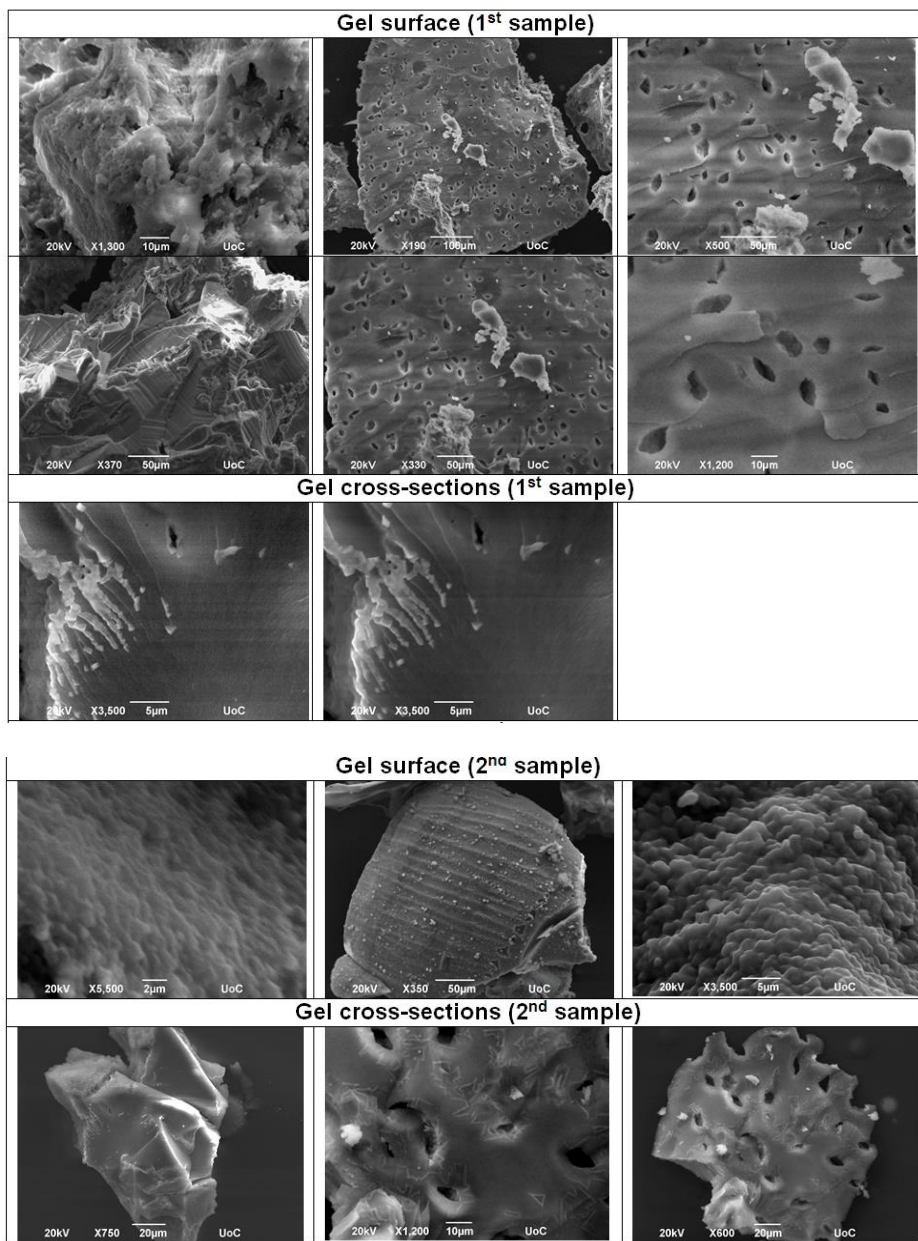
Table 3-6.SEM images of freshly "drug-loaded" gels (with ETID bisphosphonate).
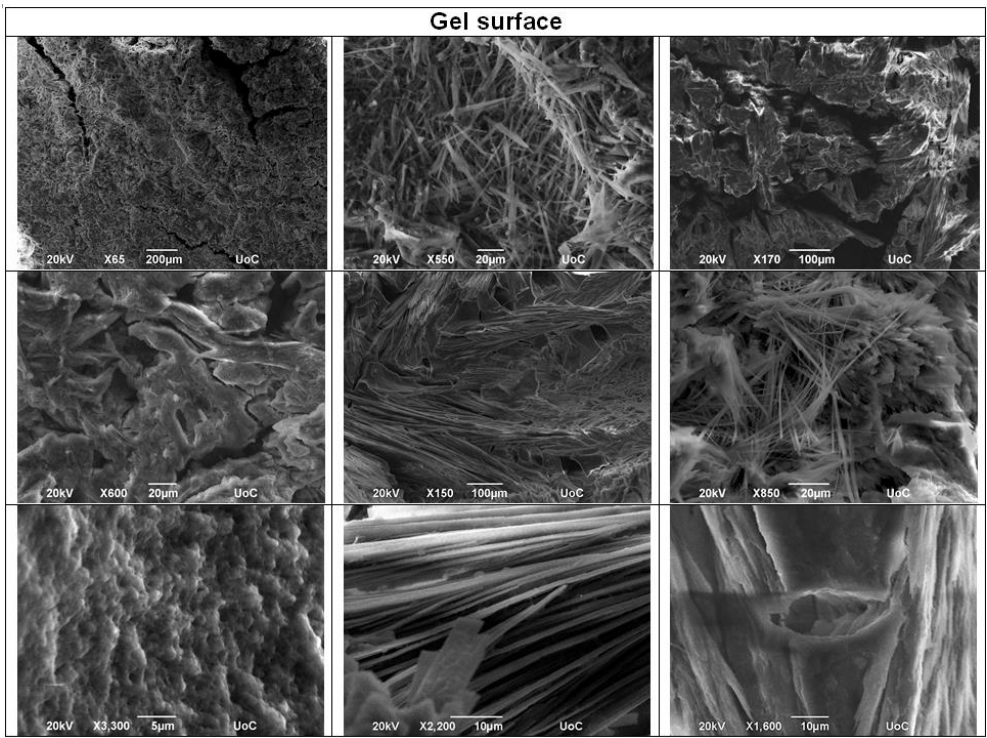
Table 3-7. SEM images of "used" gels (after 48 hour release).

Figure 3-4. SEM images of "FT" "gels" taken after 48 hour release.
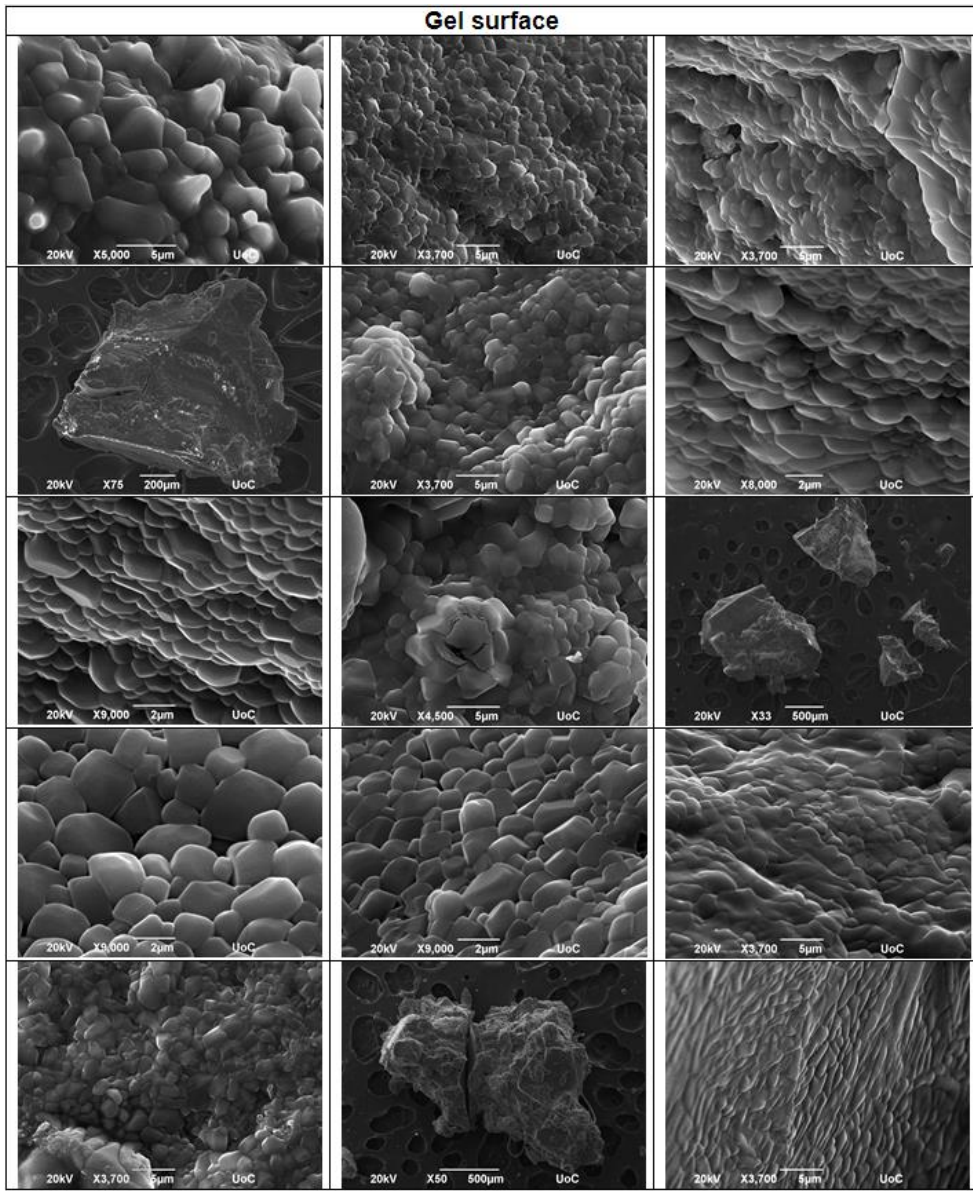
3.7.2 EDS characterization.

Table 3-8.EDS of freshly-prepared ETID-loaded gels.
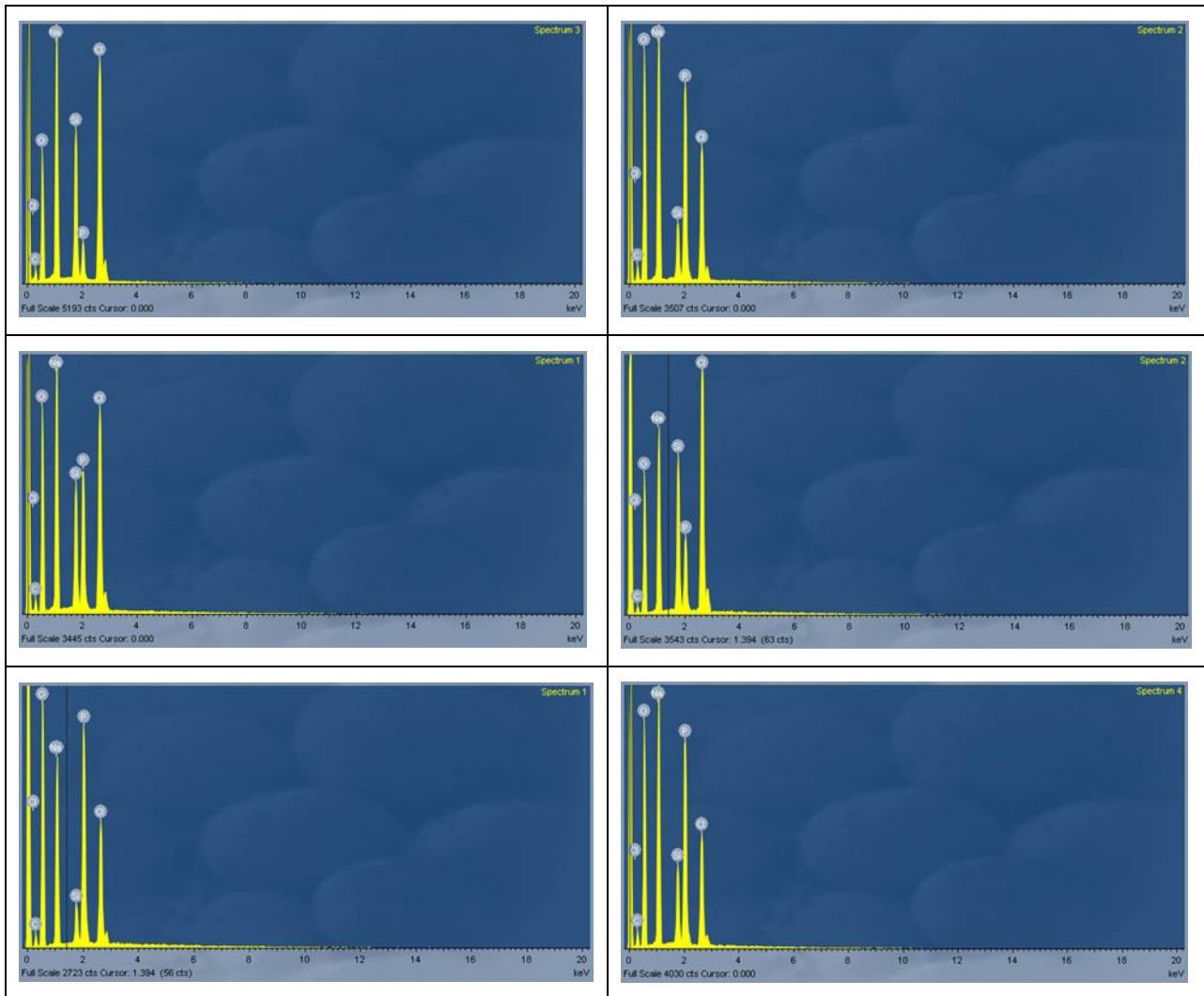
Table 3-9.EDS of "used" gels (after 48-hour release).
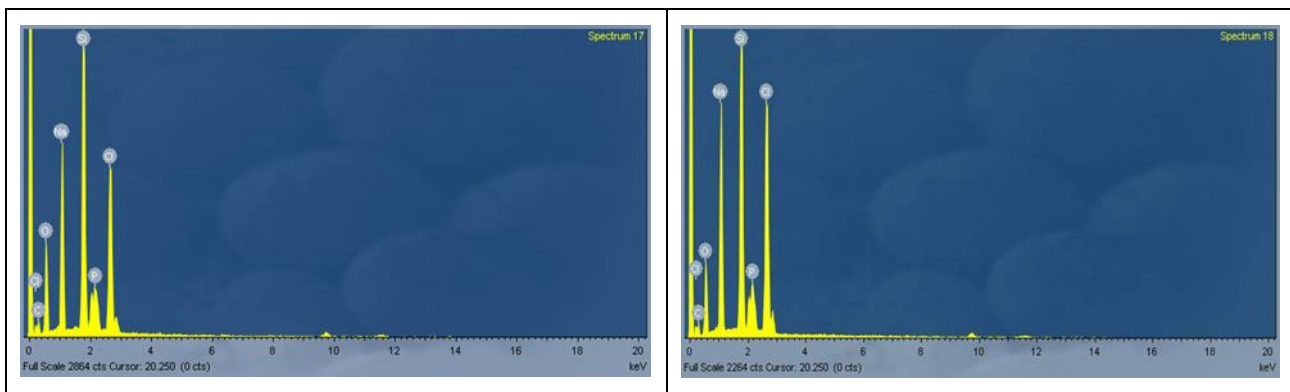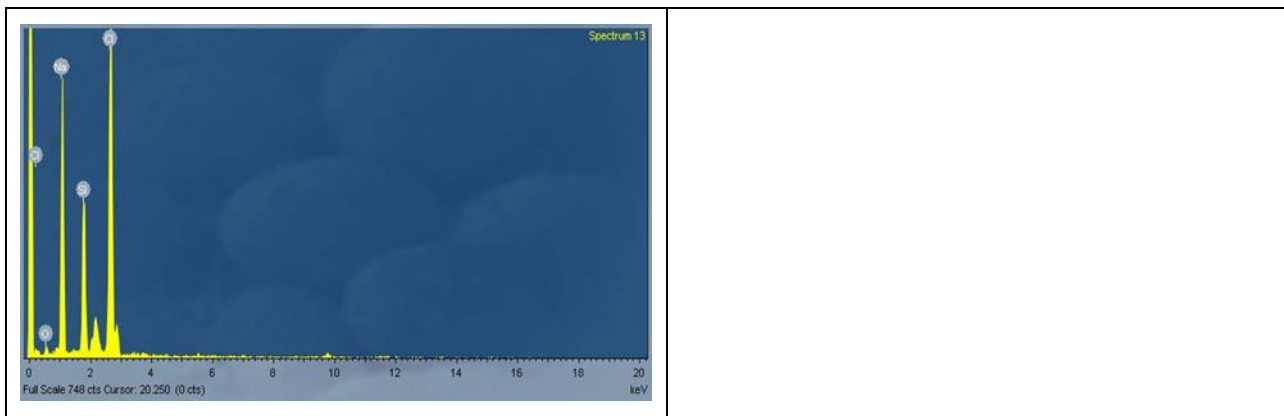
3.8 Mathematical data treatment

All aliquot samples withdrawn from the supernatant were measured using[1]H, ^{13}C, and ^{31}P NMR spectroscopy. The quantification of the released BP was based on integration of peaks in the ^{1}H spectrum and was made possible by using deuterium oxide 99.9 atom % D as solvent, that contains 0.05 wt. % 3-(trimethylsilyl)propionic-*2,2,3,3-d*4 acid sodium salt, TSP, as standard. Each release experiment was repeated 4 times in order to achieve maximum reproducibility and satisfactory statistics. Each release experiment consisting of 15 samplings/measurements, and repeated 4 times, was treated with the IGOR Pro 6.05 software.

The last step in the mathematical treatment of the results was the creation of a universal curve in the form $f(t) = a * e^{-b*t} + c$ that depicts the average value of the diffusion of the phosphonate from the silica hydrogel, including standard deviation. Factor $"a"$ of the equation is the "frequency factor" and it is related to the entropy difference between the gel and the liguid phase. Factor "b" is the exponential parameter that describes the energy statistical distribution of the molecules through desorption. Constant $"c"$ describes all the remaining interactions between the different phases (diffusion inside the gel, diffusion in the liquid, adsorption etc). The variable "t" is the time. (Table 3-10)

Table 3-10. The least square theory applied by the IGOR software on all data points (graphs to the left) and mean values (graphs to the right). In both cases the results are almost identical.
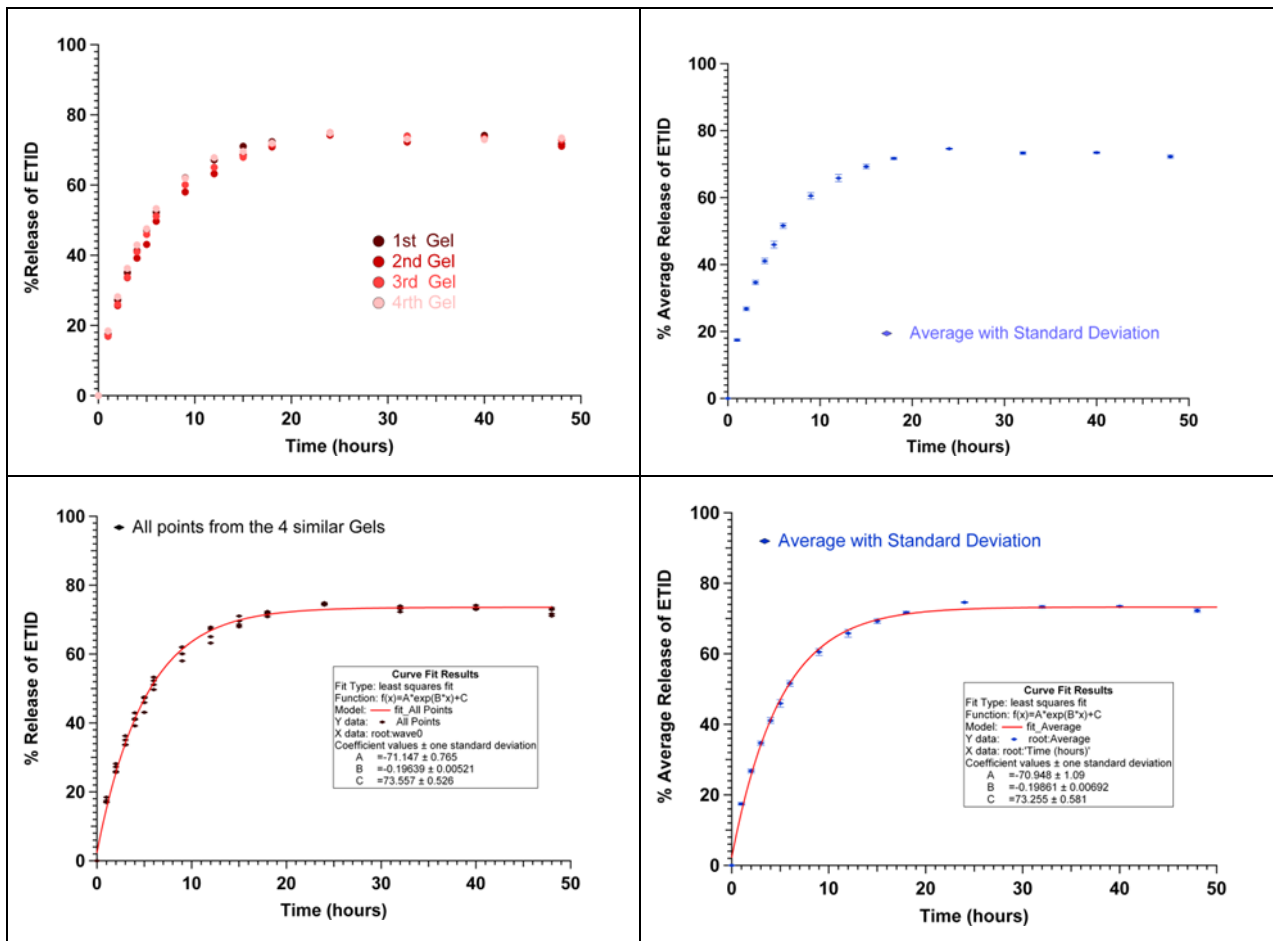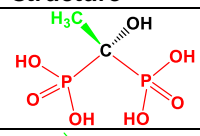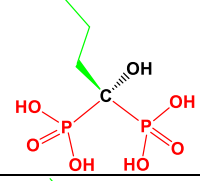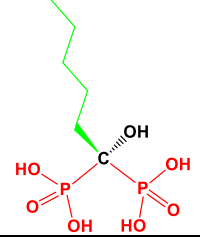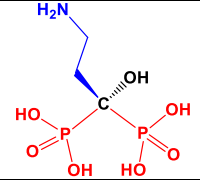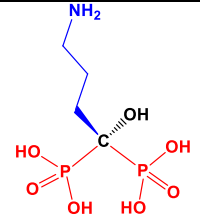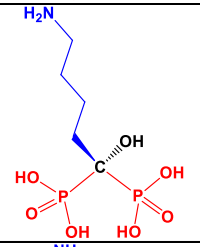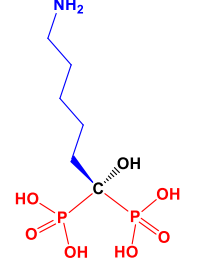
4 RESULTS AND DISCUSSION

4.1 Comments and discussion on the results

All BPs studied were synthesized by following established procedures (except the commercially available tetrasodium salt of HEDP). These BPs exhibit systematic structural differences, e.g. carbon chain length, and the presence ofthe amino end-group. These details are presented in Table 4-1.

Table 4-1.Bisphosphonate notation and structures.

Bisphosphonate common name	Bisphosphonate Chemical name	Bisphosphonate abbreviation	Bisphosphonate structure	Available as "acid"	Available as "salt"
Etidronic acid	1-hydroxyethane-1,1-bisphosphonic acid	*ETID*		YES	Tetrasodium salt
Not available	1-hydroxybutane-1,1-bisphosphonic acid disodium salt	*C3BP*		NO	Disodium salt
Not available	1-hydroxyhexane-1,1-bisphosphonic acid disodium salt	*C5BP*		NO	Disodium salt
Pamidronic acid	3-Amino-1-hydroxypropane-1,1-diphosphonic acid	*PAM*		YES	NO
Alendronic acid	3-Amino-1-hydroxybutane-1,1-diphosphonic acid	*ALE*		YES	Disodium salt
Not available	4-Amino-1-hydroxypentane-1,1-diphosphonic acid	*C4NBP*		YES	NO
Neridronic acid	6-Amino-1-hydroxyhexane-1,1-bisphosphonic acid	*NER*		YES	NO

The structural characteristics of the above BP compounds allow us to categorize them into two groups: (i) those containing an alkyl non-polar side-chain (**ETID**, **C3BP** and **C5BP**), and (ii)those containing a polar amine side-chain (**PAM**, **ALE**, **C4NBP**, and **NER**). Hence, we have bisphosphonates with one(1), three(3) and five(5) carbons in the carbon chain and bisphosphonates with two (2), three(3),four(4) and five(5) carbons and also an amine as a terminal group of the

chain. All these BPs contain an identical bis-phosphonate/hydroxyl moiety on one end, hence, their structural differences reside on the other end, which carries either a non-polar alkyl chain, or an aminoalkyl polar chain. Thus, it was interesting to see the effects of these structural variables on the possible steric interactions of the molecule with the hydrogel system and secondly the electrostatic cooperative interactions with the solvent (water).

In accordance with the above considerations we ensured the reproducibility of the experimental results in all series of experiments by keeping several variables constant, eg. Solution volume, temperature, pH, equimolar ratio of phosphonates, profile of beakers and gel surface/diameter. Thus, controlled release curves were constructed, which are presented in Figure 4-1. The traces are normalized based on the method of least squares.
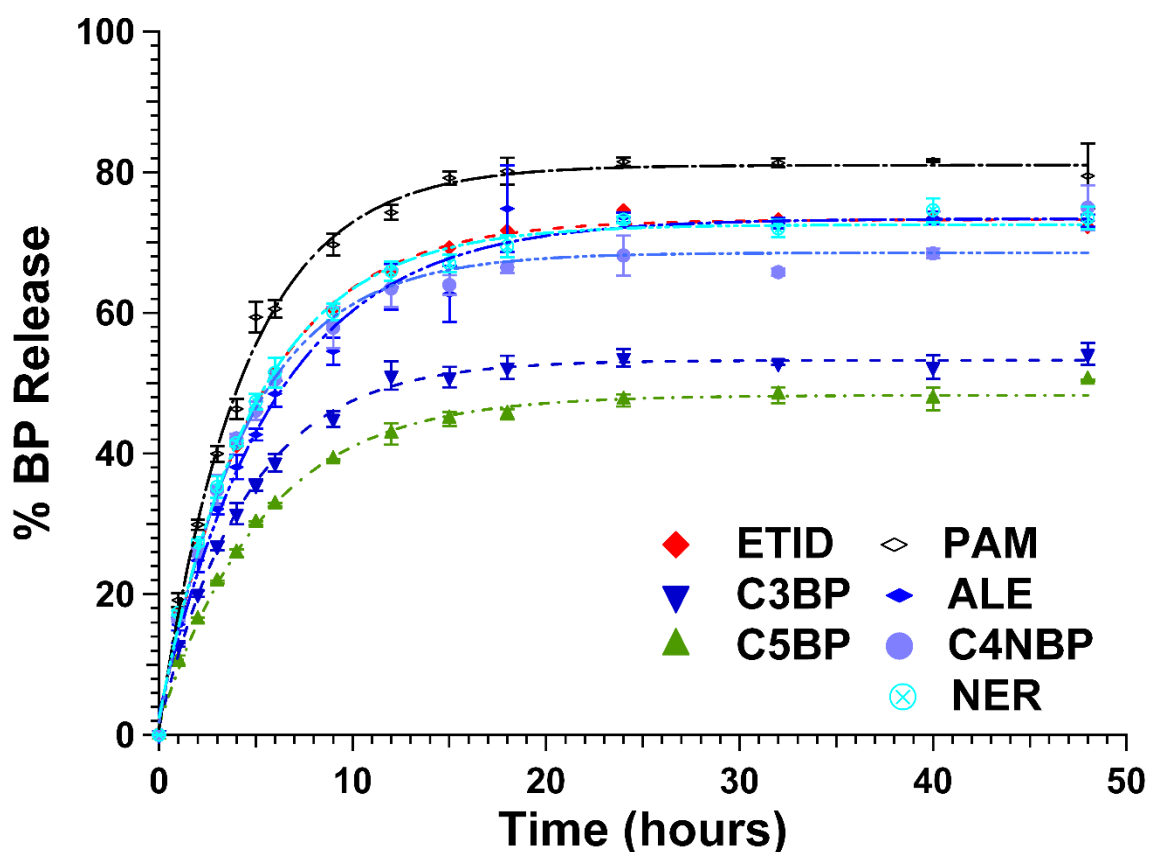
Figure 4-1. Release profiles of all BP's from identical silica gel matrices.

It is interesting to have a more careful look at the controlled release results (curves) according to the type of side-chain on the various BPs. Regarding the non-polar alkyl side-chain

BPs (see Figure 4-2) a systematic increase in the carbon chain of the substituted R side group causes both a slower release rate and final total release.
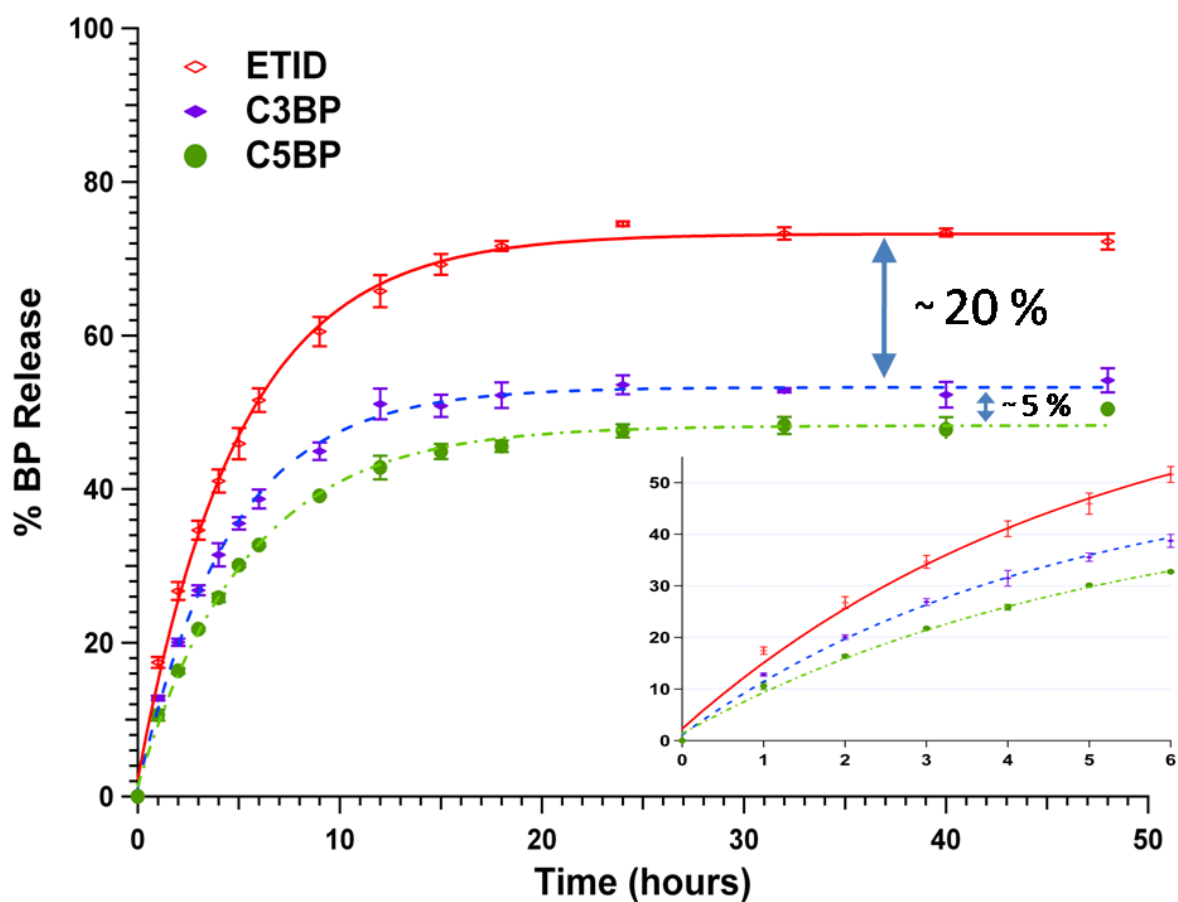
Figure 4-2. Release profiles of ETID, C3BP, C5BP. The reduction is distinctive as the carbon chain increases by two methylene groups.

As shown in Figure 4-3, there is an almost linear relationship between the carbon atoms in the alkyl side-chain and the final BP release.
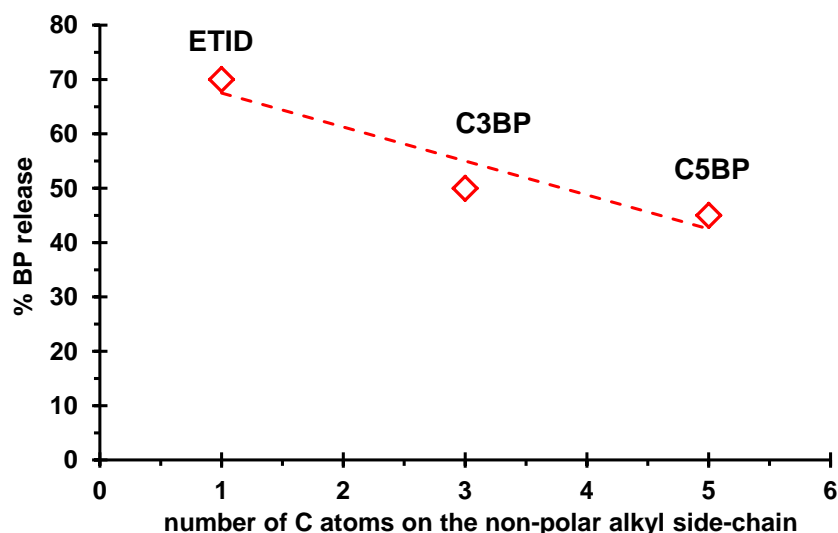
Figure 4-3. Relationship between the number of carbon atoms on the side-chain of ETID, C3BP and C5BP with the final % BP release.

Subsequently, it is revealing to examine the impact brought about by the presence of a charged group such as amino group. For such a comparison, similar molecular size BPs need to be evaluated. Therefore, comparative results between 1-hydroxybutane-1,1-diyl)bis (hydrogenphosphonic acid (C3BP) disodium salt, and (3-amino-1-hydroxypropane-1,1-diyl)bis(phosphonic acid) (Pamidronic Acid, **PAM**) are presented in Figure 4-4. In this case the two molecules have similar size but with the difference of the charged terminal. It is clear from the results shown in Figure 4-4 that the presence of the amino group profoundly enhances the diffusion rate and the final% release value.
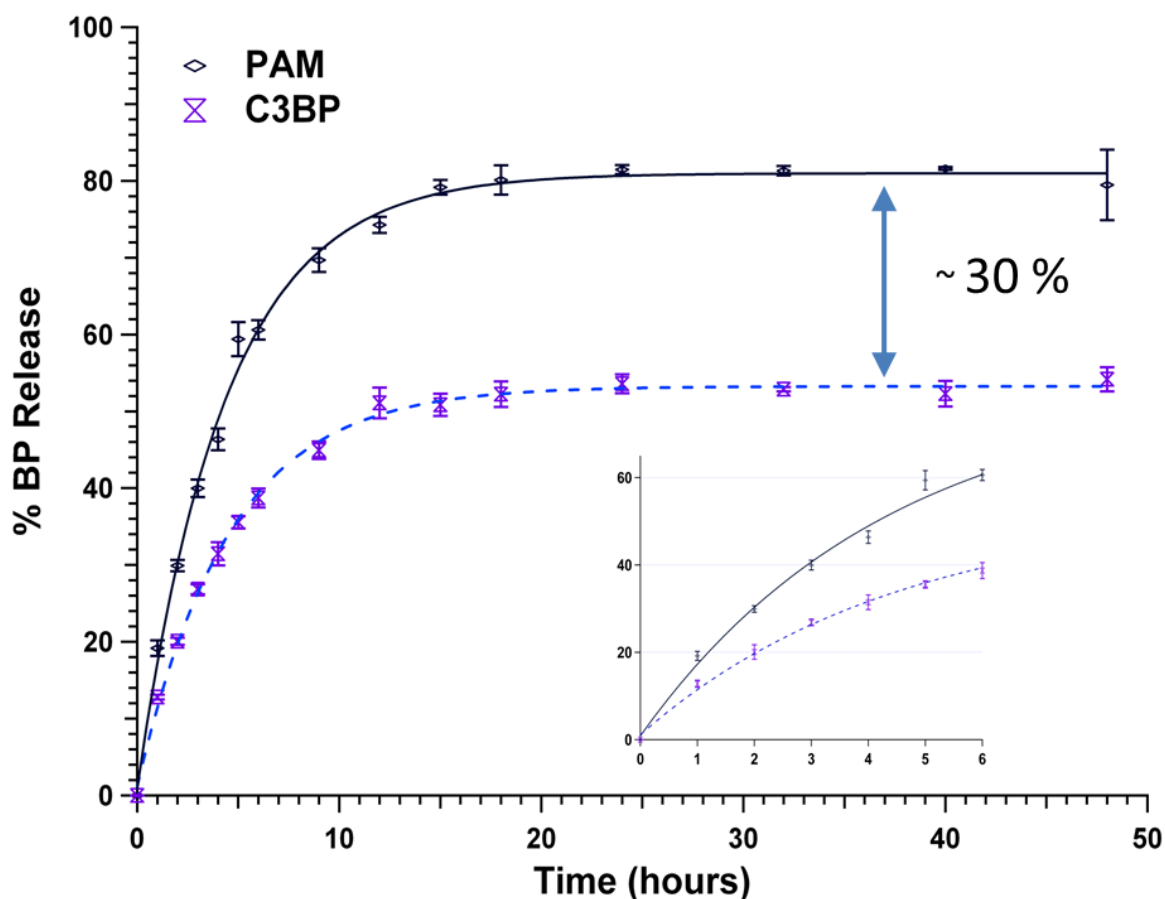
Figure 4-4. Comparison of C3BP and PAM release profiles.

An additional comparison involving larger molecular size phosphonates confirms the conclusion drawn from the comparison between **C3BP** and **PAM**. Thus, by comparing the release profiles of **C5BP** and **C4NBP** (Figure 4-5), it is evident that the amino-containing BP (**C4NBP**) demonstrates faster and higher end % release than the alkyl analog **C5BP**.
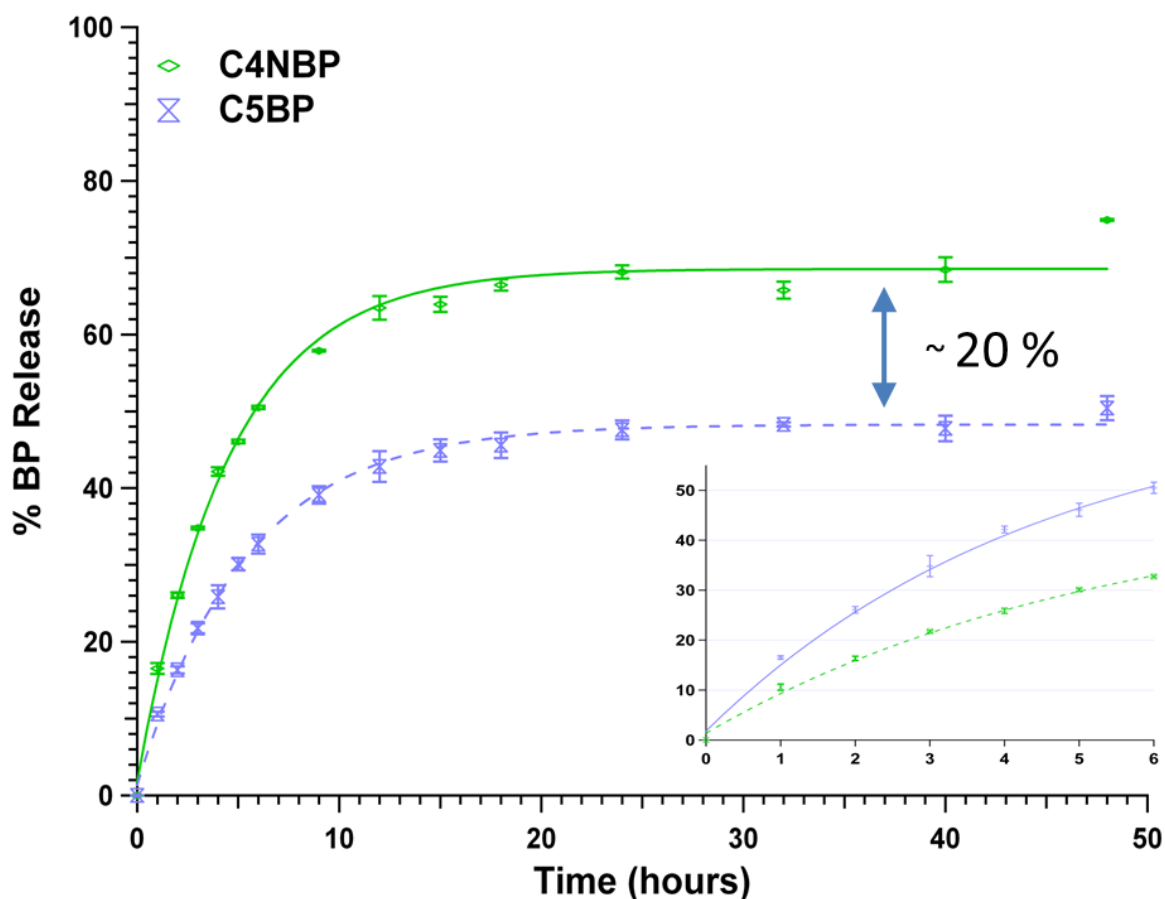
Figure 4-5. Comparison of release profiles of C5BP (a 5-atom, non-polar alkyl side-chain) and C4NBP (a 5-atom, amine-containing polar side-chain).

Another comparison, as performed for alkyl BPs, is between amino-BPs, in order to assess the influence of the systematic length increase of the aminoalkyl side chain. Figure 4-6shows comparative results of the controlled release of the family of BPs with hydrophilic, amine-containing side-chains (**PAM**, **ALE**, **C4NBP**, and **NER**). The results are quite intriguing, when compared to those for non-polar side chain BPs (Figure 4-2), as they reveal that the presence of the amine group on the side chain profoundly enhances release rates and final % release. **PAM**, with an ethylamine side chain, exhibits the fastest release and final % release (~ 80 %) of all. Side chain elongation in amino-BPs decelerates release rates and lowers final % release (*eg.* for **C4NBP** it is 70 %). Nevertheless, side chain length increase beyond 3 atoms (two C's, one N) does not induce systematic release reduction, as the results are nearly indistinguishable, thus pointing to a strong effect from the amine end-functionality surpassing that of the chain lengthening.
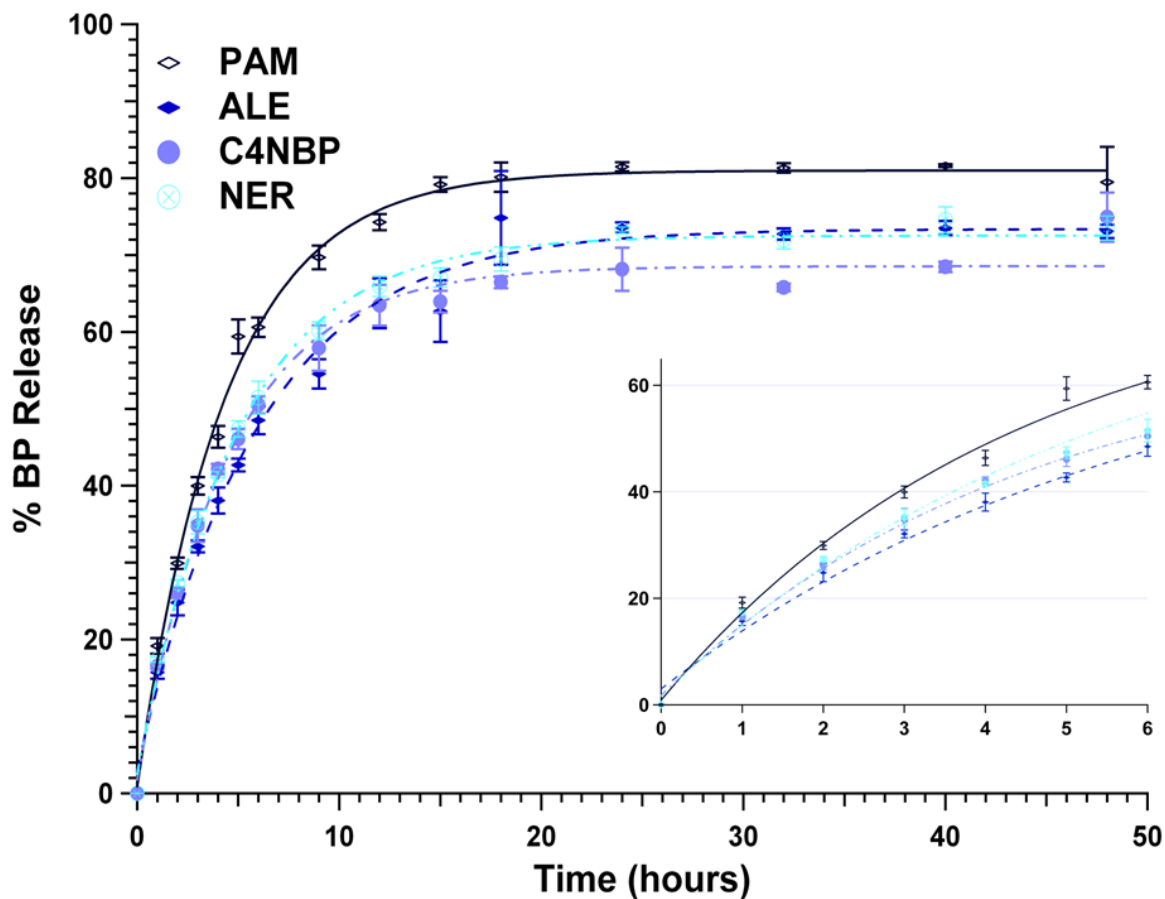
Figure 4-6. Long-term controlled release (48 hours) of BPs with hydrophilic, amine-containing side chain (PAM, ALE, C4NBP, and NER).

The release results presented in Figure 4-3 and Figure 4-6 clearly demonstrate some important trends. Both for amino-BPs and non-polar side-chain BPs, their rates and final % release correlate with their aqueous solubility trends (see Figure 4-7 and Figure 4-8).[319], [321]
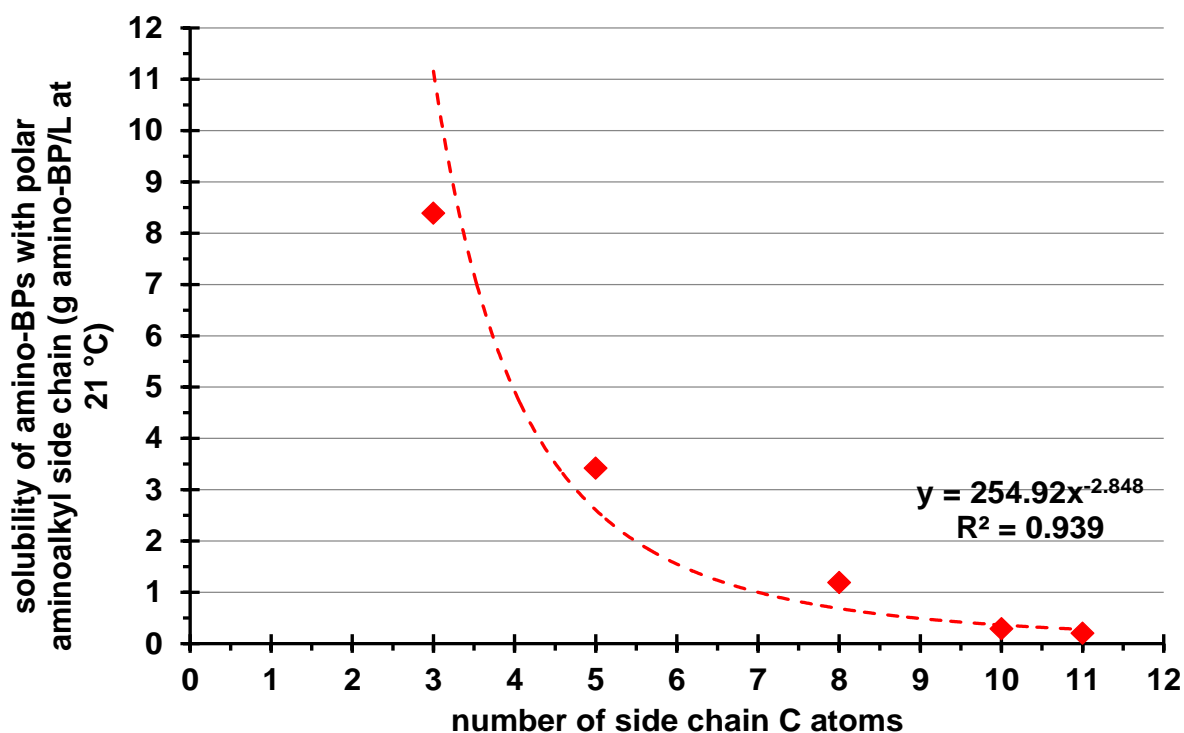
Figure 4-7. Correlation between the number of carbon atoms (length of aminoalkyl side chain) on amino-BPs and water solubility. Data taken from the SI of Reference 319.
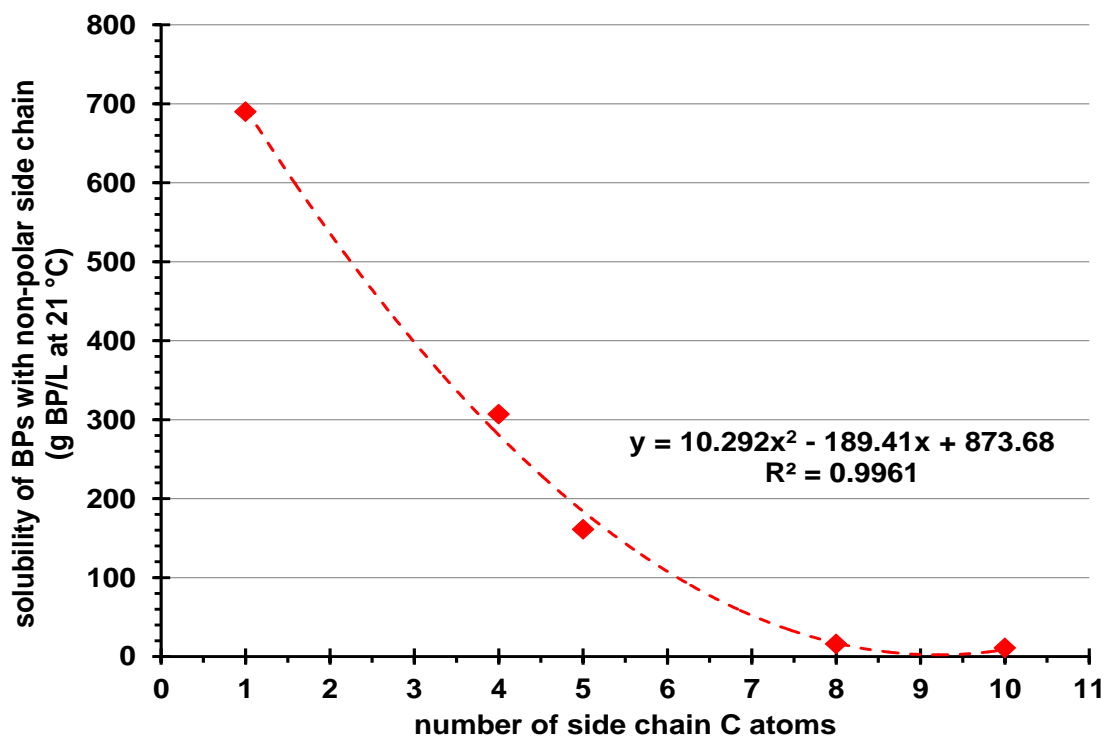
Figure 4-8. Correlation between the number of carbon atoms (length of aminoalkyl side chain) on amino-BPs and water solubility. Data taken from the SI of Reference 321.

Interestingly, none of the BP-loaded hydrogels reaches quantitative release (*eg.***ETID** reaches a ~ 75 % plateau after ~ 24 hours). In order to address whether the equilibrium reached after 24 h is final, and whether the remaining BP inside the hydrogel can be further released, step-wise experiments were performed, in which the supernatant was replaced with "fresh" aqueous medium after each release plateau was reached.

The results for **ETID**- and **PAM**-loaded gels are shown in Figure 4-9, supporting the conclusion that if equilibrium is "reset" the BPs continue to be released until a final, essentially quantitative release is achieved. Secondly, there is no detectable BP entrapped in possible inacessible gel pores, as indicated by the quantitative final release within 144 hours.
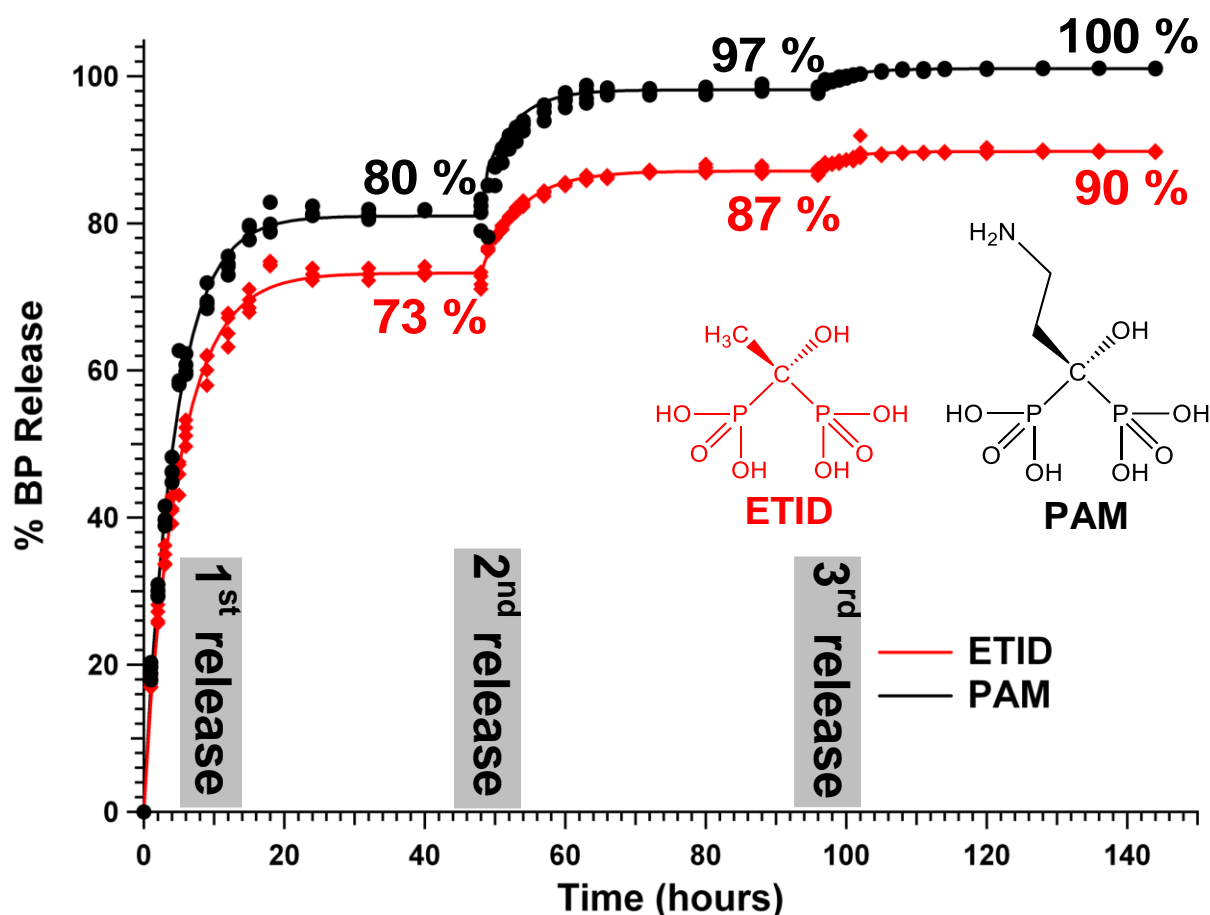
Figure 4-9. Step-wise, sustained controlled release of ETID and PAM for 144 hours.

"Empty", BP-free hydrogels were evaluated for their ability to be reloaded with drug. Thus, an "empty" (no BP) gel was prepared as "control". This gel, together with a second BP-loaded gel *after* its release, were exposed to an aqueous supernatant that contained the same content of **ETID** (as in a regular "loaded" gel) in order to assess whether the **ETID** will re-enter the gels. Indeed,

both gels absorbed ~ 20 % of dissolved **ETID**. Subsequently, both gels were subjected to the usual release conditions, delivering ~ 60 % of the absorbed **ETID** (Figure 4-10). Both gels exhibited the same behavior, proving that both "freshly-prepared" and "used" gels (after release) are robust and re-loadable.
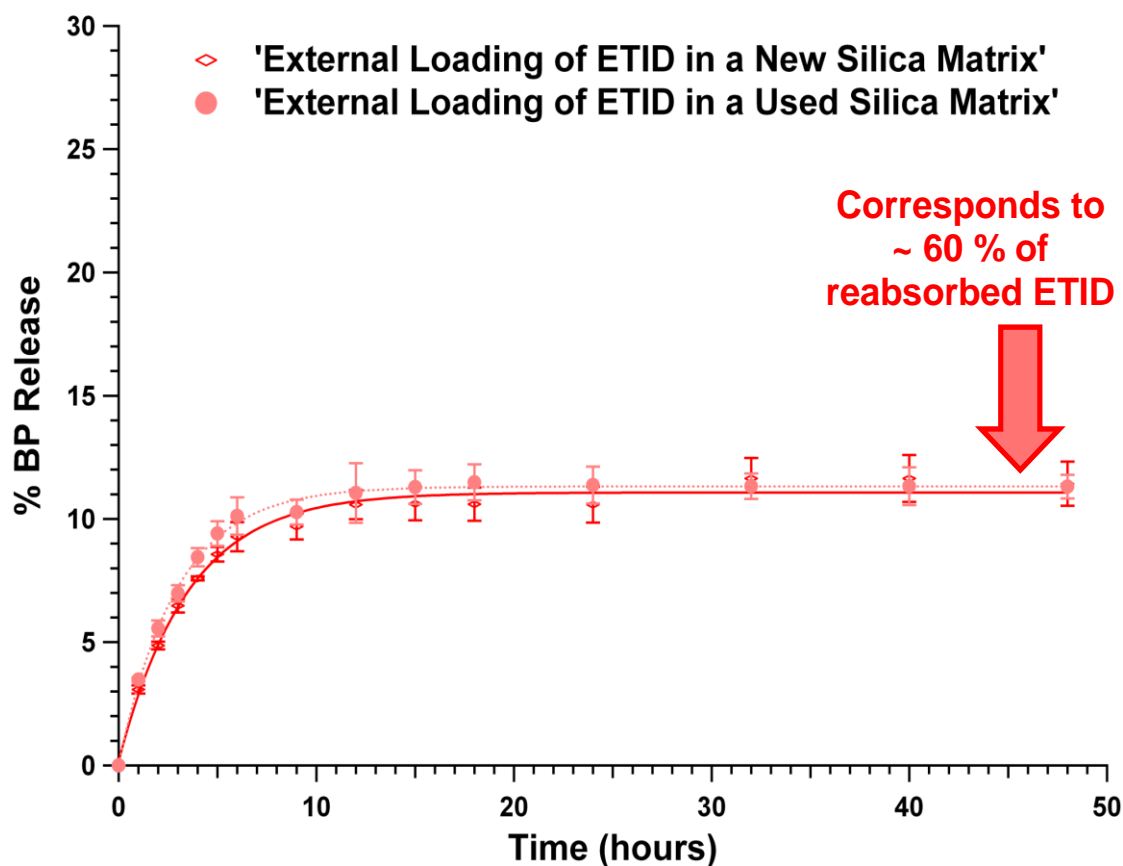
Figure 4-10. Release profiles of re-absorbed ETID from a freshly-prepared gel and from a used (emptied) gel.

All gels contain Na cations (from the silicate starting material). Next, we tried to study the effects arising from the different concentrations of sodium cations, focusing on one BP, **ETID**. For all release studies of **ETID** presented so far, the tetrasodium salt of **ETID** was used. Also, for the synthesis of the corresponding hydrogel we used disodium metasilicate pentahydrate ($Na_2SiO_3 \cdot 5H_2O$). Thus, six (6) sodium cations correspond to one (1) molecule of **ETID**. With that in mind we synthesized hydrogels using pure Etidronic acid and disodium metasilicate pentahydrate ($Na_2SiO_3 \cdot 5H_2O$), making sure to keep all other experimental parameters constant. The results are shown in Figure 4-11).

It becomes evident that the difference in concentration of sodium cations does not particularly affect the phenomenon of desorption and release. The small differences in the final value fall within the experimental error. In order to strengthen and confirm this claim, we synthesized hydrogels with the use of silicon dioxide and sodium hydroxide. For this case we used equal molar silicon mass (0.314 mmoles) as the gels resulted from the reagent sodium metasilicate pentahydrate and two and six times respectively additional molar amount of sodium hydroxide. In the first case the gel (with two molar equivalents of sodium) it was possible to keep all conditions identical (volume, temperature, pH, equimolar ratio of reagents, profile and gel surface (using exactly the same experimental beakers), while in the second case(six (6) molar equivalents of sodium) the hydrogel formed at the pH value of 10.5.
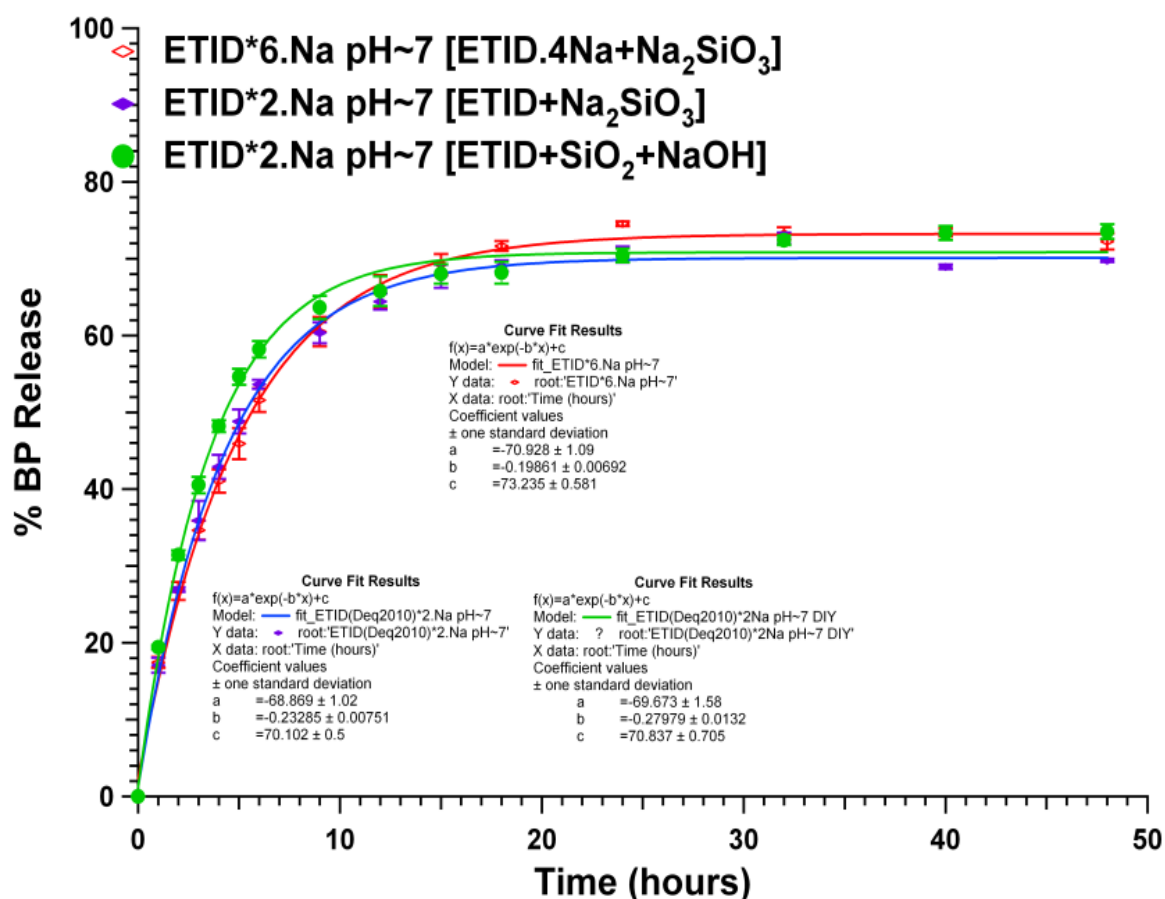
Figure 4-11. Effect of number of Na^+ ions per ETID molecule present in the gel, on ETID release.

The results and the release curves obtained thus far can be used for useful comparisons that can lead to important conclusions. As a first comparison, we can compare the release curves derived from two hydrogels: (a) the one that was synthesized using sodium metasilicate pentahydrate

($Na_2SiO_3 \cdot 5H_2O$) and "pure" **ETID** (as acid, no Na^+ cations), resulting in two Na^+ cations per **ETID** molecule, and (b) the analogous hydrogen resulting from the dilution/dissolution of silica (SiO_2) and sodium hydroxide ($2 \cdot NaOH$), resulting in four Na^+ cations per **ETID** molecule. It is evident that both exhibit consistent and very similar **ETID** diffusion/release. The slight difference in the release rate falls within the statistical error. It is important to mention that all experimental conditions were kept identical in both cases (Figure 4-11).

In order to extend the above comparison we added the release data derived from a hydrogel that was synthesized using the tetrasodium salt of **ETID**(ETID•4Na) and sodium metasilicate pentahydrate ($Na_2SiO_3 \cdot 5H_2O$), resulting in six Na^+ cations per **ETID** molecule. Again, all experimental conditions were kept identical to the previous gel syntheses. The release results were the same as with the aforementioned two gels. At the same time, it was confirmed that the nature of starting "silicon" reagent has no effect to the gel release properties. Figure 4-11 shows these combined results and leads to the conclusion that the diffusion of **ETID** remains unaffected by the method for preparing the gel and the number of Na^+ cations per **ETID** molecule (two, four or six).

Another gel was prepared from SiO_2 and 6moles of NaOH. This gel contains six Na^+ cations per **ETID** molecule, however it is different from the aforementioned gel made from the tetrasodium salt of **ETID**(ETID•4Na) and sodium metasilicate pentahydrate ($Na_2SiO_3 \cdot 5H_2O$) also containing six Na^+ cations per **ETID** molecule, in that the former can only be prepared at pH of 10.5, whereas the latter atpH 7. Hence, this was a nice opportunity to evaluate the effect of pH of gel preparation on therelease properties of these two gels. In Figure4-12 the results of these studies are shown. The comparison between the two release curves reveals that the significant difference in the pH of the hydrogel composition incurs a dramatic variation in **ETID**. This phenomenon, most likely, can be attributed to the silica gel nature that results from the polymerization of silica at these two different pH values. It should be mentioned that the curves presented and compared inFigure 4-12are derived from the fitting of the average of four repetitions (as well as the standard deviations) of these two hydrogels, enhancing the claim that the differences observed in diffusion rates are real, and beyond experimental error.
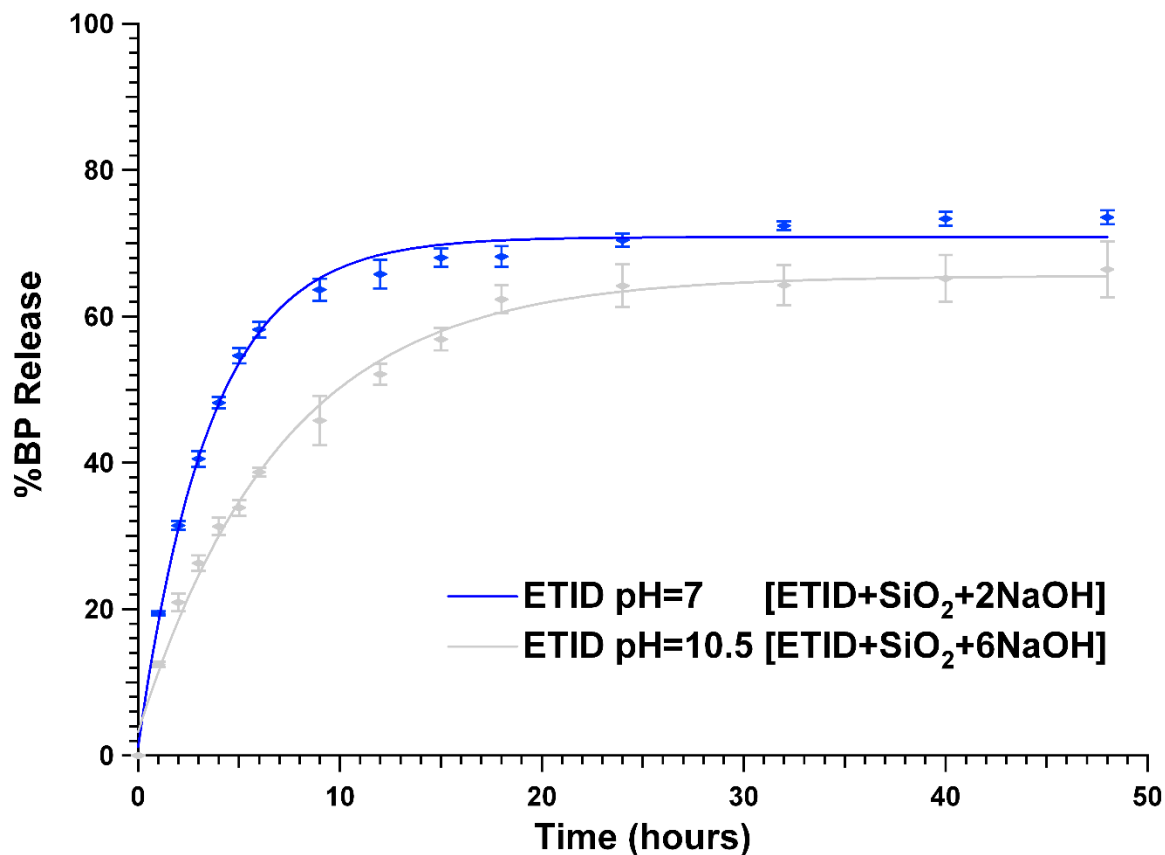
Figure 4-12. Effect of matrix's synthesis pH on ETID release.

Having reached important conclusions regarding the effects of the number of Na^+ cations per **ETID** molecule and pH of gel synthesis, we wanted to evaluate the effect of the nature of the alkali metal cations present in the hydrogel. Hence, we synthesized a number of new hydrogels, using potassium and rubidium hydroxide as bases.

In the case of potassium hydroxide (KOH),the studied hydrogel composition consisted of "pure" **ETID** (as acid, no Na^+ cations present), silicon dioxide (silica, SiO_2) and potassium hydroxide. Molar ratios were strictly followed in this case were K:Si:ETID 2:1:1. However, we were able to prepare the K-loaded gel only at thepH of10.5.Pellets of Potassium hydroxide, Silicic acid, and HEDP as acid were used for the synthesis of the matrices. The only difference between the two system was the molar ratio in KOH.
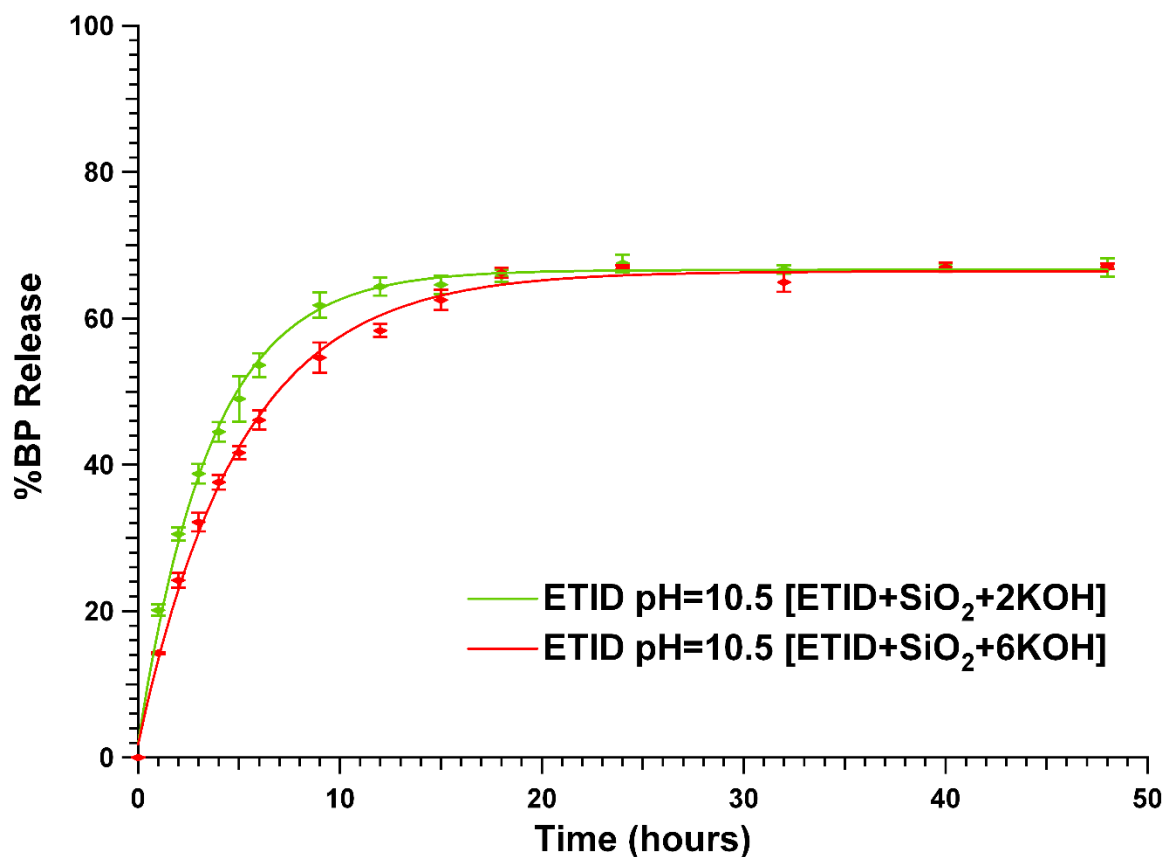
Figure 4-13. Effect of number of K$^+$ ions per ETID molecule present in the gel (the same pH value), on ETID release.

Based on the comparative curves presented in Figure 4-13 it is evident that the two identical (except for the number of K$^+$ cations) gel matrices have similar values in the final **ETID** release. A small but distinctive variation occurs in the initial rate of **ETID** release. As before, all other experimental conditions were identical (gel volume, supernatant volume, **ETID** concentration and temperature), hence the slight variation in release (slower in the case of six K$^+$ cations) observed must be due to the concentration of potassium cations. Therefore, increasing the number of potassium cations in the system slows down **ETID** release.

The comparison of the results of the two gel systems (sodium- and potassium-loaded gels) is shown in Figure 4-14. In order for the comparison to be meaningful, sodium- and potassium-loaded gels must be compared at the same pH value, while the M$^+$:Si:ETID molar ratio is the same for both gels, 6:1:1. It is evident that, while all other experimental conditions remain the same, increasing the ionic radius of the alkali metal cation contributes to small but distinct differences of the **ETID** release rate from the silica-hydrogel matrix. Final **ETID** release appears to be nearly the same for both gels. The same conclusions can be seen in comparisons presented in Figure 4-15a,b,c. On one

hand, increasing the ionic radius increases the release rate and the on the other hand the increase of the pH reduces the rate and the final release value.
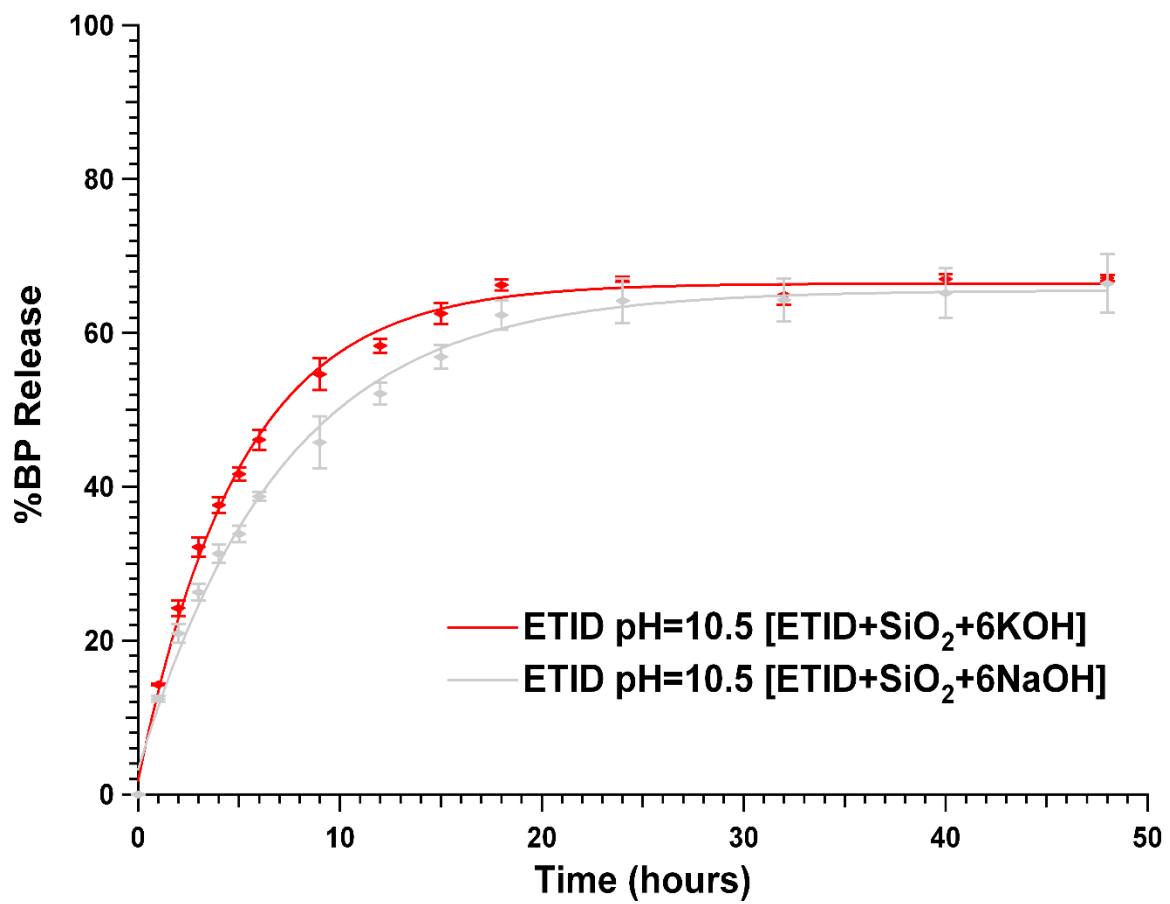
Figure 4-14. Effect of ion's nature per ETID molecule present in the gel (the same pH value) on ETID release.
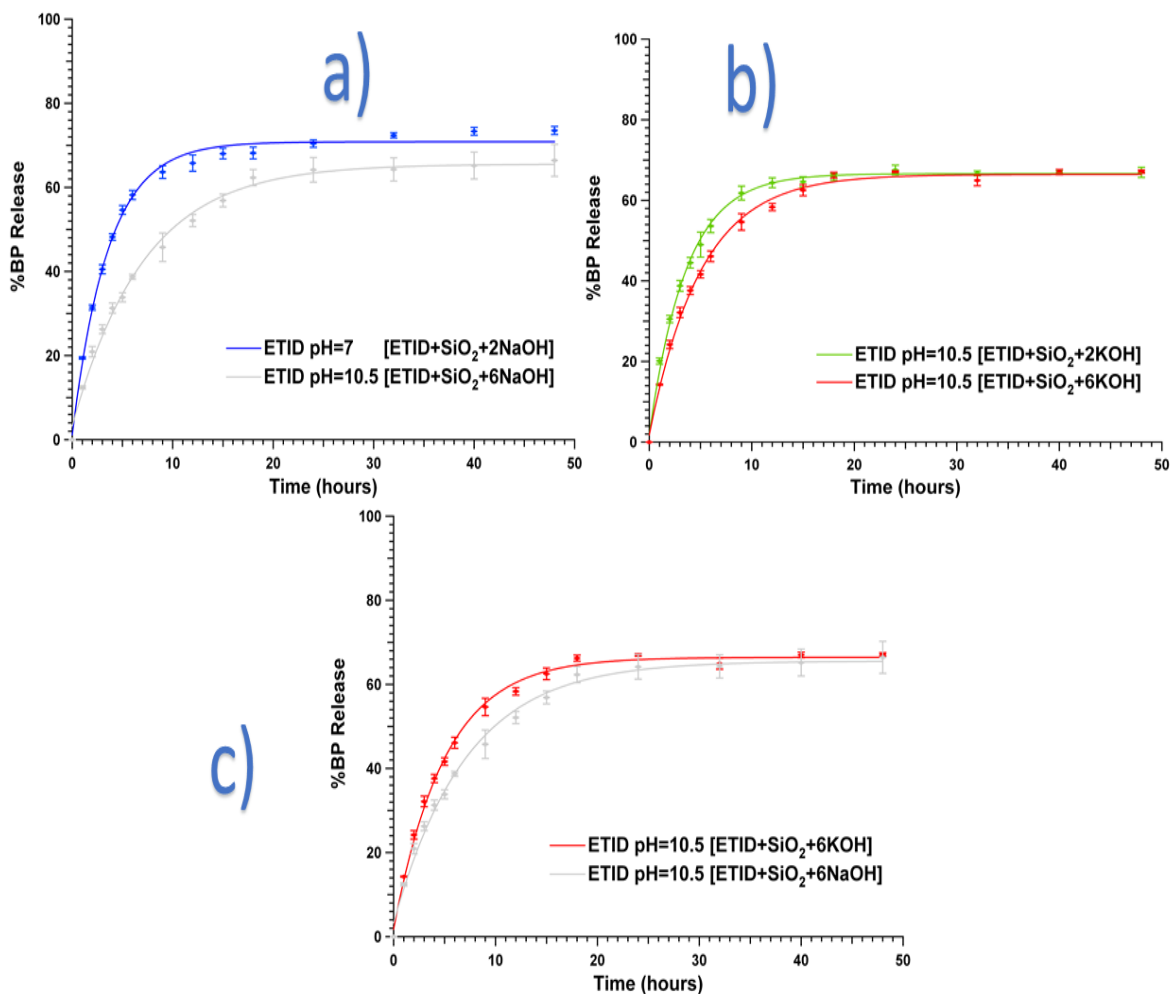
Figure 4-15. a) Effect of pH on ETID release from sodium-loaded gel matrices. b) Effect of the number of potassium cations per ETID molecule on ETID release. c) Comparison of ETID release rates between sodium- and potassium-loaded gels.

The synthesis of a rubidium-loaded hydrogel system (using 2 moles of rubidium hydroxide, RbOH) was selected as the next target. Based on the same approach, we kept all other experimental variables identical. The "complication" in the synthetic process was that no gel could form at a pH lower than 11. Figure 4-16 presents the normalized results from quadruplet experiments of the release of **ETID** from a Rb-loaded silica hydrogel matrix.
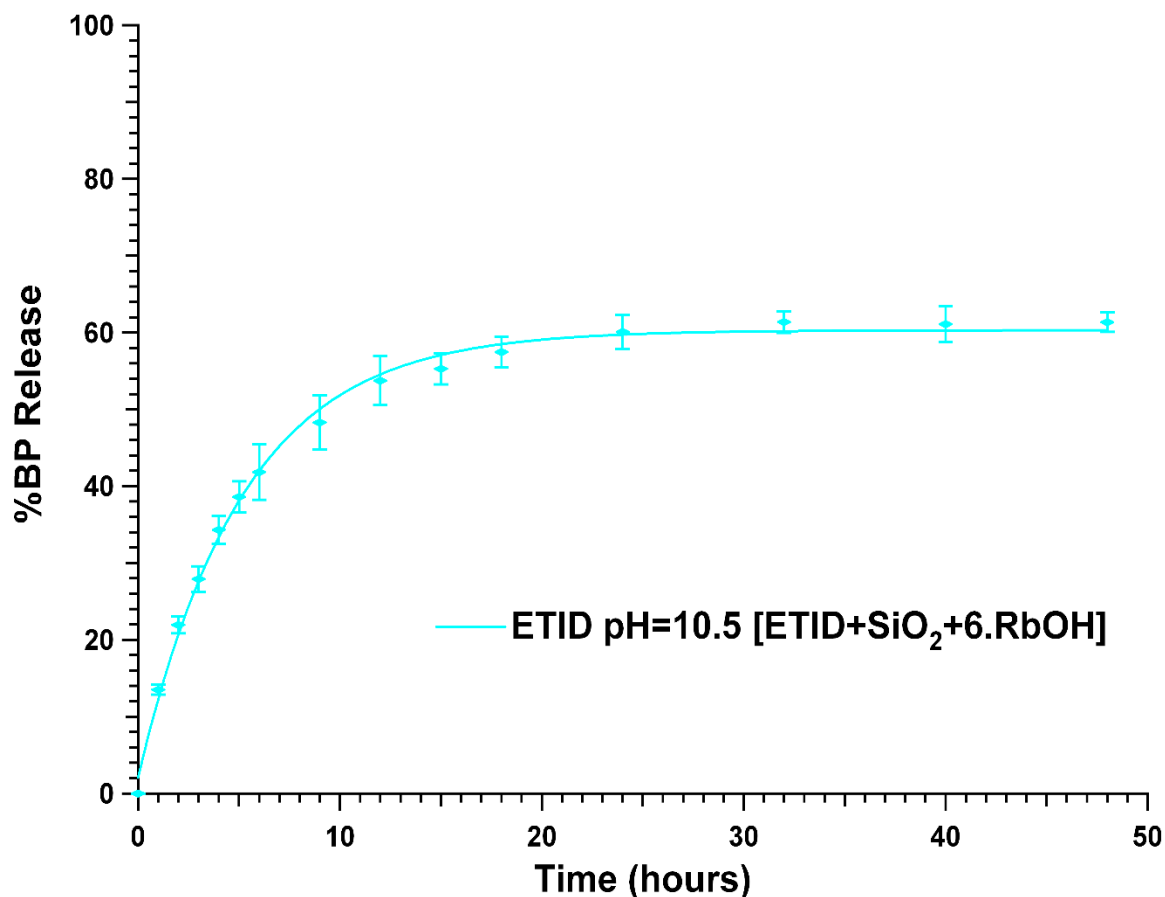
Figure 4-16. ETID release profile from a Rb-loaded hydrogel.

On the basis of the previous results obtained thus far on Na- and K-loaded hydrogels, we expected an increase in the **ETID** release rate with concurrent lowering of the final release value. In fact this new system, as indicated by the first 12hoursof the experiment, shows a behaviour that lies between the two previous systems. The final value of release is reduced considerably. In Figure 4-17 comparative curves are presented of the three different systems (sodium, potassium and rubidium) at the same pH values and identical molar ratios. Hence, the effect of the nature of the alkali metal cation (ionic radius/size) is inconclusive at this point.
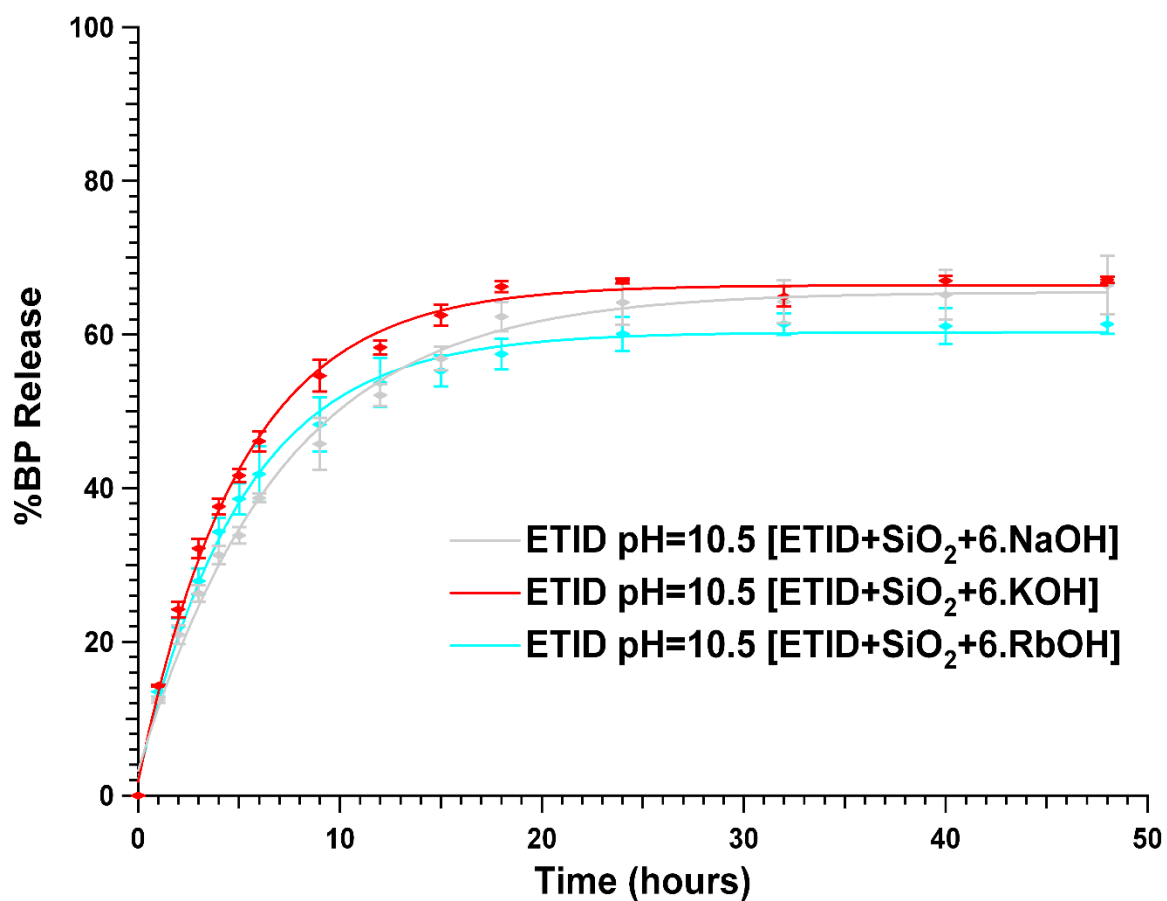
Figure 4-17. Release profiles of ETID from similar sodium-, potassium- and rubidium-loaded hydrogels.

5 CONCLUSIONS & PERSPECTIVES

In conclusion, in the present Thesis we have reported the fabrication, characterization and BP-release properties of silica-based gels. These gels can be prepared in a cost-effective manner from "cheap" reagents. They possess several attractive features such as:

(a) injectability (Figure 5-1)
(b) responsiveness to temperature
(c) re-usability
(d) re-loadability.

Furthermore, the BP drug release profiles can be fine-tuned to achieve the desired drug release, by altering several factors such as:

(a) temperature
(b) cations present
(c) pH
(d) inherent structural features of the BPs
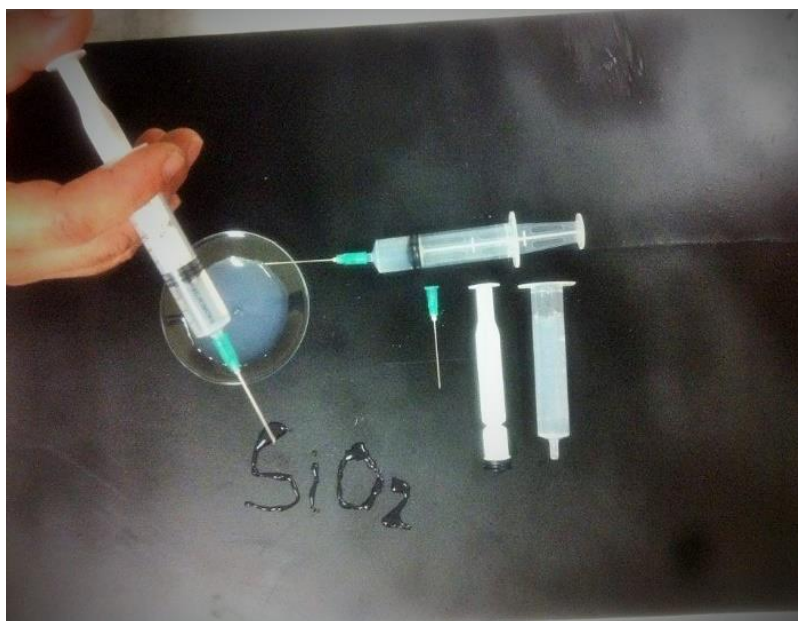
Figure 5-1. View of the silica gel-BP system injectability.

The phosphonates drugs were carefully selected and categorized into two families, ie. BPs with polar aminoalkyl side chain, and BPs with non-polar alkyl side chain. Their release from the aforementioned soft silica gel matrices into an aqueous medium mimicking that of the human stomach was systematically studied. Controllable release/diffusion was achieved. The presence and the absence of an amine group on the molecules backbones, the length of the carbon side-chain, the pH value of the matrix and the nature of the cations were the basic "tools" to control the rate and final release of the BP drugs.

The chemistry of soft silica gels presented can be extended in a number of ways. For example, functional silanes could be inserted into the silicate medium during the gel formation reaction, and, thus, modify the gel inner surface. A few representative silanes are presented below.

One such example is 3-aminopropyltrimethoxysilane (APTMOS, see Figure 5-2). Co-polymerization of APTMOS (after hydrolysis) with the silicate ions is expected to yield a modified gel, with alkylamine groups protruding from the inner gel pores. At pH regions below ~ 10 the amine groups will be protonated ($-CH_2CH_2CH_2NH_3^+$), therefore the gel should be cationic overall. This is expected to increase BP adsorption because of the anionic phosphonate groups, and hence further delay the BP release.
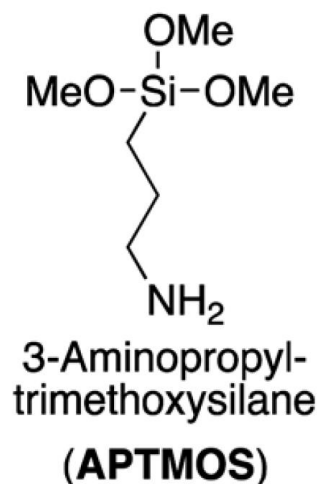
Figure 5-2. Schematic structure of 3-aminopropyltrimethoxysilane (APTMOS).

A second example of a silane-based modification of the gel is the use of TESPSA, Figure 5-3. TESPSA must undergo two processes before it can functionalize the silica gel surface. First, the silicate esters must be hydrolyzed, and secondly the succinic anhydrite ring must open, yielding the structure depicted in Figure 5-3.
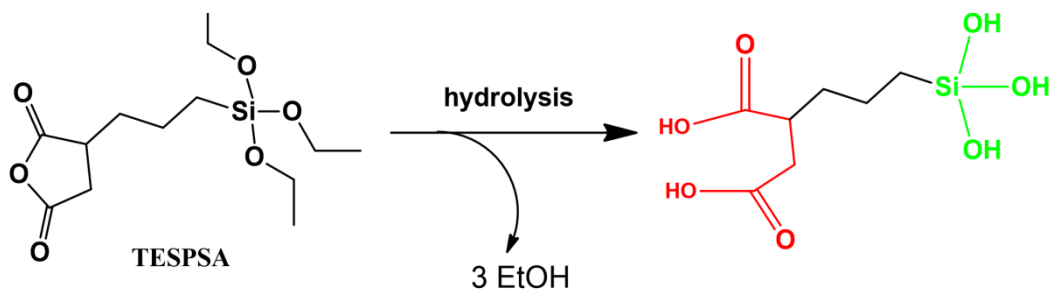
Figure 5-3. Hydrolysis and ring-opening of TESPSA yielding a polymerizable succinic acid analog.

Afterwards, grafting/copolymerization of the modified TESPSA can functionalize the gel surface, but in this case, with anionic moieties (two carboxylates), Figure 5-4. Hence, such a modified gel is expected to possess enhanced absorption properties towards cationic molecules. Therefore, in the framework of BP-related research, such a gel is expected to induce delayed release of aminoalkyl BPs.
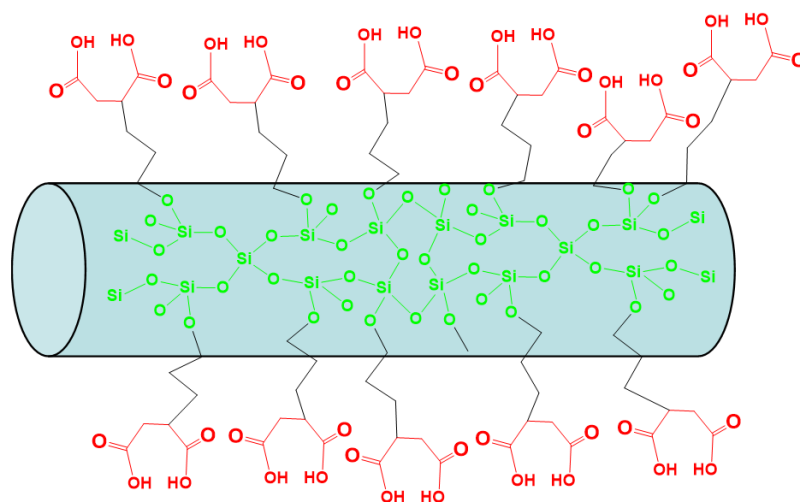
Figure 5-4. Grafting of the silica gel surface with TESPSA.

The use of soft silica gels presented could be extended beyond the field of pharmacology. For example, based on the re-loadability property of these gels, they could be used in adsorbing toxic organic substances from aqueous streams, an important environmental application for remediation of polluted aqueous systems.

6 BIBLIOGRAPHY

[1]   M. Peruzzini and L. Gonsalvi, Phosphorus Compounds: Advanced Tools in Catalysis and Material Sciences (Edited by Peruzzini, Maurizio and Gonsalvi, Luca), Dordrecht: Springer, 2011.

[2]   K. Popov, H. Rönkkömäki and L. Lajunen, "Critical evaluation of stability constants of phosphonic acids (IUPAC Technical Report)," *Pure Appl. Chem.,* no. 73, pp. 1641-1677, 2001.

[3]   K. Demadis, Water treatment processes (Edited by Konstantinos D.Demadis), New York: Nova Science Publishers, 2012.

[4]   "Human & Environmental Risk Assessment on ingredients of European household cleaning products: Phosphonates, taken from http://www.heraproject.com.," 2014.

[5]   V. Sastri, Corrosion Inhibitors: Principles and Applications. (Edited by V. S. Sastri), Chichester: Wiley, 1998.

[6]   W. Frenier and S. Barber, "Choose the best heat exchanger cleaning method.," *Chem. Eng. Progress,* no. July, pp. 37-44, 1998.

[7]   E. Valsami-Jones, Phosphorus in environmental technology: Principles and applications. (Edited by E. Valsami Jones(, London: IWA Publishing, 2004.

[8]   S. Failla, G. Consiglio and P. Finocchiaro, "New Diamine Phosphonate Monomers as Flame-

Retardant Additives for Polymers," *Phosphorus Sulfur Silicon,* vol. 186, pp. 983-988., 2011.

[9]   G. A. Consiglio, S. Failla, P. Finocchiaro and V. Siracusa, "Synthesis of new ortho-hydroxy aryl phosphonate monomers.," *Phosphorus, Sulfur Silicon Relat. Elem.,* no. 134/135, pp. 413-418, 1998.

[10] P. Finocchiaro, A. D. La Rosa και A. Recca, *Curr. Trends Polymer Sci. ,* αρ. 4, pp. 241-246, 1999.

[11] M. Frigione, A. Maffezzoli, P. Finocchiaro and S. Failla, "Cure kinetics and properties of epoxy resins containing a phosphorous-based flame retardant," *Adv. Polymer Tech.,* no. 22, pp. 329-342, 2003.

[12] A. La Rosa, S. Failla, P. Finocchiaro, A. Recca, V. Siracusa, J. Carter and P. McGrail, *J. Polymer Eng,* no. 19, pp. 151-160, 1999.

[13] M. Hagiwara, S. Koboshi and H. Kobayashi, "Pat. Eur. N 293,729," *Chem. Abstr.,* 1988.

[14] Ash, M.; Ash, I., Handbook of green chemicals (Compiled by Michael Ash and Irene Ash), New York: Synapse Information Resources Inc., 2004.

[15] J. Burns, T. Shehee, A. Clearfield and D. Hobbs, "Separation of americium from curium by oxidation and ion exchange.," *Anal. Chem.,* no. 84, pp. 6930-2, 2012.

[16] H. Someda, A. EI-Zahhar, M. Shehata and H. EI-Naggar, "Extraction studies of uranyl ion UO 22+ by dihexyl-N, N-diethyl carbamoyl methyl phosphonate (DHDECMP).," *J. Radioanal. Nucl. Chem.,* no. 228, pp. 37-41, 1998.

[17] T. Fourie and P. Van der Walt, "Complexometric titration of thorium with methylene diphosphonic acid: Application to the determination of methylene diphosphonic acid in labelling kits," *Appl. Radiat. Isot.,* no. 38, pp. 158-159, 1987.

[18] E. Brunet, L. Jiménez, M. Rodriguez, V. Luu, G. Muller, O. Juanes and J. Rodríguez-Ubis, "The use of lanthanide luminescence as a reporter in the solid state: Desymmetrization of the prochiral layers of γ-zirconium phosphate/phosphonate and circularly polarized luminescence," *Microporous Mesoporous Mater.,* no. 169, pp. 222-34, 2013.

[19] M. Wharmby and P. Wright, "Open Framework and Microporous Metal Phosphonate MOFs with Piperazine-based Bisphosphonate Linkers," in *Metal Phosphonate Chemistry: From Synthesis to Applications.*, London, Royal Society of Chemistry, 2012, pp. 317-343.

[20] P. Silva, F. Vieira, A. Gomes, D. Ananias, J. Fernandes, S. Bruno, R. Soares, A. Valente, J. Rocha and F. Almeida Paz, "Thermal transformation of a layered multifunctional network into a metal-organic framework based on a polymeric organic linker.," *J. Am. Chem. Soc,* no. 133, pp. 15120-38, 2011.

[21] K. Popov, V. Yachmenev, A. Kolosov and N. Shabanova, "Effect of soil electroosmotic flow enhancement by chelating reagents.," *Colloids Surf. A,* no. 160, pp. 135-140, 1999.

[22] R. Hilderbrand, The role of phosphonates in living systems. (Edited by Richard L. Hilderbrand), Boca Raton, FL,: CRC Press, 1983.

[23] M. Notelovitz, Osteoporosis: Prevention, diagnosis and management, New York: Professional Communications Inc., 2008.

[24] B. Nowack, "The behavior of phosphonates in wastewater treatment plants of Switzerland," *Wat. Res,* vol. 32, pp. 1271-1279, 1998.

[25] A. Popov, H. Ronkkomaki, K. Popov, L. Lajunen and A. Vendilo, "31P NMR protonation equilibrium study of iminobis(methylenephosphonic acid) and its derivatives at high pH," *Inorg. Chim. Acta,* no. 8, pp. 1-7, 2003.

[26] E. Ruiz-Agudo, C. Rodriguez-Navarro and E. Sebastian-Pardo, "Sodium Sulfate Crystallization in the Presence of Phosphonates: Implications in Ornamental Stone Conservation.," *Cryst. Growth Des.,* no. 6, pp. 1575-1583, 2006.

[27] V. Deluchat, J. Bollinger, B. Serpaud and C. Caullet, "Divalent cations speciation with three phosphonate ligands in the pH-range of natural waters.," *Talanta,* no. 44, pp. 897-907, 1997.

[28] M. B. Tomson, A. T. Kan and J. E. Oddo, "Acid/Base and Metal Complex Solution Chemistry of the Polyphosphonate DTPMP versus Temperature and Ionic Strength.," *Langmuir,* vol. 10, no. 5, pp. 1442-1449, 1994.

[29] A.-L. Alanne, H. Hyvönen, M. Lahtinen, M. Ylisirniö, P. Petri Turhanen, E. Kolehmainen, S. Peräniemi and J. Vepsäläinen, "Systematic study of the physicochemical properties of a homologous series of aminobisphosphonates.," *Molecules,* vol. 17, pp. 10928-45, 2012.

[30] K. Popov, E. Niskanen, H. Ronkkomaki and L. Lajunen, "31 P NMR Study of organophosphonate protonation equilibrium at high pH.," *New J. Chem,* no. 23, pp. 1209-13, 1999.

[31] K. Sawada, T. Miyagawa, T. Sakaguchi and K. Doi, "Structure and thermodynamic properties of aminopoly-phosphonate complexes of the alkaline-earth metal Ions," *J. Chem. Soc. Dalton Trans.,* pp. 3777-84, 1993.

[32] K. Sawada, T. Araki, T. Suzuki and K. Doi, "Complex formation of aminopolyphosphonates. 2. Stability and structure of nitrilotris(methylenephosphonato) complexes of the divalent transition metal ions in aqueous solution," *Inorg. Chem.,* no. 28, pp. 2687-2688, 1989.

[33] K. Sawada, T. Araki and T. Suzuki, "Complex formation of amino polyphosphonates. 1. Potentiometric and nuclear magnetic resonance studies of nitrilotris(methylenephosphonato) complexes of the alkaline-earth-metal ions," *Inorg. Chem.,* no. 26, pp. 1199-1204, 1987.

[34] R. Motekaitis, I. Murase and M. A.E., "Equilibriums of ethylenediamine-N,N,N',N'-tetrakis(methylenephosphonic) acid with copper(II), nickel(II), cobalt(II), zinc(II), magnesium(II), calcium(II), and iron(III) ions in aqueous solution," *Inorg. Chem.,* no. 15, pp. 2303-2306, 1976.

[35] R. Motekaitis, I. Murase and A. Martell, "New multidentate ligands. XIII. Ethylenediaminetetra(methylenephosphonic) acid.," *Inorg. Nucl. Chem. Lett.,* no. 7, pp. 1103-07, 1971.

[36] V. Deluchat, B. Sepraud, E. Alves, C. Caullet and J. Bollinger, "Protonation and Complexation Constants of Phosphonic Acids with Cations of Environmental Interest.," *Phosphorus Sulfur Silicon,* no. 209, pp. 109-110, 1996.

[37] Stone, A.T.; Knight, M.A.; Nowack, B.;, "Speciation and Chemical Reactions of Phosphonate Chelating Agents in Aqueous Media.," in *Chemicals in the environment*, ACS Symposium Series 806,, 2002, pp. 59-94.

[38] J. Gałezowska, P. Kafarski, H. Kozłowski, P. Młynarz, V. Nurchi and T. Pivetta, *Inorg. Chim. Acta.,* no. 362, pp. 707-13, 2009.

[39] P. Garczarek, J. Janczak and J. Zon, "New multifunctional phosphonic acid for metal phosphonate synthesis.," *J. Mol. Struct.,* vol. 1036, no. 505, pp. 505-509, 2013.

[40] D. Boczula, A. Cały, D. Dobrzynska, J. Janczak and J. Zon, "Structural and vibrational characteristics of amphiphilic phosphonate salts," *J. Mol. Struct.,* vol. 1007, no. 11, pp. 220-6, 2012.

[41] Z. Du, C. Zhao, Z. Zhou and K. Wang, "Two intricate hydrogen-bonded networks formed by m-sulfophenylphosphonic acid, melamine, and water molecules," *J. Mol. Struct.,* vol. 1035, no. 183, pp. 183-189, 2013.

[42] K. Demadis, E. Barouda, H. Zhao and R. Raptis, "Structural architectures of charge-assisted, hydrogen-bonded, 2D layered amine···tetraphosphonate and zinc···tetraphosphonate ionic materials," *Polyhedron,* no. 29, pp. 3361-67, 2009.

[43] K. Demadis, R. Raptis and P. Baran, "Chemistry of Organophosphonate Scale Growth Inhibitors: 2. Structural Aspects of 2-Phosphonobutane-1,2,4-Tricarboxylic Acid Monohydrate (PBTC.H2O).," *Bioinorg. Chem. Appl.,* Vols. 3-4, pp. 119-34, 2005.

[44] T. Grawe, G. Schäfer and T. Schrader, "Molecular Recognition of Amidines in Water.," *Org. Lett.,* no. 5, pp. 1641-4, 2003.

[45] A. Clearfield and K. Demadis, Metal Phosphonate Chemistry: From Synthesis to Applications. (Edited by Clearfield, A. and Demadis, K.D.), London: Royal Society of Chemistry, 2012.

[46] C. Cheng and K. Lin, "A lithium ethylenediphosphonate containing lithium chains and symmetric hydrogen bonds.," *Acta Cryst. C.,* vol. 62, no. 8, pp. 363-5, 2006.

[47] D. Vega, D. Fernaandez and J. Ellena, "Disodium pamidronate.," *Acta Cryst.,* vol. 57, no. 2, pp. 77-80, 2002.

[48] N. Padalwar, C. Pandu and K. Vidyasagar, "Monovalent metal phenylphosphonates and phenylarsonates: Single crystal X-ray structures of A(HO3PPh)(H2O3PPh) (A = K, Rb, Cs, Tl) and Na(HO3AsPh)(H2O3AsPh) and methylamine intercalation of A(HO3PPh)(H2O3PPh) (A = Li, Na, K, Tl)," *J. Solid State Chem.,* no. 203, pp. 321-25.

[49] A. Ayi, A. Burrows, M. Mahon and V. Pop, "Sodium Trihydrogen-1,4-Benzenediphosphonate: An Extended Coordination Network.," *J. Chem. Crystallogr.,* no. 41, pp. 1165-68, 2011.

[50] T. Kinnibrugh, N. Garcia and A. Clearfield, "Structural differences of metal biphenylenebisphosphonate with change in the alkali metal.," *J. Solid State Chem.,* no. 187, pp. 149-58, 2012.

[51] J. Mazurek, T. Lis, G. Rusek and K. Krajewski, "Nitro Derivatives of 3-Acetamidobenzyl

Acetate.," *Acta Cryst. C.,* vol. 54, no. 6, pp. 863-867, 1998.

[52] K. Demadis and P. J. Baran, "Chemistry of organophosphonate scale growth inhibitors: two-dimensional, layered polymeric networks in the structure of tetrasodium 2-hydroxyethyl-amino-bis(methylenephosphonate)," *J. Sol. St. Chem.,* no. 177, pp. 4768-76, 2004.

[53] K. Demadis, J. Sallis, R. Raptis and P. Baran, "A crystallographically characterized nine-coordinate calcium-phosphocitrate complex as calcification inhibitor in vivo.," *J. Am. Chem. Soc.,* no. 123, pp. 10129-30, 2001.

[54] K. Demadis and S. Katarachia, "Metal-Phosphonate Chemistry: Synthesis, Crystal Structure of Calcium-Amnotris (Methylene Phosphonate) and Inhibition of CaCO3 Crystal Growth," *Phosphorus Sulfur Silicon,* no. 179, pp. 627-48, 2004.

[55] K. Demadis, S. Katarachia, H. Zhao, R. Raptis and P. Baran, "Alkaline Earth Metal Organotriphosphonates: Inorganic−Organic Polymeric Hybrids from Dication−Dianion Association.," *Cryst. Growth Des.,* vol. 6, no. 4, pp. 836-38, 2006.

[56] K. Demadis, P. Lykoudis, R. Raptis and G. Mezei, "Phosphonopolycarboxylates as Chemical Additives for Calcite Scale Dissolution and Metallic Corrosion Inhibition Based on a Calcium-Phosphonotricarboxylate Organic−Inorganic Hybrid," *Cryst. Growth Des.,* vol. 6, no. 5, pp. 1064-67, 2006.

[57] E. Barouda, K. Demadis, S. Freeman, F. Jones and M. Ogden, "Barium Sulfate Crystallization in the Presence of Variable Chain Length Aminomethylenetetraphosphonates and Cations (Na+ or Zn2+)," *Cryst. Growth Des.,* no. 7, pp. 321-327, 2007.

[58] K. Demadis, M. Papadaki, R. Raptis and H. Zhao, "2D and 3D alkaline earth metal carboxyphosphonate hybrids: Anti-corrosion coatings for metal surfaces," *J. Solid State Chem.,* no. 181, pp. 679-683, 2008.

[59] K. Demadis, M. Papadaki, R. Raptis and H. Zhao, "Corrugated, Sheet-Like Architectures in Layered Alkaline-Earth Metal R,S-Hydroxyphosphonoacetate Frameworks: Applications for Anticorrosion Protection of Metal Surfaces.," *Chem. Mater.,* vol. 20, no. 15, pp. 4835-46, 2008.

[60] K. Demadis, E. Barouda, R. Raptis and H. Zhao, "Metal tetraphosphonate "wires" and their corrosion inhibiting passive films.," *Inorg. Chem.,* no. 48, pp. 819-21, 2009.

[61] K. Demadis, Z. Anagnostou and H. Zhao, "Novel Calcium

Carboxyphosphonate/polycarboxylate Inorganic−Organic Hybrid Materials from Demineralization of Calcitic Biomineral Surfaces.," *ACS Appl. Mater. Interfaces,* vol. 1, no. 1, pp. 35-38, 2009.

[62] K. Demadis, E. Barouda, N. Stavgianoudaki and H. Zhao, "Inorganic−Organic Hybrid Molecular Ribbons Based on Chelating/Bridging, "Pincer" Tetraphosphonates, and Alkaline-Earth Metals.," *Cryst. Growth Des.,* vol. 9, no. 3, pp. 1250-3, 2009.

[63] E. Akyol, M. Öner, E. Barouda and K. Demadis, "Systematic structural determinants of the effects of tetraphosphonates on gypsum crystallization.," *Cryst. Growth Des.,* no. 9, pp. 5154-5154, 2009.

[64] K. Demadis, M. Papadaki and I. Cisarova, "Single-Crystalline Thin Films by a Rare Molecular Calcium Carboxyphosphonate Trimer Offer Prophylaxis From Metallic Corrosion," *ACS-Appl. Mater. Interf.,* vol. 2, no. 7, pp. 1814-16, 2010.

[65] R. Colodrero, A. Cabeza, P. Olivera-Pastor, J. Rius, D. Choquesillo-Lazarte, J. García-Ruiz, M. Papadaki, K. Demadis and M. Aranda, "Common Structural Features in Calcium Hydroxyphosphonoacetates. A High-Throughput Screening.," *Cryst. Growth Des.,* vol. 11, no. 5, pp. 1713-22, 2011.

[66] K. Demadis, S. Katarachia and M. Koutmos, "Crystal growth and characterization of zinc-(amino-tris-(methylenephosphonate)) organic-inorganic hybrid networks and their inhibiting effect on metallic corrosion," *Inorg. Chem. Comm.,* no. 8, pp. 254-8, 2005.

[67] K. Demadis, C. Mantzaridis, R. Raptis and G. Mezei, "Metal-organotetraphosphonate inorganic-organic hybrids: crystal structure and anticorrosion effects of zinc hexamethylenediaminetetrakis(methylenephosphonate) on carbon steels.," *Inorg. Chem.,* no. 44, pp. 4469-71, 2005.

[68] S. Lodhia, A. Turner, M. Papadaki, K. Demadis and G. Hix, "Polymorphism, composition, and structural variability in topology in 1D, 2D, and 3D copper phosphonocarboxylate materials.," *Cryst. Growth Des.,* no. 9, pp. 1811-22, 2009.

[69] K. Demadis, M. Papadaki, M. Aranda, A. Cabeza, P. Olivera-Pastor and Y. Sanakis, "tepwise Topotactic Transformations (1D to 3D) in Copper Carboxyphosphonate Materials: Structural Correlations," *Cryst. Growth Des.,* no. 10, pp. 357-64, 2010.

[70] R. Colodrero, A. Cabeza, P. Olivera-Pastor, D. Choquesillo-Lazarte, J. Garcia-Ruiz, A.

Turner, G. Ilia, B. Maranescu, K. Papathanasiou, K. Demadis, G. Hix and M. Aranda, "Divalent Metal Vinylphosphonate Layered Materials: Compositional Variability, Structural Peculiarities, Dehydration Behavior, and Photoluminescent Properties," *Inorg. Chem.,* vol. 50, no. 21, pp. 11202-11, 2011.

[71] J. Weber, G. Grossmann, K. Demadis, N. Daskalakis, E. Brendler, M. Mangstl and J. Schmedt auf der Günne, "Linking 31P magnetic shielding tensors to crystal structures: experimental and theoretical studies on metal(II) amino-tris(methylenephosphonates)," *Inorg. Chem.,* no. 51, pp. 11466-77, 2012.

[72] X.-Q. Zhao, B. Zhao, Y. Ma, W. Shi, P. Cheng, Z.-H. Jiang, D.-Z. Liao and S.-P. Yan, "Lanthanide(III)−Cobalt(II) Heterometallic Coordination Polymers with Radical Adsorption Properties," *Inorg. Chem.,* no. 46, pp. 5832-5834, 2007.

[73] S. Kunnas-Hiltunen, E. Laurila, M. Haukka, J. Vepsäläinen and M. Ahlgrén, "Organic-Inorganic Hybrid Materials: Syntheses, X-ray Diffraction Study, and Characterisations of Manganese, Cobalt, and Copper Complexes of Modified Bis(phosphonates)," *Z. Anorg. Allg. Chem.,* no. 636, pp. 710-720, 2010.

[74] G. Hix and K. Harris, "Synthesis of layered nickel phosphonate materials based on a topotactic approach.," *J. Mater. Chem.,* no. 8, pp. 579-84, 1998.

[75] K. Gholivand and A. Farrokhi, "Supramolecular hydrogen-bonded frameworks from a new bisphosphonic acid and transition metal ions," *Z. Anorg. Allg. Chem.,* no. 637, pp. 263-68, 2011.

[76] N. Calin and S. Sevov, "Novel Mixed-Valence Heteropolyoxometalates: A Molybdenum Diphosphonate Anion [MoV7MoVIO16(O3PPhPO3H)4]3- and its One- and Two-Dimensional Assemblies.," *Inorg. Chem.,* no. 42, pp. 7304-08, 2003.

[77] E. Dumas, C. Sassoye, K. Smith and S. Sevov, "Synthesis and characterization of [Mo(7)O(16)(O(3)PCH(2)PO(3))(3)]:(8-) a mixed-valent polyoxomolybdenum diphosphonate anion with octahedrally and tetrahedrally coordinated molybdenum.," *Inorg. Chem.,* no. 41, pp. 4029-32, 2002.

[78] C. du Peloux, A. Dolbecq, P. Mialane, J. Marrot and F. Sécheresse, "Template synthesis of {(MoV2O4)(O3PCH2PO3)}n clusters (n = 3, 4, 10): solid state and solution studies.," *J. Chem. Soc. Dalton Trans.,* no. 8, pp. 1259-1263, 2004.

[79] H. Li, L. Zhang, G. Li, Y. Yu, Q. Huo and Y. Liu, "Synthesis, characterization, and crystal structure of two novel 3D cadmium organotriphosphonates complexes.," *Microporous Mesoporous Mater.,* no. 131, pp. 186-191, 2010.

[80] J. Mao, Z. Wang and A. Clearfield, "The role of deprotonation of the ligand on the structures of metal phosphonates: synthesis, characterization and crystal structures of two new metal diphosphonates with a 1D double chain and a 2D layer structure.," *J. Chem. Soc., Dalton Trans.,,* pp. 4457-63, 2002.

[81] R.-L. Sang and L. Xu, "Unprecedented helix-based microporous metal–organic frameworks constructed from a single ligand," *Chem. Commun.,* pp. 6143-6145, 2008.

[82] S.-F. Tang, X.-B. Pan, X.-X. Lu and X.-B. Zhao, "Investigation on three new metal carboxydiphosphonates: Syntheses, structures, magnetic and luminescent properties.," *J. Solid State Chem.,* no. 197, pp. 139-146, 2013.

[83] Z. Du, C. Zhao, L. Dong, X. Deng and Y. Sun, "Tube- or cage-containing layered cadmium(II) and zinc(II) phosphonates decorated by sulfone groups," *J. Coord. Chem.,* no. 65, pp. 813-822, 2012.

[84] C. Samanamu, E. Zamora, L. Lesikar, J. Montchamp and A. Richards, "5-Pyrimidyl phosphonic acid as a building block for the synthesis of coordination polymers.," *CrystEngComm,* vol. 10, no. 10, pp. 1372-78, 2008.

[85] D. Sagatys, C. Dahlgren, G. Smith, R. Bott and J. White, "The complex chemistry of N-(phosphonomethyl)glycine (glyphosate): preparation and characterization of the ammonium, lithium, sodium (4 polymorphs) and silver(I) complexes.," *J. Chem. Soc., Dalton Trans.,* vol. 2000, no. 19, pp. 3404-10, 2000.

[86] J. Fry, C. Samanamu, J. Montchamp and A. Richards, "A Mild Synthetic Route to Zinc, Cadmium, and Silver Polymers with 2-Pyridyl Phosphonic Acid: Synthesis and Analysis," *Eur. J. Inorg. Chem.,* pp. 463-70, 2008.

[87] W. Power, M. Lumsden and R. Wasylishen, "Solid-state 31P NMR studies of mercury(II) phosphonates. Anisotropies of the 31P chemical shift and the 31P-199Hg indirect spin-spin coupling," *Inorg. Chem.,* no. 30, pp. 2997-3002, 1991.

[88] P. Vojtíšek, J. Rohovec and I. Lukeš, "COMPLEXES OF MERCURY(II) WITH TETRAETHYL 2,2'-BIPYRIDYL-4,4'-DIPHOSPHONATE," *Collect. Czech. Chem.*

Commun., no. 62, pp. 1710-1720, 1997.

[89] J. Mao, Z. Wang and A. Clearfield, "Building layered structures from hydrogen bonded molecular units and 1D metal phosphonate chains: synthesis, characterization and crystal structures of N,N′-dimethyl-N,N′-ethylenediamine-bis(methylenephosphonic acid), its Ni(II) and Pb(II) complexes," *J. Chem. Soc., Dalton Trans.,* pp. 4541-46, 2002.

[90] S.-M. Ying and J.-G. Mao, "Novel Layered Lead(II) Aminodiphosphonates with Carboxylate-Sulfonate and 1,3,5-Benzenetricarboxylate Ligands as Pendant Groups or Intercalated Species," *Eur. J. Inorg. Chem.,* pp. 1270-76, 2004.

[91] D. Poojary, B. Zhang, A. Cabeza, M. Aranda, S. Bruque and A. Clearfield, "Synthesis and crystal structures of two metal phosphonates, M(HO3PC6H5)2(M = Ba, Pb)," *J. Mater. Chem.,* no. 6, pp. 639-44, 1996.

[92] A. Cabeza, M. Aranda and S. Bruque, "New lead triphosphonates: synthesis, properties and crystal structures.," *J. Mater. Chem.,* no. 9, pp. 571-9, 1999.

[93] F. Yi, T. Zhou and J. Mao, "Novel lead(II) coordination polymers based on p-sulfophenylarsonic acid," *J. Mol. Struct.,* no. 987, pp. 51-57, 2011.

[94] C. Lei, J. Mao and Y. Sun, "Two isomeric lead(II) carboxylate-phosphonates: syntheses, crystal structures and characterizations.," *J. Solid State Chem.,* vol. 177, no. 7, pp. 2449-55, 2004.

[95] J. Wu, H. Hou, H. Han and Y. Fan, "Highly selective ferric ion sorption and exchange by crystalline metal phosphonates constructed from tetraphosphonic acids.," *Inorg. Chem.,* no. 46, pp. 7960-70, 2007.

[96] F. Costantino, P. Gentili and N. Audebrand, "A new dual luminescent pillared cerium(IV)sulfate–diphosphonate.," *Inorg. Chem. Comm.,* vol. 12, no. 5, pp. 406-08, 2009.

[97] G. Cao, V. Lynch, J. Swinnea and T. Mallouk, "Synthesis and structural characterization of layered calcium and lanthanide phosphonate salts," *Inorg. Chem.,* vol. 29, no. 11, pp. 2112-17, 1990.

[98] J. Legendziewicz, P. Gawryszewska, E. Gałdecka and Z. Gałdecki, "Novel polynuclear compound of europium with N-phosphonomethylglycine; spectroscopy and structure.," *J. Alloys Comp.,* no. 356, pp. 275-277, 1998.

[99] J.-Y. Zhang, C.-M. Liu, D.-Q. Zhang, S. Gao and D.-B. Zhu, "Syntheses, crystal structures, and magnetic properties of two cyclic dimer M2L2 complexes constructed from a new nitronyl nitroxide ligand and M(hfac)2 (M = Cu2+, Mn2+)," *Acta Cryst.,* vol. 360, no. 11, pp. 3553-3559, 2007.

[100] S.-M. Ying, X.-R. Zeng, X.-N. Fang, X.-F. Li and S.-D. Liu, "Synthesis, crystal structure and fluorescent characterization of a novel lanthanide tetraphosphonate with a layered structure.," *Inorganica Chimica Acta,* no. 259, p. 1589, 2006.

[101] P. Silva, J. Fernandes and F. Almeida Paz, "Redetermination at 180 K of a layered lanthanide-organic framework.," *Acta Cryst.,* vol. E68, no. m294, 2012.

[102] L. Tei, A. Blake, C. Wilson and M. Schröder, "Lanthanide complexes of new nonadentate imino-phosphonate ligands derived from 1,4,7-triazacyclononane: synthesis, structural characterisation and NMR studies.," *Dalton Trans.,* no. 13, pp. 1945-52, 2004.

[103] R. Wang, Y. Zhang, H. Hu, R. Frausto and A. Clearfield, *Chem. Mater.,* no. 4, p. 864, 1992.

[104] F. Serpaggi and G. Ferey, "Hybrid Organic−Inorganic Frameworks (MIL-n). Hydrothermal Synthesis of a Series of Pillared Lanthanide Carboxyethylphosphonates and X-ray Powder ab Initio Structure Determination of MIL-19, Pr[O3P(CH2)2CO2].," *Inorg. Chem.,* vol. 38, no. 21, pp. 4741-44, 1999.

[105] T. Zhou, F. Yi, P. Li and J. Mao, "Synthesis, crystal structures, and luminescent properties of two series' of new lanthanide (III) amino-carboxylate-phosphonates.," *Inorg. Chem.,* no. 49, pp. 905-15, 2010.

[106] A. Alsobrook, E. Alekseev, W. Depmeier and T. Albrecht-Schmitt, "Uranyl carboxyphosponates that Incorporate Cd(II)," *J. Solid State Chem.,* no. 184, pp. 1195-1200, 2011.

[107] D. Poojary, D. Grohol and A. Clearfield, "Synthesis and X-Ray Powder Structure of a Novel Porous Uranyl Phenylphosphonate Containing Unidimensional Channels Flanked by Hydrophobic Regions.," *Angew. Chem. Int. Ed.,* no. 34, pp. 1508-1510, 1995.

[108] A. Alsobrook, B. Hauser, J. Hupp, E. Alekseev, W. Depmeier and T. Albrecht-Schmitt, "Cubic and rhombohedral heterobimetallic networks constructed from uranium, transition metals, and phosphonoacetate: new methods for constructing porous materials.," *Chem. Commun.,* no. 46, pp. 9167-69, 2010.

[109] K. Knope and C. Cahill, "Synthesis and characterization of 1-, 2-, and 3-dimensionalbimetallic UO22+/Zn2+ Phosphonoacetates.," *Eur. J. Inorg. Chem.,* pp. 1177-85, 2010.

[110] Z. Liao, J. Ling, L. Reinke, J. Szymanowski, G. Sigmona and P. Burns, "Cage clusters built from uranyl ions bridged through peroxo and 1-hydroxyethane-1,1-diphosphonic acid ligands.," *Dalton Trans.,* no. 42, pp. 6793-6802, 2013.

[111] R. Fu, S. Xia, S. Xiang, S. Hu and X. Wu, "Syntheses, characterization and electrical property of a new silver diphosphonate with zeolite-like framework and three-dimensional silver interactions: [Ag4(O3PCH2CH2PO3)]," *J. Solid State Chem.,* no. 177, pp. 4626-31, 2004.

[112] R. Colodrero, P. Olivera-Pastor, A. Cabeza, M. Papadaki, K. Demadis and M. Aranda, "Structural Mapping and Framework Interconversions in 1D, 2D, and 3D Divalent Metal R,S-Hydroxyphosphonoacetate Hybrids," *Inorg. Chem.,* no. 49, pp. 761-768, 2010.

[113] P. Forster, N. Stock and A. Cheetham, "A High-Throughput Investigation of the Role of pH, Temperature, Concentration, and Time on the Synthesis of Hybrid Inorganic-Organic Materials.," *Angew. Chem. Int. Ed.,* no. 44, pp. 7608-7611, 2005.

[114] S. Natarajan and P. Mahata, "Non-carboxylate based metal-organic frameworks (MOFs) and related aspects.," *Curr. Opin. Solid State Mater. Sci.,* no. 13, pp. 46-53, 2009.

[115] A. Bhattacharya and G. Thyagarajan, "Michaelis-Arbuzov rearrangement," *Chem. Rev.,* vol. 81, no. 4, pp. 415-30, 1981.

[116] K. Moedritzer and R. Irani, "The Direct Synthesis of α-Aminomethylphosphonic Acids. Mannich-Type Reactions with Orthophosphorous Acid," *J. Org. Chem.,* no. 31, pp. 1603-1607, 1966.

[117] J. Zon, P. Garczarek and M. Bialek, "Synthesis of Phosphonic Acids and Their Esters as Possible Substrates for Reticular Chemistry," in *Metal Phosphonate Chemistry: From Synthesis to Applications.*, A. Clearfield and K. Demadis, Eds., 2012, Royal Society of Chemistry, London, pp. 170-191..

[118] P. Lebduskova, J. Kotek, P. Hermann, L. Vander Elst, R. Muller, I. Lukes and J. Peters, "A Gadolinium(III) Complex of a Carboxylic-Phospherous Acid Derivative of Diethylentriamine Covalently Bound to Inulin, a Potential Macromolecular MRI Contrast Agent," *Bioconjugate Chem.,* no. 15, pp. 881-9, 2004.

[119] A. Heras, N. Rodriguez, V. Ramos and E. Agullo, "N-methylene phosphonic chitosan: a novel soluble derivative.," *Carbohydrate Polymers,* no. 44, pp. 1-8, 2001.

[120] V. Ramos, N. Rodrıguez, M. Dıaz, M. Rodrıguez, A. Heras and E. Agullo, "N-methylene phosphonic chitosan. Effect of preparation methods on its properties.," *Carbohydrate Polymers,* vol. 52, no. 1, pp. 39-46, 2003.

[121] V. Ramos, N. Rodrıguez, M. Rodrıguez, A. Heras and E. Agullo, "Modified chitosan carrying phosphonic and alkyl groups.," *Carbohydrate Polymers,* no. 51, pp. 425-429, 2003.

[122] A. Zuñiga, A. Debbaudt, A. Albertengo and M. Rodríguez, "Synthesis and characterization of N-propyl-N-methylene phosphonic chitosan derivative.," *Carbohydrate Polymers,* no. 79, pp. 475-480, 2010.

[123] G. Matevosyan, Y. Yukha and P. Zavlin, "Phosphorylation of Chitosan," *Rus. J. Gen. Chem.,* no. 73, pp. 1725-28, 2003.

[124] Z. Zhong, P. Li, R. Xing, X. Chen and S. Liu, "Preparation, characterization and antifungal properties of 2-(α-arylamino phosphonate)-chitosan.," *Int. J. Biol. Macromol,* vol. 45, no. 3, pp. 255-59, 2009.

[125] R. Jayakumara, N. Selvamurugan, S. Nair, S. Tokura and H. Tamura, "Preparative methods of phosphorylated chitin and chitosan—An overview.," *Int. J. Biol. Macromol.,* no. 43, pp. 221-225, 2008.

[126] X. Wang, J. Ma, Y. Wang and B. He, "Structural characterization of phosphorylated chitosan and their applications as effective additives of calcium phosphate cements.," *Biomaterials,* vol. 22, no. 16, pp. 2247-55, 2001.

[127] H. Kang, Y. Cai, J. Deng, H. Zhang, Y. Tang and P. Liu, "Synthesis and aqueous solution behavior of phosphonate-functionalized chitosans.," *Eur. Polym. J.,* no. 42, pp. 2678-85, 2006.

[128] F. Lebouc, I. Dez, M. Gulea, P. Madec and P. Jaffres, "Synthesis of phosphorus-containing chitosan derivatives.," *Phosphorus Sulfur Silicon,* no. 184, pp. 872-89, 2009.

[129] A. Cengiz and N. Bayramgil, "Phosphonic Acid Containing Superporous Hydrogels and their Adsorption Properties.," *Soft Materials,* vol. 11, no. 4, pp. 476-82, 2013.

[130] A. Popa, C.-M. Davidescu, N. Petru, I. Gheorghe, A. Katsaros and K. Demadis, "Synthesis

and Characterization of Phosphonate Ester/Phosphonic Acid Grafted Styrene−Divinylbenzene Copolymer Microbeads and Their Utility in Adsorption of Divalent Metal Ions in Aqueous Solutions," *Ind. Eng. Chem. Res.,* no. 47, pp. 2010-2017, 2008.

[131] R. Navarro, S. Wada and K. Tatsumi, "Heavy Metal Flocculation by Phosphonomethylated-Polyethyleneimine and Calcium Ions.," *Sep. Sci. Technol.,* no. 38, pp. 2327-2345, 2003.

[132] R. Navarro, S. Wada and K. Tatsumi, "Heavy Metal Flocculation by Phosphonomethylated-Polyethyleneimine and Calcium Ions.," *Sep. Sci. Technol.,* vol. 38, no. 10, pp. 2327-45, 2002.

[133] S. Hong and F. Raushel, "Inhibitors directed towards the binuclear metal center of phosphotriesterase.," *J. Enzymol. Inhib.,* no. 12, pp. 191-203, 1997.

[134] C. Temperini, A. Innocenti, A. Guerri, A. Scozzafava, S. Rusconi and S. Supuran, "Phosph(on)ate as a zinc-binding group in metalloenzyme inhibitors: X-ray crystal structure of the antiviral drug foscarnet complexed to human carbonic anhydrase I," *Bioorganic & Medicinal Chemistry Letters,* vol. 17, no. 8, pp. 2210-5, 2007.

[135] F. Cheng and E. Oldfield, "Inhibition of Isoprene Biosynthesis Pathway Enzymes by Phosphonates, Bisphosphonates, and Diphosphates," *J. Med. Chem.,* no. 47, pp. 5149-58, 2004.

[136] S. Rusconi, A. Innocenti, D. Vullo, A. Mastrolorenzo, A. Scozzafava and C. Supuran, "Carbonic anhydrase inhibitors. Interaction of isozymes I, II, IV, V, and IX with phosphates, carbamoyl phosphate, and the phosphonate antiviral drug foscarnet.," *Bioorg. Med. Chem. Lett.,* no. 14, pp. 5763-5767, 2004.

[137] O. Shekhah, L. Fu, R. Sougrat, Y. Belmabkhout, A. Cairns, E. Giannelis and M. Eddaoudi, "Successful implementation of the stepwise layer-by-layer growth of MOF thin films on confined surfaces: mesoporous silica foam as a first case study," *Chem. Commun.,* no. 48, pp. 11434-36, 2012.

[138] P. Van Nieuwenhuyse, V. Bounor-Legare, F. Boisson, P. Cassagnau and A. Michel, "Hydrolysis–condensation reactions of diethylphosphato-ethyltriethoxysilane with tetraethoxysilane studied by 29Si-NMR: Solvent and phosphonate catalytic effect," *J. Non-Cryst. Solids,* no. 354, pp. 1654-1663, 2008.

[139] M. Jaber, O. Larlus and J. Miehe-Brendle, "Layered metal (II) and silico-phosphonate with ion exchange properties," *Solid State Sci.,* no. 9, pp. 144-148, 2007.

[140] A. Matsuda, N. Nakamoto, K. Tadanaga, T. Minami and M. Tatsumisago, "Preparation and characterization of thermally stable proton-conducting composite sheets composed of phosphosilicate gel and polyimide.," *Solid State Ionics,* Vols. 162-163, pp. 247-252, 2003.

[141] A. Matsuda, T. Kanzaki, K. Tadanaga, M. Tatsumisago and T. Minami, "Proton conductivities of sol–gel derived phosphosilicate gels in medium temperature range with low humidity.," *Solid State Ionics,* no. 687, pp. 154-154, 2002.

[142] A. Clearfield, "Organically Pillared Micro- and Mesoporous Materials.," *Chem. Mater,* vol. 10, no. 10, pp. 2801-10, 1998.

[143] K. Maeda, "Metal phosphonate open-framework materials.," *Microporous Mesoporous Mater,* vol. 73, no. 1-2, pp. 47-55, 2004.

[144] K. Demadis, "Alkaline Earth Metal Phosphonates: From Synthetic Curiosities to Nanotechnology Applications," in *Solid State Chemistry Research Trends*, New York, Nova Science Publishers, 2007, pp. 109-172.

[145] A. Clearfield, "Metal Phosphonate Chemistry," in *Progress in Inorganic Chemistry (Edited by Kenneth D. Karlin)*, N.Y, Wiley, 1998, pp. 371-510.

[146] A. Vioux, L. Le Bideau, P. Hubert Mutin and D. Leclercq, "Hybrid organic-inorganic materials based on organophosphorus derivatives.," *Top. Curr. Chem.,* no. 232, pp. 145-174, 2004.

[147] A. Cheetham, G. Ferey and T. Loiseau, "Open-Framework Inorganic Materials.," *Angew. Chem. Int. Ed.,* no. 38, pp. 3268-3292, 1999.

[148] B. Breeze, M. Shanmugam, F. Tuna and R. Winpenny, "A series of nickel phosphonate–carboxylate cages," *Chem. Commun.,* pp. 5185-87, 2007.

[149] U. Costantino, M. Nocchetti and R. Vivani, "Preparation, characterization, and structure of zirconium fluoride alkylamino-N, N-bis methylphosphonates: A new design for layered zirconium diphosphonates with a poorly hindered interlayer region.," *J. Am. Chem. Soc,* vol. 124, no. 28, pp. 8428-34, 2002.

[150] K. Demadis, "Chemistry of Organophosphonate Scale Inhibitors,Part 4: Stability of Amino-tris-(Methylene Phosphonate)Towards Degradation by Oxidizing Biocides," *Phosphorus Sulfur Silicon,* no. 181, pp. 167-176, 2006.

[151] S. Dyer, C. Anderson and G. Graham, "Thermal stability of amine methyl phosphonate scale inhibitors.," *J. Pet. Sci. Eng.,* no. 43, pp. 259-270, 2004.

[152] J. Oddo and M. Tomson, "The solubility and stoichiometry of calcium-diethylenetriaminepenta(methylene phosphonate) at 70° in brine solutions at 4.7 and 5.0 pH.," *Appl. Geochem.,* no. 5, pp. 527-532, 1990.

[153] J. Xiao, A. Kan and M. Tomson, "Prediction of BaSO4 precipitation in the presence and absence of a polymeric inhibitor: Phosphino-polycarboxylic acid.," *Langmuir,* no. 17, pp. 4668-73, 2001.

[154] S. Friedfeld, S. He and M. Tomson, "The temperature and ionic strength dependence of the solubility product constant of ferrous phosphonate.," *Langmuir,* no. 14, pp. 3698-3703, 1998.

[155] V. Tantayakom, H. Fogler, P. Charoensirithavorn and S. Chavadej, "Kinetic study of scale inhibitor precipitation in squeeze treatment.," *Cryst. Growth Des.,* vol. 5, no. 1, pp. 329-35, 2005.

[156] F. Browning and H. Fogler, "Fundamental Study of the Dissolution of Calcium Phosphonates from Porous Media," *Chemical Engineering,* no. 42, pp. 2883-96, 1996.

[157] R. Pairat, C. Sumeath, F. Browning and H. Fogler, "Precipitation and dissolution of calcium-ATMP precipitates for the inhibition of scale formation in porous media," *Langmuir,* no. 13, pp. 1791-1798, 1997.

[158] V. Tantayakom, H. Fogler, F. De Moraes, M. Bualuang, S. Chavadej and P. Malakul, "Study of Ca-ATMP Precipitation in the Presence of Magnesium Ion.," *Langmuir,* vol. 20, no. 6, pp. 2220-6, 2004.

[159] A. Penard, F. Rossignol, H. Nagaraja, C. Pagnoux and T. Chartier, "Dispersion of alpha-alumina ultrafine powders using 2-phosphonobutane-1, 2, 4-tricarboxylic acid for the implementation of a DCC process.," *Eur. J. Ceram. Soc,* no. 25, pp. 1109-1118, 2005.

[160] M. Pearse, "An overview of the use of chemical reagents in mineral processing.," *Minerals Engineering,* no. 15, pp. 139-149, 2005.

[161] I. Sekine, T. Shimode, M. Yuasa and K. Takaoka, "Corrosion inhibition of structural steels in the carbon dioxide absorption process by organic inhibitors.," *Ind. Eng. Chem. Res.,* no. 31, pp. 434-439, 1992.

[162] B. Mosayebi, M. Kazemeini and A. Badakhshan, "Effect of phosphonate based corrosion inhibitors in a cooling water system.," *Br. Corr. J.,* vol. 37, no. 3, pp. 217-24, 2002.

[163] Y. Kuznetsov, "Role of the Complexation Concept in the Present Views on the Initiation and Inhibition of Metal Pitting.," *Prot. Met.,* no. 37, pp. 434-9, 2001.

[164] Y. Balaban-Irmenin, A. Rubashov and N. Fokina, "The effect of phosphonates on the corrosion of carbon steel in heat-supply water.," *Protection of Metals,* vol. 42, no. 2, pp. 133-136, 2006.

[165] J. Fang, Y. Li, X. Ye, Z. Wang and Q. Liu, "Passive Films and Corrosion Protection Due to Phosphonic Acid Inhibitors," *Corrosion,,* no. 49, pp. 266-271, 1993.

[166] A. Paszternák, S. Stichleutner, I. Felhősi, Z. Keresztes, Z. Nagy, E. Kuzmann, E. Vértes, Z. Homonnay, G. Pető and E. Kálmán, "Surface modification of passive iron by alkyl-phosphonic acid layers.," *Electrochim. Acta,* no. 53, pp. 337-345, 2007.

[167] B. Nowack and J. VanBriesen, Biogeochemistry of Chelating Agents (Edited by Bernd Nowack and Jeanne M. VanBriesen), vol. 910, Washington DC: American Chemical Society, 2005.

[168] T. Knepper, "Synthetic chelating agents and compounds exhibiting complexing properties in the aquatic environment.," *Trends Anal. Chem.,* no. 22, pp. 708-24, 2003.

[169] K. Miyazaki, T. Horibe, J. Antonucci, S. Takagi and L. Chow, "Polymeric calcium phosphate cements: setting reaction modifiers.," *Dent. Mater.,* no. 9, pp. 46-50, 1993.

[170] M. Atai, M. Nekoomanesh, S. Hashemi and S. Amani, "Physical and mechanical properties of an experimental dental composite based on a new monomer.," *Dent. Mater.,* no. 20, pp. 663-8, 2004.

[171] J. Nicholson and G. Singh, "The use of organic compounds of phosphorus in clinical dentistry.," *Biomaterials,* vol. 17, pp. 2023-30, 1996.

[172] H. Tschernitschek, L. Borchers and W. Geurtsen, "Nonalloyed titanium as a bioinert metal—A review," *J. Prosth. Dent.,* no. 96, pp. 12-23, 2006.

[173] M. Bottrill, L. Kwok and N. Long, "Lanthanides in magnetic resonance imaging.," *Chem. Soc. Rev.,* no. 35, pp. 557-71, 2006.

[174] I. Finlay, M. Mason and M. Shelley, "Radioisotopes for the palliation of metastatic bone cancer: a systematic review.," *Lancet Oncol.,* no. 6, pp. 392-400, 2005.

[175] V. Kubíček, J. Rudovský, J. Kotek, P. Hermann, L. Vander Elst, R. Muller, Z. Kolar, H. Wolterbeek, J. Peters and L. I., "A Bisphosphonate Mono-Amide Analogue of DOTA: a Potential Agent for Bone-Targeting.," *J. Am. Chem. Soc,* no. 127, pp. 16477-16485, 2005.

[176] H. Kung, R. Ackerhalt and M. Blau, "Uptake of Tc-99m monophosphate complexes in bone and myocardial necrosis in animals.," *J. Nucl. Med.,* no. 19, pp. 1027-31, 1978.

[177] S. Padalecki and T. Guise, "The role of bisphosphonates in breast cancer: Actions of bisphosphonates in animal models of breast cancer," *Breast Cancer Res.,* no. 4, p. 35, 2001.

[178] V. Stresing, F. Daubiné, I. Benzaid, H. Mönkkönen and P. Clézardin, "Bisphosphonates in cancer therapy.," *Cancer Lett.,* vol. 257, no. 1, pp. 16-35, 2007.

[179] R. Layman, K. Olson and C. Van Poznak, "Bisphosphonates for Breast Cancer: Questions Answered, Questions Remaining.," *Hematol. Oncol. Clinics North Amer.,* no. 21, pp. 341-367, 2007.

[180] S. Horike, D. Umeyama and S. Kitagawa, "Ion conductivity and transport by porous coordination polymers and metal-organic frameworks.," *Accounts Chem. Res.,* no. 46, pp. 2376-84, 2013.

[181] K. Kreuer, "Proton conductivity: materials and applications.," *Chem. Mater.,* no. 8, pp. 610-41, 1996.

[182] M. Yoon, K. Suh, S. Natarajan and K. Kim, "Proton conduction in metal-organic frameworks and related modularly built porous solids.," *Angew. Chem. Int. Ed.,* no. 52, pp. 2688-700, 2013.

[183] J. Lee, O. Farha, J. Roberts, K. Scheidt, S. Nguyen and J. Hupp, "Metal-organic framework materials as catalysts.," *Chem. Soc. Rev.,* no. 38, pp. 1450-9, 2009.

[184] S. Isikli, S. Tuncagil, A. Bozkurt and L. Toppare, "Immobilization of Invertase in a Novel Proton Conducting Poly(vinylphosphonic acid) − poly(1-vinylimidazole) Network," *J. Macromolecular Science, Part A,* no. 47, pp. 639-646, 2010.

[185] V. Zima, J. Svoboda, K. Melánová, L. Beneš, M. Casciola, M. Sganappa, J. Brus and M. Trchová, "Synthesis and characterization of new zirconium 4-sulfophenylphosphonates.,"

Solid State Ionics, vol. 181, no. 15-16, pp. 705-13, 2010.

[186] R. Colodrero, A. Cabeza, P. Olivera-Pastor, E. Losilla, K. Papathanasiou, N. Stavgianoudaki, J. Sanz, I. Sobrados, D. Choquesillo-Lazarte, J. García-Ruiz, L. León Reina, M. Aranda, P. Corvillo and K. C. M. 2. Demadis, "Multifunctional Luminescent and Proton-Conducting Lanthanide Carboxyphosphonate Open-Framework Hybrids Exhibiting Crystalline-to-Amorphous-to-Crystalline Transformations," *Chem. Mater.,* vol. 24, no. 19, pp. 3780-3792, 2012.

[187] S. Kim, K. Dawson, B. Gelfand, J. Taylor and G. Shimizu, "Enhancing proton conduction in a metal-organic framework by isomorphous ligand replacement.," *J. Am. Chem. Soc.,* vol. 135, no. 3, pp. 963-6, 2013.

[188] R. Colodrero, P. Olivera-Pastor, E. Losilla, M. Aranda, M. Papadaki, A. McKinlay, R. Morris, K. Demadis and A. Cabeza, "Multifunctional lanthanum tetraphosphonates: Flexible, ultramicroporous and proton-conducting hybrid frameworks.," *Dalton Trans.,* vol. 41, no. 14, pp. 4045-51, 2012.

[189] R. Colodrero, P. Olivera-Pastor, E. Losilla, D. Alonso, M. Aranda, L. Leon-Reina, J. Rius, K. Demadis, B. Moreau, D. Villemin, F. Rey and A. Cabeza, "High Proton Conductivity in a Flexible, Cross-Linked, Ultramicroporous Magnesium Tetraphosphonate Hybrid Framework.," *Inorg. Chem.,* vol. 51, no. 14, pp. 7689-98, 2012.

[190] J. Taylor, K. Dawson and G. Shimizu, "A Water-Stable Metal–Organic Framework with Highly Acidic Pores for Proton-Conducting Applications," *J. Am. Chem. Soc.,* no. 135, pp. 1193-96, 2013.

[191] G. Shimizu, J. Taylor and K. Dawson, "Metal Organophosphonate Proton Conductors," in *Metal Phosphonate Chemistry: From Synthesis to Applications.*, London, Royal Society of Chemist\y, 2012, pp. 493-524..

[192] M. Arkas, D. Tsiourvas and C. Paleos, "Functional Dendritic Polymers for the Development of Hybrid Materials for Water Purification.," *Macromol. Mater. Eng.,* no. 295, pp. 883-898, 2010.

[193] M. Plabst, L. McCusker and T. Bein, "Exceptional ion-exchange selectivity in a flexible open framework lanthanum (III) tetrakisphosphonate.," *J. Am. Chem. Soc,* no. 131, pp. 18112-18, 2009.

[194] J. Wu, H. Hou, H. Han and Y. Fan, "Highly selective ferric ion sorption and exchange by crystalline metal phosphonates constructed from tetraphosphonic acids.," *Inorg. Chem.,* vol. 46, pp. 7960-70, 2007.

[195] O. Abderrahim, M. Didi, B. Moreau and D. Villemin, "A New Sorbent for Selective Separation of Metal: Polyethylenimine Methylenephosphonic Acid.," *Solv. Extract. Ion Exchange,* no. 24, pp. 943-55, 2006.

[196] R. Navarro, S. Wada and S. Tatsumi, "Heavy metal precipitation by polycation–polyanion complex of PEI and its phosphonomethylated derivative.," *J. Hazardous Mater.,* no. B123, pp. 203-209, 2005.

[197] O. Abderrahim, M. Didi and D. Villemin, "Polyethyleneimine Methylenephosphonic Acid for the Solid-Phase Sorption of Lead(II).," *Analytical Letters,,* no. 42, pp. 1233-1244, 2009.

[198] A. Bortun, L. Bortun, A. Clearfield, S. Khainakov and J. García, "Synthesis and ion exchange properties of novel inorganic adsorbents tin(IV)–nitrilotris(methylene)triphosphonates.," *Solv. Extr. Ion Exch.,* no. 16, pp. 651-667, 1998.

[199] T.-Y. Ma, X.-J. Zhang, G.-S. Shao, J.-L. Cao and Z.-Y. Yuan, "Ordered macroporous titanium phosphonate materials: synthesis, photocatalytic activity, and heavy metal ion adsorption," *J. Phys. Chem. C,* no. 112, pp. 3090-96, 2008.

[200] X.-J. Zhang, T.-Y. Ma and Z.-Y. Yuan, "Titania–phosphonate hybrid porous materials: preparation, photocatalytic activity and heavy metal ion adsorption," *J. Mater. Chem.,* no. 18, pp. 2003-2010, 2008.

[201] M. Marma, B. Kashemirov and C. McKenna, "Synthesis and stability studies of phosphonoformate-amino acid conjugates: a new class of slowly releasing foscarnet prodrugs.," *Bioorg. Med. Chem. Lett.,* no. 14, pp. 1787-90, 2004.

[202] B. Oberg, "Antiviral effects of phosphonoformate (PFA, foscarnet sodium).," *Pharmac. Ther.,* no. 40, pp. 213-85, 1989.

[203] J. Choi, H. Kim, Y. Lee, B. Cho, H. Seong, M. Cho and S. Kim, "Inhibition of bone healing by pamidronate in calvarial bony defects," *Oral Surg Oral Med Oral Pathol Oral Radiol Endod,* no. 103, pp. 321-28, 2007.

[204] H. Nakayama, K. Takeshita and M. Tsuhako, "Preparation of 1-hydroxyethylidene-1,1-

diphosphonic acid-intercalated layered double hydroxide and its physicochemical properties.," *J. Pharm. Sci.,* no. 92, pp. 2419-26, 2003.

[205] G. Golomb, R. Langer, F. Schoen, M. Smith, Y. Choi and R. Levy, "Controlled release of diphosphonate to inhibit bioprosthetic heart valve calcification: Dose-response and mechanistic studies," *J. Controlled Release,* no. 4, pp. 181-94, 1986.

[206] K. Demadis, I. Theodorou and M. Paspalaki, "Controlled Release of Bis(phosphonate) Pharmaceuticals from Cationic Biodegradable Polymeric Matrices," *Ind. Eng. Chem. Res.,* no. 50, pp. 5873-76, 2011.

[207] G. Gunasekaran, R. Natarajan, V. Muralidharan, N. Palaniswamy and B. Appa Rao, "Inhibition by phosphonic acids - an overview.," *Anti-Corr. Meth. Mater.,* vol. 44, no. 4, pp. 248-259, 1997.

[208] S. Cohen, "Review: Replacements for Chromium Pretreatments on Aluminum.," *Corrosion,* no. 51, pp. 71-78, 1995.

[209] K. Demadis and N. Stavgianoudaki, "Structural Diversity in Metal Phosphonate Frameworks: Impact on Applications.," in *Metal Phosphonate Chemistry: From Synthesis to Applications (Edited by A Clearfield and K.D. Demadis)*, London, The Royal Society of Chemistry, 2012, pp. 438-492.

[210] K. Demadis, M. Papadaki and D. Varouchas, "Metal–Phosphonate Anticorrosion Coatings," in Green Corrosion Chemistry and Engineering: Opportunities and Challenges (Edited by Sanjay K. Sharma, Foreworded by Nabuk Okon Eddy), Germany, Wiley-VCH Verlag GmbH & Co., 2012, pp. 243-296..

[211] M. Papadaki and K. Demadis, "STRUCTURAL MAPPING OF HYBRID METAL PHOSPHONATE CORROSION INHIBITING THIN FILMS.," *Comments Inorg. Chem.,* no. 30, pp. 89-118, 2009.

[212] K. Demadis and G. Angeli, ""Good Scale"–"Bad Scale" How Metal–Phosphonate Materials Contribute to Corrosion Inhibition.," in *Mineral Scales in Biological and Industrial Systems (Edited by Zahid Amjad)*, New York, Taylor and Francisv RCPress, 2013, pp. 343-360.

[213] K. Demadis, "Alkaline Earth Metal Phosphonates: From Synthetic Curiosities to Nanotechnology ApplicationS," in *Solid State Chemistry Research Trends (Edited by Ronald W. Buckley)*, New York, Nova Science Publishers, Inc., 2007, pp. 109-172.

[214] H. Li, M. Eddaoudi, M. O'Keeffe and O. Yaghi, "Design and synthesis of an exceptionally stable and highly porous metal-organic framework.," *Nature,* no. 402, pp. 276-79, 1999.

[215] G. Ferey, C. Mellot-Draznieks, C. Serre and F. Millange, "Crystallized frameworks with giant pores: are there limits to the possible?," *Acc. Chem. Res.,* no. 38, pp. 217-25, 2005.

[216] S. Chui, J. Charmant, A. Orpen and I. Williams, "A chemically functionalizable nanoporous material.," *Science,* no. 283, pp. 1148-50, 1999.

[217] K. Park, Z. Ni, A. Côté, J. Choi, R. Huang, F. Uribe-Romo, H. Chae, M. O'Keeffe and O. Yaghi, "Exceptional chemical and thermal stability of zeolitic imidazolate frameworks.," *Proc. Natl. Acad. Sci. U.S.A.,* no. 103, pp. 10186-91, 2006.

[218] R. Vaidhyanathan, D. Bradshaw, J. Rebilly, J. Barrio, J. Gould, N. Berry and M. Rosseinsky, "A Family of Nanoporous Materials Based on an Amino Acid Backbone," *Angew. Chem. Int. Ed.,* no. 45, pp. 6495-6499, 2006.

[219] R. Matsuda, R. Kituara, S. Kitagawa, Y. Kubota, R. Belosludov, T. Kobayashi, H. Sakamoto, T. Chiba, M. Takata, Y. Kawazoe and Y. Mita, "Highly controlled acetylene accommodation in a metal-organic microporous material.," *Nature,* no. 436, pp. 238-241, 2005.

[220] J. Groves, S. Miller, S. Warrender, C. Mellot-Draznieks, R. Lightfoot and P. Wright, "The first route to large pore metal phosphonates.," *Chem. Commun.,* pp. 3305-07, 2006.

[221] S. Miller, G. Pearce, P. Wright, F. Bonino, S. Chavan, S. Bordiga, I. Margiolaki, N. Guillou, G. Ferey, S. Bourrelly and P. Liewellyn, "Structural Transformations and adsorption of fuel-related gases of a structurally responsive nickel phosphonate metal-organic framework, Ni-STA-12.," *J. Am. Chem. Soc.,* no. 130, pp. 159678-81, 2008.

[222] E. Brunet, C. Cerro, O. Juanes, J. Rodriguez-Ubis and A. Clearfield, "Hydrogen storage in highly microporous solids derived from aluminium biphenyldiphosphonate," *J. Mater. Sci.,* no. 43, pp. 1155-58, 2008.

[223] K. Peeters, P. Grobet and E. Vansant, "Intercalation ability of hydrolysed aluminium species in n-alkylmonoamine α-zirconium phosphate compounds," *J. Mater. Chem.,* no. 6, pp. 239-46, 1996.

[224] R. Hoppe, G. Alberti, U. Contantino, C. Dionigi, G. Ekloff and R. Vivani, "Intercalation of dyes in layered zirconium phosphates. 1. Preparation and spectroscopic characterization of α-

zirconium phosphate crystal violet compounds," *Langmuir,* no. 13, pp. 7252-57, 1997.

[225] S. Suib, "Zeolitic and layered materials.," *Chem. Rev.,* vol. 93, no. 2, pp. 803-826, 1993.

[226] A. Lazarin and C. Airoldi, "Layered crystalline barium phenylphosphonate as host support for n-alkylmonoamine intercalation.," *J. Inclusion Phen. Macrocyclic Chem.,* no. 51, pp. 33-40, 2005.

[227] C. Lima and C. Airoldi, "Layered crystalline calcium phenylphosphonate—synthesis, characterization and n-alkylmonoamine intercalation.," *Solid State Sci,* vol. 4, no. 10, pp. 1321-29, 2002.

[228] B. Zhang, D. Poojary, A. Clearfield and G. Peng, "Synthesis, Characterization, and Amine Intercalation Behavior of Zirconium N-(Phosphonomethyl)iminodiacetic Acid Layered Compounds.," *Chem. Mater.,* vol. 8, no. 6, pp. 1333-40, 1996.

[229] P. Gendraud, M. De Roy and J. Besse, "Intercalation Reactions of Layered Vanadyl Organophosphonates with Alkylamines," *Inorg. Chem.,* no. 35, pp. 6108-12, 1996.

[230] T. Kijima, S. Watanabe and M. Machida, "Carbon Number Dependence of the Intercalation and Interlayer Amidation Properties of .alpha.,.omega.-Alkylidiamines for Layered Zirconium (Carboxyethyl)phosphonate.," *Inorg. Chem.,* no. 33, pp. 2586-91, 1994.

[231] A. Lazarin and C. Airoldi, "Corrigendum to "Calorimetric data on intercalation of some aromatic amines into barium phenylphosphonate at the solid/liquid interface.," *J. Chem. Thermodynamics,* no. 37, pp. 243-48, 2005.

[232] T. Kijima, K. Ohe, F. Sasaki, M. Yada and M. Machida, "Intercalation of Dendritic Polyamines by α and γ-Zirconium Phosphates.," *Bull. Chem. Soc. Jpn.,* no. 71, pp. 141-8, 1998.

[233] V. Ruiz and C. Airoldi, "Thermochemical data for n-alkylmonoamine intercalation into crystalline lamellar zirconium phenylphosphonate," *Thermochim. Acta,* no. 420, pp. 73-78, 2004.

[234] A. Lazarin and C. Airoldi, "Corrigendum to "Calorimetric data on intercalation of some aromatic amines into barium phenylphosphonate at the solid/liquid interface.," *J. Chem. Thermodynamics,* no. 37, pp. 243-48, 2005.

[235] Y. Zhang, K. Scott and A. Clearfield, "Intercalation of alkylamines into dehydrated and

hydrated zinc phenyiphosphonates.," *J. Mater. Chem.,* vol. 5, no. 2, pp. 315-18, 1995.

[236] K. Scott, Y. Zhang, R.-C. Wang and A. Clearfield, "Synthesis, Characterization, and Amine Intercalation Behavior of Zinc Phosphite Phenylphosphonate Mixed Derivatives.," *Inorg. Chem.,* no. 7, pp. 1095-1102, 1995.

[237] C. Lima and C. Airoldi, "Crystalline calcium phenylphosphonate—thermodynamic data on n-alkylmonoamine intercalations.," *Thermochim. Acta,* vol. 400, no. 1-2, pp. 51-59, 2003.

[238] C. Lima and C. Airoldi, "Synthesis, characterization and thermodynamics of the reaction of calcium methylphosphonate with n-alkylmonoamines.," *Int. J. Inorg. Mater.,* vol. 3, no. 7, pp. 907-14, 2001.

[239] G. Hix and K. Harris, "Synthesis of layered nickel phosphonate materials based on a topotactic approach.," *J. Mater. Chem.,* vol. 8, no. 3, pp. 579-84, 1998.

[240] F. Fredoueil, D. Massiot, P. Janvier, F. Gingl, M. Doeuff, M. Evain, A. Clearfield and B. Bujoli, "Synthesis and X-ray Powder Structure of a New Pillared Layered Cadmium Phosphonate, Giving Evidence that the Intercalation of Alkylamines into Cd(O3PR)·H2O Is Topotactic.," *Inorg. Chem.,* vol. 38, no. 8, pp. 1831-33, 1999.

[241] D. Poojary and A. Clearfield, "Coordinative Intercalation of Alkylamines into Layered Zinc Phenylphosphonate. Crystal Structures from X-ray Powder Diffraction Data," *J. Am. Chem. Soc.,* vol. 117, no. 45, pp. 11278-84, 1995.

[242] Mashkevich B.O, New York: Nova Science Publishers, Inc., 2007.

[243] S. Binauld and M. Stenzel, "Acid-degradable polymers for drug delivery: a decade of innovation," *Chem. Commun.,* no. 49, pp. 2082-2102, 2013.

[244] K. Soppimath, T. Aminabhavi, A. Kulkarni and W. Rudzinski, "Biodegradable polymeric nanoparticles as drug delivery devices.," *J Control Release,* no. 70, pp. 1-20, 2001.

[245] Z. Zhao, "Adsorption of phenylalanine from aqueous solution onto active carbon and silica gel.," *Chin. J. Chem.,* no. 10, pp. 325-330, 1992.

[246] J. Kennedy, "HPLC Purification of pergolide using silica gel.," *Org. Process Res. Dev.,* no. 1, pp. 68-71, 1997.

[247] H. Ehrlich, D. K. P. Koutsoukos and O. Pokrovsky, "Modern views on desilicification: Biosilica and abiotic silica dissolution in natural and artificial environments," *Chem. Rev.,* no.

110, pp. 4556-4689, 2010.

[248] K. Demadis, "Silica scale inhibition relevant to desalination technologies: Progress and recent developments.," in *Desalination research progress. (Edited by Daniel J. Delgado and Pablo Moreno)*, New York, Nova Science Publishers, Inc., 2008, pp. 249-259..

[249] C. Perry and T. Keeling-Tucker, "Aspects of the bioinorganic chemistry of silicon in conjunction with the biometals calcium, iron and aluminium.," *J Inorg Biochem.,* no. 69, pp. 181-191, 1998.

[250] S. Mann, C. Perry, R. Williams, C. Fyfe, G. Gobbi and G. Kennedy, "The characterisation of the nature of silica in biological systems," *J Chem. Soc. Chem. Commun.,* no. 4, pp. 168-170., 1983.

[251] T. Coradin, D. Eglin and J. Livage, "The silicomolybdic acid spectrophotometric method and its application to silicate/biopolymer interaction studies.," *Spectroscopy,* no. 18, pp. 567-576, 2004.

[252] R. Ning, "Reactive silica in natural waters—A review.," *Des. Wat. Treat.,* no. 21, pp. 79-86, 2010.

[253] G. Wang και L. Zhang, «Manipulating formation and drug-release behavior of new sol-gel silica matrix by hydroxypropyl guar gum.,» *J. Phys. Chem. B.,* αρ. 111, pp. 10665-10670., 2007.

[254] C. Gommes, S. Blacher, B. Goderis, R. Pirard, B. Heinrichs, C. Alie and J. Pirard, "In situ SAXS analysis of silica gel formation with an additive.," *J. Phys. Chem. B.,* no. 108, pp. 8983-8991, 2004.

[255] E. Martin del Valle, M. Galan and R. Carbonell, "Drug delivery technologies: The way forward in the new decade.," *Ind. Eng. Chem. Res.,* no. 48, pp. 2475-2486, 2009.

[256] S. Ramakrishna, J. Mayer, E. Wintermantel and K. Leong, "Biomedical applications of polymer-composite materials: a review.," *Composite Sci. Technol.,* no. 61, pp. 1189-1224, 2001.

[257] M. Mestiri, J. Benoit, P. Hernigou, J. Devissaguet and F. Puisieux, "Cisplatin-loaded poly(methyl methacrylate) implants: a sustained drugdelivery system.," *J. Controlled Release,* no. 33, pp. 107-113, 1995.

[258] J. Hughes, L. Vick and T. Wang, "European Patent 1250164."Coated Implants."," 2004.

[259] J. Szymura-Oleksiak, A. Slosarczyk, A. Cios, B. Mycek, Z. Paszkiewicz, S. Szklarczyk and D. Stankiewicz, "The kinetics of pentoxifyllinerelease in vivo from drug-loaded hydroxyapatite implants.," *Ceram. Int.,* no. 27, p. 767–772, 2001.

[260] R. Siegel and M. Rathbone, "Overview of controlled release mechanisms.," in *Fundamentals and Applications of Controlled Release Drug Delivery.*, New York, Springer, 2012, pp. 19-43..

[261] V. Hengst, C. Oussoren, T. Kissel and G. Storm, "Bone targeting potential of bisphosphonate-targeted liposomes. Preparation, characterization and hydroxyapatite binding in vitro..," *Int J Pharm,* no. 331, pp. 224-227, 2007.

[262] K. Uhrich, S. Cannizzaro, R. Langer and K. Shakesheff, "Polymeric systems for controlled drug release.," *Chem. Rev.,* no. 99, pp. 3181-3198.

[263] K. Walter, R. Tamargo, A. Olivi, P. Burger and H. Brem, "Intratumoral chemotherapy.," *Neurosurgery,* no. 37, pp. 1129-1145, 1995.

[264] M. Francis, R. Graham, R. Russell and H. Fleisch, "Diphosphonates inhibit formation of calcium phosphate crystals in vitro and pathological calcification in vivo.," *Science,* no. 165, pp. 1264-1266, 1969.

[265] R. Russell, N. Watts, F. Ebetino and M. Rogers, "Mechanisms of action of bisphosphonates: similarities and differences and their potential influence on clinical efficacy.," *Osteoporos Int.,* no. 19, p. 733–759, 2008.

[266] J. Frith, J. Mönkkönen, G. Blackburn, R. Russell and M. Rogers, "Clodronate and liposome-encapsulated clodronate are metabolized to a toxic ATP analog, adenosine 5′-(β, γ-dichloromethylene) triphosphate, by mammalian cells in vitro.," *J. Bone Miner. Res.,* no. 12, pp. 1358-1367, 1997.

[267] P. Lehenkari, M. Kellinsalmi, J. Näpänkangas, K. Ylitalo, J. Mönkkönen, M. Rogers, A. Azhayev, H. Väänänen and I. Hassinen, "Further insight into mechanism of action of clodronate: inhibition of mitochondrial ADP/ATP translocase by a nonhydrolyzable, adenine-c," *Mol. Pharmacol.,* no. 61, pp. 1255-1262, 2002.

[268] J. Dunford, K. Thomspson, F. Coxon, S. Luckman, F. Hahn, C. Poulter, E. F.H. and M.

Rogers, "Structure-activity relationships for inhibition of farnesyl disphosphate syntase in vitro and inhibition of bone resorption in vivo by nitrogen-containing bisphosphonates.," *J. Pharm. Exp. Ther.,* no. 296, pp. 235-242, 2001.

[269] R. M. H. J. L. S. H. D. M. P. W. G. R. R. R. G. R. A. Fisher J.E, «Alendronate mechanism of action: geranylgeraniol, an intermediate in the mevalonate pathway, prevents inhibition of osteoclast formation, bone resorption and kinase activation in vitro.,» *Proc. Natl. Acad. Sci. USA,* αρ. 96, pp. 133-138, 1999.

[270] S. Luckman, D. Hughes, F. Coxon, R. Graham, R. Russell and M. Rogers, "Nitrogen-Containing Bisphosphonates Inhibit the Mevalonate Pathway and Prevent Post-Translational Prenylation of GTP-Binding Proteins, Including Ras," *J. Bone Miner. Res.,* no. 13, pp. 581-589, 1998.

[271] E. Van Beek, E. Pieterman, L. Cohen, C. Lowik and S. Papapoulos, "Nitrogen-containing bisphosphonates inhibit isopentenyl pyrophosphate isomerase/farnesyl pyrophosphate synthase activity with relative potencies corresponding to their antiresorptive potencies in vitro and in vivo.," *Biochem. Biophys. Res. Commun.,* no. 255, pp. 491-494, 1999.

[272] H. Fleisch, A. Reszka, G. Rodan and G. Rogers, "Bisphosphonates: mechanisms of action," in *Principles of bone biology (Edited by:John P. Bilezikian, Lawrence G. Raisz and Gideon A. Rodan)*, San Diego, Academic Press, 2002, pp. 1361-1385.

[273] G. Rodan and A. Reszka, "Bisphophonate mechanism of action.," *Curr. Mol. Med.,* no. 2, pp. 571-577, 2002.

[274] G. Mundy, "Mechanisms of bone metastasis.," *Cancer,* no. 80, pp. 1546-1556, 1997.

[275] E. Shane, "Evolving data about subtrochanteric fractures and bisphosphonates.," *N. Engl. J. Med.,* no. 326, pp. 1825-1827, 2010.

[276] R. Weinstein, P. Robertson and S. Manolagas, "Giant osteoclast formation and long-term oral bisphosphonate therapy.," *N. Engl. J. Med.,* no. 360, pp. 53-62, 2009.

[277] T. Chen, J. Berenson, R. Vescio, R. Swift, A. Gilchick, S. Goodin, P. LoRusso, P. Ma, C. Ravera, F. Deckert, H. Schran, J. Seaman and A. Skerjanec, "Pharmacokinetics and pharmacodynamics of zoledronic acid in cancer patients with bone metastases.," *J. Clin. Pharmacol.,* no. 42, pp. 1228-1236, 2002.

[278] W. Thompson, D. Thompson, P. Anderson and G. Rodan, "European Patent 0341961 :

Polymalonic acids as bone affinity agents.," 1989.

[279] L. Gil, Y. Han, E. Opas, G. Rodan, R. Ruel, J. Seedor, P. Tyler and R. Young, "Prostaglandin E2–bisphosphonate conjugates: potential agents for treatment of osteoporosis.," *Bioorg. Med. Chem.,* no. 7, pp. 901-919, 1999.

[280] W. Shakespeare, C. Metcalf III, Wang. Y, R. Sundaramoorthi, T. Keenan, M. Weigele, R. Bohacek, D. Dalgarno and T. Sawyer, "Novel bone-targeted Src tyrosine kinase inhibitor drug discovery. Curr Opin Drug Discov Devel.," *Curr. Opin. Drug Discov. Devel.,* no. 6, pp. 729-741, 2003.

[281] H. Hirabayashi, T. Takahashi, J. Fujisaki, T. Masunaga, S. Sato, J. Hiroi, Y. Tokunaga, S. Kimura and T. Hata, "Bone specific delivery and sustained release of diclofenac, a non-steroidal anti-inflammatory drug, via bisphosphonic prodrug based on Osteotropic Drug Delivery System (ODDS)," *J. Control Release,* no. 70, pp. 183-191, 2001.

[282] F. Hosain, R. Spencer, H. Couthon and G. Sturtz, "Targeted delivery of antineoplastic agent to bone: biodistribution studies of technetium-99m-labeled gembisphosphonate conjugate of methotrexate.," *J. Nucl. Med.,* no. 37, pp. 105-107, 1996.

[283] M. Francis and I. Fogelman, "99mTc diphosphonate uptake mechanism on bone.," in *Bone scanning in clinical practice. (Edited by Fogelman Ignac)*, New York,, Springer-Verlag, 1987, pp. 7-17.

[284] H. Lamb and D. Faulds, "Samarium 153Sm lexidronam.," *Drugs Aging,* no. 11, pp. 413-418, 1997.

[285] E. Giger, B. Castagner and J. Leroux, "Biomedical applications of bisphosphonates.," *J. Controlled Release,* no. 167, pp. 175-188, 2013.

[286] S. Gittens, G. Bansal, R. Zernicke and H. Uludag, "Designing proteins for bone targeting.," *Adv. Drug Deliv. Rev,* no. 57, pp. 1011-1036, 2005.

[287] X. Liu, A. Wiswall, J. Rutledge, M. Akhter, D. Cullen, R. Reinhardt and D. Wang, "Osteotropic β-cyclodextrin for local bone regeneration.," *Biomaterials,* no. 29, pp. 1686-1692, 2008.

[288] R. Levy, X. Qu, T. Underwood, J. Trachy and F. Schoen, "Calcification of valved aortic allografts in rats: Effects of age, crosslinking, and inhibitors.," *J. Biomed. Mater. Res.,* no. 29, pp. 217-226, 1995.

[289] R. Levy, J. Wolfrum, F. Schoen, M. Hawley, S. Lund and R. Langer, "Inhibition of calcification of bioprosthetic heart valves by local controlled-release diphosphonate.," *Science,* no. 228, pp. 190-192, 1985.

[290] R. Levy, T. Johnson, A. Sintov and G. Golomb, "Controlled release implants for cardiovascular disease. J Controlled Release 11:245-254.," *J Controlled Release,* no. 11, pp. 245-254, 1990.

[291] G. Golomb, M. Dixon, M. Smith, F. Schoen and R. Levy, "Controlled-release drug delivery of diphosphonates to inhibit bioprosthetic heart valve calcification: release rate modulation with silicone matrices via drug solubility and membrane coating.," *J. Pharm. Sci.,* no. 76, pp. 271-276, 1987.

[292] S. Cremers, G. Pillai and S. Papapoulos, "Pharmacokinetics/pharmacodynamics of bisphosphonates: use for optimisation of intermittent therapy for osteoporosis.," *Clin Pharmacokinet,* no. 44, pp. 551-570, 2005.

[293] J. Fujisaki, Y. Tokunaga, T. Takahashi, T. Hirose, F. Shimojo, A. Kagayama and T. Hata, "Osteotropic drug delivery system (ODDS) based on bisphosphonic prodrug. I: synthesis and in vivo characterization of osteotropic carboxyfluorescein.," *J. Drug Target.,* vol. 3, no. 4, pp. 273-82, 1995.

[294] J. Fujisaki, Y. Tokunaga, T. Sawamoto, T. Takahashi, S. Kimura, F. Shimojo and T. Hata, "Osteotropic drug delivery system (ODDS) based on bisphosphonic prodrug. III: Pharmacokinetics and targeting characteristics of osteotropic carboxyfluorescein," *J Drug Target.,* no. 4, pp. 117-123, 1996.

[295] J. Fujisaki, Y. Tokunaga, T. Takahashi, S. Murata, F. Shimojo and T. Hata, "Physicochemical characterization of bisphosphonic carboxyfluorescein for osteotropic drug delivery.," *J Pharm Pharmacol,* no. 48, pp. 798-800, 1996.

[296] S. Patwardhan, S. Clarson and C. Perry, "On the role(s) of additives in bioinspired silicification.," *Chem. Commun.,* pp. 1113-1121, 2005.

[297] D. Belton, S. Patwardhan, V. Annenkov, E. Danilovtseva and C. Perry, "From biosilicification to tailored materials: Optimizing hydrophobic domains and resistance to protonation of polyamines.," *Proc. Natl. Acad.. Sci. USA,* no. 105, pp. 5963-5968, 2008.

[298] C. Steven, G. Busby, C. Mather, B. Tariq, M. Lucia-Briuglia, D. Lamprou, A. Urquhart, M.

Grant and S. Patwardhan, "Bioinspired silica as drug delivery systems and their biocompatibility.," *J. Mater. Chem. B,* no. 2, pp. 5028-5042, 2014.

[299] D. Belton, S. Patwardhan and C. Perry, "Spermine, spermidine and their analogues generate tailored silicas.," *J. Mater. Chem.,* vol. 15, no. 43, pp. 4629-4638, 2005.

[300] F. Balas, M. Manzano, P. Horcajada and M. Vallet-Regí, "Confinement and controlled release of bisphosphonates on ordered mesoporous silica-based materials.," *J. Am. Chem. Soc.,* no. 128, pp. 8116-8117, 2006.

[301] J. Thomas, B. Johnson, R. Raja, G. Samkar and P. Midgley, "High-performance nanocatalysts for single-step hydrogenations..," *Acc Chem Res,* no. 36, pp. 20-30, 2003.

[302] A. Chong and X. Zhao, "Functionalization of SBA-15 with APTES and characterization of functionalized materials.," *J. Phys. Chem. B,* no. 107, pp. 12650-12657, 2003.

[303] A. Walcarius, M. Etienne and B. Lebeau, "Rate of access to the binding sites in organically modified silicates.Ordered mesoporous silicas grafted with amine or thiol groups.," *Chem. Mate.,* no. 15, pp. 2161-2173, 2003.

[304] J. Crank, The Mathematics of Diffusion, 2nd Revised ed. Edition (Edited by J. Crank), Oxford: Oxford University Press, 1975.

[305] P. Costa and J. Sousa-Lobo, "Modeling and comparison of dissolution profiles.," *Eur. J. Pharm. Sci.,* no. 13, pp. 123-133, 2001.

[306] W. Patrick, "US 1297724-A Patented : Silica gel and process of making same.," Mar. 18, 1919.

[307] Z. Amjad, Mineral Scale Formation and Inhibition. (Edited by Amjad, Z.), New York: Springer, 1995.

[308] Z. Amjad, Advances in Crystal Growth Inhibition Technologies (Edited by Amjad, Z), New York: Plenum Press, 2002.

[309] M. Quraishi, I. Farooqi and P. Saini, "Investigation of Some Green Compounds as Corrosion and Scale Inhibitors for Cooling Systems," *Corrosion,* no. 55, pp. 493-497, 1999.

[310] K. Demadis, E. Neofotistou, E. Mavredaki, M. Tsiknakis, E. Sarigiannidou and S. Katarachia, "Inorganic Foulants in Membrane Systems: Chemical Control Strategies and the Contribution of "Green Chemistry," *Desalination,* no. 179, pp. 281-295, 2005.

[311] K. Demadis and E. Neofotistou, "Inhibition and Growth Control of Colloidal Silica: Designed Chemical Approaches.," *Mater. Performance,* no. 43, pp. 38-42, 2004.

[312] E. Neofotistou and K. Demadis, "Silica Scale Growth Inhibition By Polyaminoamide STARBURST Dendrimers.," *Coll. Surf. A: Physicochem. Eng. Asp.,* no. 242, pp. 213-216, 2004.

[313] E. Neofotistou and K. Demadis, "Use of Antiscalants for Mitigation of Silica (SiO) Fouling and Deposition: Fundamentals and Applications in Desalination Systems.," *Desalination,* no. 167, pp. 257-272, 2004.

[314] K. Demadis, "Focus on Operation & Maintenance: Scale Formation and Removal," *Power,* no. 148, pp. 19-23, 2004.

[315] K. Demadis, "A Structure/Function Study of Polyaminoamide (PAMAM) Dendrimers As Silica Scale Growth Inhibitors.," *J. Chem. Technol. Biotechnol.,* no. 80, pp. 630-640, 2005.

[316] E. Mavredaki, E. Neofotistou and D. K.D., "Inhibition and Dissolution as Dual Mitigation Approaches for Colloidal Silica Fouling and Deposition in Process Water Systems: Functional Synergies," *Ind. Engin. Chem. Res.,* no. 44, pp. 7019-7026, 2005.

[317] K. Demadis and E. Mavredaki, "Dissolution Enhancement of Colloidal Silica By Environmentally Benign Additives. Potential Applications in Silica-Laden Water Systems," *Env. Chem. Lett.,* no. 3, pp. 127-131, 2005.

[318] K. Demadis and A. Stathoulopoulou, "Novel, Multifunctional, Environmentally Friendly Additives for Effective Control of Inorganic Foulants in Industrial Water and Process Applications.," *Mater.Performance,* no. 45, pp. 40-44, 2005.

[319] A. Alanne, H. Hyvönen, M. Lahtinen, M. Ylisirniö, P. Turhanen, E. Kolehmainen, S. Peräniemi and J. Vepsäläinen, "Systematic study of the physicochemical properties of a homologous series of aminobisphosphonates.," *Molecules,* no. 17, pp. 10928-10945, 2012.

[320] M. Egorov, S. Aoun, M. Padrines, F. Redini, D. Heymann, J. Lebreton and M. Mathé-Allainmat, "A One-Pot Synthesis of 1-Hydroxy-1,1-bis(phosphonic acid)s Starting from the Corresponding Carboxylic Acids.," *Eur. J. Org. Chem.,* pp. 7148-7154, 2011.

[321] A. Alanne, M. Tuikka, K. Tõnsuaadu, M. Ylisirniö, L. Hämäläinen, P. Turhanen, J. Vepsäläinen and S. Peräniemi, "A novel bisphosphonate-based solid phase method for

effective removal of chromium(III) from aqueous solutions and tannery effluent," *s. RSC-Adv.,* no. 3, pp. 14132-14138, 2013.

[322] K. Popov, E. Niskanen, H. Ronkkomaki and L. L.H.J., "31 P NMR Study of organophosphonate protonation equilibrium at high pH.," *New J. Chem.,* no. 23, pp. 1209-13, 1999.